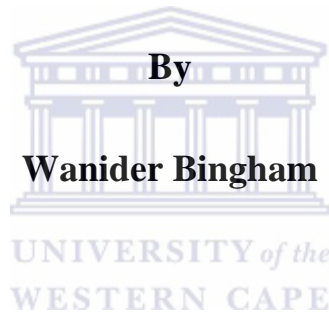




**Immunohistochemical Analysis of a Panel of Human and
Murine Markers on Xenografted Human Vaginal Mucosa:
A Comparative Study**



**Thesis Presented in Partial Fulfillment of the Requirements for the Degree of Magister
Scientiae**

In the Department of Medical Biosciences

University of the Western Cape

Supervisors: Prof D Hiss

Co-Supervisor: Prof J Hille

15 November 2012

Immunohistochemical Analysis of a Panel of Human and Murine Markers on Xenografted Human Vaginal Mucosa: A Comparative Study

Wanider Bingham

KEYWORDS

Athymic Nude Mice

Vaginal Mucosa

Xenografts

Cytokeratins

Collagen Type IV

Laminin

Elastin

Fibronectin

Langerhans Cells

Vascular Endothelial Growth Factor Receptor (VEGFR)

Immunohistochemistry



ABSTRACT

Immunohistochemical Analysis of a Panel of Human and Murine Markers on Xenografted Human Vaginal Mucosa: A Comparative Study

W. Bingham

MSc Thesis, Department of Medical Biosciences, University of the Western Cape

Athymic nude mouse models have been extensively used to study biological behaviour of normal and diseased human tissues. In such models, immune-deficient mice act as hosts for cysts constructed from human material. A unique biocyst model that entails transplantation of human vaginal cysts into athymic nude mice has been implemented to study diseases of oral mucosa. To date, only one immunohistochemical study of this biocyst model has been reported. Nevertheless, conclusions made in that study were only based on the observed expression patterns of human and murine markers. Statistical assessment of immunohistochemical data had been omitted by the investigator. Therefore, the objective of this study was to further delineate the immunohistochemical profile of normal human vaginal tissue and human vaginal tissue that had been xenografted into nude mice.

Experimental cysts constructed from human vaginal mucosa were xenografted into athymic nude mice and harvested 9-weeks post transplantation. Immunohistochemical analysis of normal human vaginal tissue and human vaginal tissue that had been xenografted into nude mice was performed using a panel of human and murine markers. Expression patterns of human and murine markers were assessed. Human markers included cytokeratin 1, cytokeratin 5, cytokeratin 13, cytokeratin 14, collagen type IV, laminin, elastin, fibronectin, Langerhans cells and VEGFR-3. Murine markers included collagen type IV, laminin,

fibronectin, Langerhans cells and VEGFR-2. Staining intensities were quantified and statistically analysed using one-way ANOVA with subsequent Friedman's test for multiple comparisons. Since the sample size was small, the power of the test statistic was enhanced by including Dunn's post-test for further multiple comparisons.

A strong positive expression of all cytokeratins was detected in both normal and xenografted vaginal tissues. Human markers that exhibited weak to moderate positive expression were collagen IV, laminin, fibronectin and VEGFR-3. Human elastin and human Langerhans cells exhibited strong and varying expression patterns respectively. Weak expression patterns for all murine markers were reported, with an exception of VEGFR-2 which was negatively expressed in all xenografted vaginal tissues. Significant differences ($P < 0.05$) in the mean staining intensities between normal and xenografted vaginal tissues were reported for cytokeratin 1, fibronectin and Langerhans cells. There were no statistical differences ($P > 0.05$) in the mean staining intensities for other markers.

In conclusion, immunohistochemical studies proved that human vaginal tissue could not only survive in nude mice, but could also become active and develop structures necessary for survival, in this case, a newly formed stromal layer. The epithelium and stromal layer exhibited a human ecosystem.

November 2012

DECLARATION

I declare that '*Immunohistochemical Analysis of a Panel of Human and Murine Markers on Xenografted Human Vaginal Mucosa: A Comparative Study*' is my own work, that it has not been submitted for any degree or examination in any other university, and that all the sources I have used or quoted have been indicated and acknowledged by complete references.

.....

Wanider Bingham

15 November 2012



DEDICATION

This dissertation is dedicated to the memory of the most amazing grandfather, George Bingham. I thank you for the love and care you always showed when you were still in this world.



ACKNOWLEDGEMENTS

To **Prof. D Hiss**, I sincerely thank you for supervising the project and teaching me a million things throughout my study. I also wish to extend my gratitude to my co-supervisor **Prof. J Hille** for idealizing the study.

To **Mr. C Kok**, many thanks for playing a critical role in this study. I extend my immense gratitude for your constant guidance and patience throughout this project. All the comments and inputs have been vital to the successful completion of this thesis.

To **my family**, particularly my grandmother, my heartfelt thanks for your financial and emotional support throughout my life. Your continuous support and unconditional love has given me strength to accomplish what I have thus far.

Mr. Y Mnyamana and **Mr. D Jwambi**, I appreciate all the technical assistance you offered with regards to computers.

To **Prof G Van' Der Horst**, **Dr L Marie** and **Mrs. C Opuwari**, I am grateful for your availability whenever I needed assistance. You are the reason behind my improved microscopy skills.

Many thanks to the **Department of Anatomical Pathology, University of Stellenbosch**, for providing the resources used in the study and the **Department of Medical Biosciences, University of the Western Cape** for providing all the equipment I needed to compile this write-up.

Finally, I thank the **National Health Laboratory Service Research Trust** for their financial contribution to the project.

TABLE OF CONTENTS

TITLE PAGE.....	ii
ABSTRACT.....	iii
DECLARATION.....	v
DEDICATION.....	vi
ACKNOWLEDGEMENTS.....	vii
TABLE OF CONTENTS.....	viii
LIST OF ABBREVIATIONS.....	xiii
LIST OF FIGURES.....	xvi
LIST OF TABLES.....	xvii
LIST OF APPENDIXES.....	xviii
CHAPTER ONE: INTRODUCTION.....	1
1.1 Background.....	1
1.2 Rationale.....	2
1.3 Purpose of the study.....	3
1.3.1 Aim.....	3
1.3.2 Objectives.....	3
1.3.3 Research Question.....	3
1.4 Research Methodology.....	4
1.5 Organization of Chapters.....	4
1.6 Concluding Remarks.....	4
CHAPTER TWO: LITERATURE REVIEW.....	5
2.1 Organization of Human Vaginal Mucosa.....	5
2.1.1 The Epithelium.....	6
2.1.2 The Basement Membrane.....	7
2.1.3 The Connective Tissue.....	8
2.2 Animal Models.....	8
2.2.1 Significance of Athymic Nude Mice in the Medical World.....	8
2.3 Cytokeratins.....	9
2.4 Collagen Type IV.....	10



2.4.1	The α -Chains of Collagen IV.....	10
2.4.2	Expression and Interaction of Collagen IV.....	11
2.4.3	Collagen IV Assembly.....	11
2.5	Laminin.....	12
2.5.1	Family of Laminin Glycoproteins.....	12
2.5.2	Tissue Distribution of Laminin Isoforms and Receptors.....	13
2.5.3	The Interaction of Laminin with Cell Surface Receptors.....	14
2.5.4	Prominent Role of Laminins.....	15
2.5.5	The Role of Laminin in Pathology.....	15
2.6	Elastin.....	16
2.6.1	The Synthesis of Elastin from Tropoelastin.....	16
2.6.2	Structural Properties of Elastin.....	16
2.6.3	Elastogenesis.....	17
2.7	Fibronectin.....	18
2.7.1	Brief Overview of Fibronectin.....	18
2.7.2	Fibronectin as a Constituent of the Plasma and Extracellular Matrix.....	18
2.7.3	Fibronectin as a Mediator of Cellular Interactions.....	19
2.7.4	Functional Domains of Fibronectin.....	20
2.7.5	The Association of Fibronectin Depletion with Tumorigenicity.....	23
2.8	Langerhans Cells.....	23
2.8.1	Langerhans Cells as Regulators of Immune Responses.....	24
2.9	Vascular Endothelial Growth Factor Receptor (VEGFR).....	25
2.9.1	Angiogenesis.....	25
2.9.2	VEGF Family and Receptors.....	26
2.9.3	Expression and Differential Roles of VEGFs and VEGFRs.....	27
2.10	Immunohistochemistry.....	30
2.10.1	Immunohistochemical Stain.....	31
2.10.2	Immunohistochemistry Detection Systems.....	32
2.11	Concluding Remarks.....	32
CHAPTER THREE: MATERIALS AND METHODS.....		33
3.1	Ethical Approval.....	33

3.2	Experimental Design - Part 1: Tissue Preparation.....	33
3.2.1	Cyst Production.....	33
3.2.2	Athmic Nude Mice.....	34
3.2.3	Cyst Xenografts.....	34
3.2.4	Cyst Retrieval.....	34
3.3	Experimental Design - Part 2: Immunohistochemistry.....	35
3.3.1	Principle.....	35
3.3.2	Antibodies.....	36
3.3.3	Procedure.....	37
3.3.4	Light Microscopy.....	38
3.3.5	Scoring Criteria.....	39
3.4	Statistical Analysis.....	40
3.5	Positive Controls.....	40
3.5.1	Positive Human Tissue Controls.....	40
3.5.2	Positive Mouse Tissue Controls.....	41
3.6	Negative Controls.....	42
3.6.1	1 st Negative Control Tissue.....	42
3.6.2	2 nd Negative Control Tissue.....	42
3.7	Acronyms used in the Study.....	42
CHAPTER FOUR: RESULTS.....		43
4.1	Human Cytokeratin 1 Expression Profile.....	43
4.1.1	Immunohistochemical Scores for Cytokeratin 1.....	43
4.1.2	Statistical Comparisons of Cytokeratin 1 Staining Intensities.....	44
4.1.3	Photomicrographs of Vaginal Mucosae Stained for Cytokeratin 1.....	45
4.2	Human Cytokeratin 5 Expression Profile.....	46
4.2.1	Immunohistochemical Scores for Cytokeratin 5.....	46
4.2.2	Statistical Comparisons of Cytokeratin 5 Staining Intensities.....	47
4.2.3	Photomicrographs of Vaginal Mucosae Stained for Cytokeratin 5.....	48
4.3	Human Cytokeratin 13 Expression Profile.....	49
4.3.1	Immunohistochemical Scores for Cytokeratin 13.....	49
4.3.2	Statistical Comparisons of Cytokeratin 13 Staining Intensities.....	50

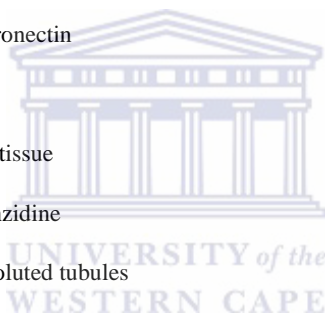


4.3.3	Photomicrographs of Vaginal Mucosae Stained for Cytokeratin 13.....	51
4.4	Human Cytokeratin 14 Expression Profile.....	52
4.3.1	Immunohistochemical Scores for Cytokeratin 14.....	52
4.4.2	Statistical Comparisons of Cytokeratin 14 Staining Intensities.....	53
4.4.3	Photomicrographs of Vaginal Mucosae Stained for Cytokeratin 14.....	54
4.5	Collagen Type IV Expression Profile.....	55
4.5.1	Immunohistochemical Scores for Collagen IV.....	55
4.5.2	Statistical Comparisons of Collagen IV Staining Intensities.....	56
4.5.3	Photomicrographs of Vaginal Mucosae Stained for Human Collagen IV.....	57
4.5.4	Photomicrographs of Vaginal Mucosae Stained for Mouse Collagen IV.....	58
4.6	Laminin Expression Profile.....	59
4.6.1	Immunohistochemical Scores for Laminin.....	59
4.6.2	Statistical Comparisons of Laminin Staining Intensities.....	60
4.6.3	Photomicrographs of Vaginal Mucosae Stained for Human Laminin.....	61
4.6.4	Photomicrographs of Vaginal Mucosae Stained for Mouse Laminin.....	62
4.7	Human Elastin Expression Profile.....	63
4.7.1	Immunohistochemical Scores for Elastin.....	63
4.7.2	Statistical Comparisons of Elastin Staining Intensities.....	64
4.7.3	Photomicrographs of Vaginal Mucosae Stained for Human Elastin.....	65
4.8	Fibronectin Expression Profile.....	66
4.8.1	Immunohistochemical Scores for Fibronectin.....	66
4.8.2	Statistical Comparisons of Fibronectin Staining Intensities.....	67
4.8.3	Photomicrographs of Vaginal Mucosae Stained for Human Fibronectin.....	68
4.8.4	Photomicrographs of Vaginal Mucosae Stained for Mouse Fibronectin.....	69
4.9	Langerhans Cells Expression Profile.....	70
4.9.1	Immunohistochemical Scores for Langerhans Cells.....	70
4.9.2	Statistical Comparisons of Langerhans Cells Staining Intensities.....	71
4.9.3	Photomicrographs of Vaginal Mucosae Stained for Human Langerhans Cells.....	72
4.9.4	Photomicrographs of Human and Murine Tissues Stained for Mouse Langerhans Cells.....	73
4.10	Vascular Endothelial Growth Factor Receptor (VEGFR) Expression Profile.....	74
4.10.1	Immunohistochemical Scores for VEGFR.....	74

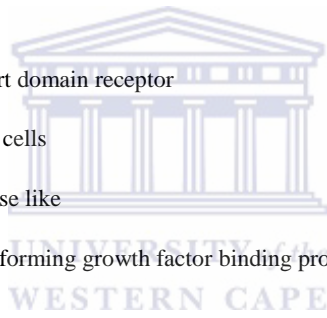
4.10.2	Statistical Comparisons of VEGFR Staining Intensities.....	75
4.10.3	Photomicrographs of Vaginal Mucosae Stained for VEGFR.....	76
CHAPTER FIVE: DISCUSSION AND CONCLUSION.....		77
5.1	Interpretation of Results.....	77
5.1.1	Analysis of Cytokeratin 1 Expression Profile.....	77
5.1.2	Analysis of Cytokeratin 5 Expression Profile.....	78
5.1.3	Analysis of Cytokeratin 13 Expression Profile.....	78
5.1.4	Analysis of Cytokeratin 14 Expression Profile.....	79
5.1.5	Analysis of Collagen Type IV Expression Profile.....	79
5.1.6	Analysis of Laminin Expression Profile.....	80
5.1.7	Analysis of Elastin Expression Profile.....	81
5.1.8	Analysis of Fibronectin Expression Profile.....	82
5.1.9	Analysis of Langerhans Cells Expression Profile.....	82
5.1.10	Analysis of Vascular Endothelial Growth Factor Receptor Expression Profile.....	83
5.2	Conclusion.....	84
CHAPTER SIX: LIMITATIONS OF THE STUDY AND FUTURE PROSPECTS.....		86
6.1	Problems Encountered and Recommendations.....	86
6.2	Future Directions.....	86
REFERENCES.....		88
APPENDIX I: Immunohistochemical Staining Protocol.....		94
APPENDIX II: Immunohistochemistry Washing Buffers.....		96
APPENDIX III: Antigen Retrieval Buffers.....		97
APPENDIX IV: Blocking Solutions.....		98
APPENDIX V: Immunohistochemistry Diluent Solution.....		99
APPENDIX VI: Novocastra™ Lyophilized Monoclonal Antibodies.....		100
APPENDIX VII: Statistical Analysis Data.....		104

LIST OF ABBREVIATIONS

Acronym	Description
Ab	-Antibody
ABC	-Avidin-biotin conjugates
AFM	-Atomic force microscopy
ANOVA	-Analysis of variance
BM	-Basement membrane
B-SA	-Biotin-streptavidin
BVs	-Blood vessels
C	-Carboxyl
CD	-Circular dichroism
cFN	-Cellular fibronectin
CK	-Cytokeratin
CT	-Connective tissue
DAB	-Diaminobenzidine
DCT	-Distal convoluted tubules
DPX	-Mountant (glue)
DC	-Dendritic cell
DDR-1	-Discoidin domain receptor-1
dH ₂ O	-Distilled water
EBP	-Elastin binding protein
ECs	-Endothelial cells
ECM	-Extra cellular matrix
EDTA	-Ethylene diamine tetracetic acid
EHS	-Engelbreth-Holm-Swarm
ELISA	-Enzyme linked immunosorbent assay
Ep	-Epithelium
FFPE	-Formalin fixed paraffin embedded
FGR	-Fibroblast growth factor
FK506	-Tacrolimus / fujimycin



FKBP65	-Tatrolimus binding protein
Flk	-Fetal liver kinase
FN	-Fibronectin
GBM	-Glomerular basement membrane
GM-CSF	-Granulocyte-macrophage colony-stimulating factor
HIV	-Human immunodeficiency virus
H ₂ O	-Water
H ₂ O ₂	-Hydrogen peroxide
HRP	-Horseradish peroxidase
IGF	-Insulin-like growth factor
IHC	-Immunohistochemistry
JCT	-Juxtacanalicular tissue
Kd	-Kilodalton
KDR	-Kinase insert domain receptor
LCs	-Langerhans cells
LOXL	-Lysyl oxidase like
LTBP	-Latent transforming growth factor binding protein
M	-Molar
MAGP	-Microfibril associated glycoprotein
Mcg	-Small membrane coated granules
MFAP	-Microfibril associated protein
Mm	-Millimolar
ml	-Milliliters
mRNA	-Messenger ribonucleic acid
N	-Amino
NHLS	-National Health Laboratory Services
NC	-Non-collagenous
nm	-Nanometer
NM	-Nude mouse
NVT	-Normal vaginal tissue
NVT ^α	-Normal vaginal tissue of the previous study



PAP	-Peroxidase anti-peroxidase
PBS	-Phosphate buffer solution
PCR	-Polymerase chain reaction
PCT	-Proximal convoluted tubules
PDGF	-Platelet derived growth factor
pFN	-Plasma fibronectin
PIGF	-Placental growth factor
RTK	-Receptor tyrosine kinase
sECM	-Specialized extracellular matrix
Sv	-Snake venom-derived
TEM	-Transmission electron microscopy
TGF	-Transforming growth factor
TGF- β 2	- Transforming growth factor beta-2
TK	-Tyrosine kinase
TM	-Trabecular meshwork
TNF	-Tumor necrosis factor
VEGF	-Vascular endothelial growth factor
VEGFR	-Vascular endothelial growth factor receptor
VPF	-Vascular permeability factor
XVT	-Xenografted vaginal tissue
XVT-h	-Xenografted vaginal tissue – human antigen localization
XVT-m	-Xenografted vaginal tissue – mouse antigen localization
XVT ^a	-Xenografted vaginal tissue of the previous study
α	-Alpha
β	-Beta
$^{\circ}\text{C}$	-Degree Celsius
μg	-Microgram
$\mu\text{g/ml}$	-Microgram per milliliters
μm	-Micrometer
μl	-Microliter
γ	-Gamma

LIST OF FIGURES

Figure	Description	Page
Figure 2.1	Classical Model of Elastogenesis	17
Figure 3.1	Indirect Conjugate (Sandwich) Method	36
Figure 4.1	Mean Cytokeratin 1 Staining Intensity by Vaginal Mucosal Type	44
Figure 4.2	Immunohistochemical Staining of Cytokeratin 1 on Vaginal Mucosal Tissues	45
Figure 4.3	Mean Cytokeratin 5 Staining Intensity by Vaginal Mucosal Type	47
Figure 4.4	Immunohistochemical Staining of Cytokeratin 5 on Vaginal Mucosal Tissues	48
Figure 4.5	Mean Cytokeratin 13 Staining Intensity by Vaginal Mucosal Type	50
Figure 4.6	Immunohistochemical Staining of Cytokeratin 13 on Vaginal Mucosal Tissues	51
Figure 4.7	Mean Cytokeratin 14 Staining Intensity by Vaginal Mucosal Type	53
Figure 4.8	Immunohistochemical Staining of Cytokeratin 14 on Vaginal Mucosal Tissues	54
Figure 4.9	Mean Collagen IV Staining Intensity by Vaginal Mucosal Type	56
Figure 4.10	Immunohistochemical Staining of Human Collagen IV on Vaginal Mucosal Tissues	57
Figure 4.11	Immunohistochemical Staining of Mouse Collagen IV on Human and Murine Tissues	58
Figure 4.12	Mean Laminin Staining Intensity by Vaginal Mucosal Type	60
Figure 4.13	Immunohistochemical Staining of Human Laminin on Vaginal Mucosal Tissues	61
Figure 4.14	Immunohistochemical Staining of Mouse Laminin on Human and Murine Tissues	62
Figure 4.15	Mean Elastin Staining Intensity by Vaginal Mucosal Type	64
Figure 4.16	Immunohistochemical Staining of Human Elastin on Vaginal Mucosal Tissues	65
Figure 4.18	Mean Fibronectin Staining Intensity by Vaginal Mucosal Type	67
Figure 4.19	Immunohistochemical Staining of Human Fibronectin on Vaginal Mucosal Tissues	68
Figure 4.20	Immunohistochemical Staining of Mouse Fibronectin on Human and Murine Tissues	69
Figure 4.21	Mean Langerhans Cells Staining Intensity by Vaginal Mucosal Type	71
Figure 4.22	Immunohistochemical Staining of Human Langerhans Cells on Vaginal Mucosal Tissues	72
Figure 4.23	Immunohistochemical Staining of Mouse Langerhans Cells on Human and Murine Tissues	73
Figure 4.24	Mean VEGFR-3 and VEGFR-2 Staining Intensity by Vaginal Mucosal Type	75
Figure 4.25	Immunohistochemical Staining of Human VEGFR-3 and VEGFR-2 on Vaginal Mucosal Tissues	76

LIST OF TABLES

Table	Description	Page
Table 2.1	Functional Domains of Laminin	13
Table 3.1	Antibodies used for Immunohistochemical Analysis of Mouse Antigens	36
Table 3.2	Antibodies used for Immunohistochemical Analysis of Human Antigens	37
Table 3.3	Immunohistochemical Scoring Criteria for Human and Murine Markers	39
Table 3.4	Immunohistochemical Scoring Criteria for Collagen IV and Laminin	39
Table 3.5	Positive Human Control Tissues Used for Human Antigen Retrieval	41
Table 3.6	Positive Mouse Control Tissues Used for Mouse Antigen Retrieval	41
Table 4.1	Immunohistochemical Scoring of Human Vaginal Mucosa for Human Cytokeratin 1 Antigens	43
Table 4.2	Immunohistochemical Scoring of Human Vaginal Mucosa for Human Cytokeratin 5 Antigens	46
Table 4.3	Immunohistochemical Scoring of Human Vaginal Mucosa for Human Cytokeratin 13 Antigens	49
Table 4.4	Immunohistochemical Scoring of Human Vaginal Mucosa for Human Cytokeratin 14 Antigens	52
Table 4.5	Immunohistochemical Scoring of Human Vaginal Mucosa for Human and Mouse Collagen IV Antigens	55
Table 4.6	Immunohistochemical Scoring of Human Vaginal Mucosa for Human and Mouse Laminin Antigens	59
Table 4.7	Immunohistochemical Scoring of Human Vaginal Mucosa for Human Elastin Antigens	63
Table 4.8	Immunohistochemical Scoring of Human Vaginal Mucosa for Human and Mouse Fibronectin Antigens	66
Table 4.9	Immunohistochemical Scoring of Human Vaginal Mucosa for Human and Mouse Langerhans Cells Antigens	70
Table 4.10	Immunohistochemical Scoring of Human Vaginal Mucosa for Human VEGFR-3 and Mouse VEGFR-2 Antigens	74

LIST OF APPENDIXES

Appendix	Description	Page
Appendix I	Immunohistochemical Staining Protocol	94
Appendix II	Immunohistochemistry Washing Buffers	96
Appendix III	Antigen Retrieval Buffers	97
Appendix IV	Blocking Solutions	98
Appendix V	Immunohistochemistry Diluent Solution	99
Appendix VI	Novocastra™ Lyophilized Monoclonal Antibodies	100
Appendix VII	Statistical Analysis Data	104



CHAPTER ONE

INTRODUCTION

1.1 BACKGROUND

Animal models have been extensively used to identify clinically efficacious agents of various human disorders. Amongst these models is the athymic nude (nu/nu) mouse model. The discovery of athymic nude mice has led to effective transplantation and propagation of various human tissues and cell lines into mice [1-3]. On the contrary, the predictive value of these athymic nude mouse models still remains a subject of controversial debate.

Thompson *et al.*, [4] implemented a biocyst model in which human vaginal epithelium was used to construct cysts which were then transplanted into athymic nude mice. They proposed this model as an *in vivo* biotest system to study oral mucosal disorders in humans [4]. Moreover, they hypothesized that the epithelium of the cyst remains unchanged after transplantation into immune-deficient mice. Thompson *et al.*, [4] established that allowing cysts to remain in mice for 9-weeks was an ample period to allow integration of cysts into a murine environment. Nevertheless, Thompson and colleagues' work was not entirely successful due to infection incurred by the cysts. Further investigation of this remarkable model was therefore undertaken by Wang and Hille [5]. They identified possible sources of infection that had initially affected the integrity of the experimental cysts. With stringent infection control measures, Wang and Hille obtained intact cysts 9-weeks post transplantation. They presented evidence that the structure of the epithelium remained unchanged, thus confirming the hypothesis made by Thompson *et al.*, [4]. Although Wang and Hille refined Thompson's cyst model, immunohistochemical profiling of the transplanted epithelial cysts remained unknown. For that reason, Kok [6] undertook a study in which he

characterized and compared normal human vaginal mucosa and transplanted epithelial cysts. The study entailed histological and immunohistochemical profiling of normal vaginal tissues and transplanted experimental cysts [6]. Kok's immunohistochemical data had not been statistically assessed. Therefore, conclusions made were based on the observed expression patterns of human and murine markers.

To the best of our knowledge, Kok's study of this biocyst model is the only one with relatively extensive immunohistochemical results. We therefore undertook this study in an attempt to reassess the immunohistochemical profile of normal vaginal tissues in comparison to xenografted vaginal tissues. To clarify the discussion of the comparative results, our study, incorporates for the first time, statistical assessment of the staining intensities of human and murine markers. We attempted to elucidate the nature of the epithelium, the basement membrane and stromal layer of the xenografted tissue based, not only on the expression patterns of markers, but also on the level of statistical significance.

1.2 RATIONALE

Human vaginal mucosa serves as a portal for various micro-organisms, including those that are pathogenic. The penetration of human vaginal mucosa by micro-organisms often leads to infections. Some of the infections are strongly associated with the development of carcinoma of the cervix, vagina and vulva. Carcinoma of the cervix, ovaries and vagina affect a significant number of women worldwide, with approximately 80, 720 cases reported annually, with an estimated mortality rate of 28, 120 women per year [7]. Advances in surgery and chemotherapy have improved survival for carcinomas, but such improvements have not been that remarkable [7]. Several researchers rely on athymic nude mouse models to study carcinomas [2, 8], and to establish diagnostic and therapeutic modalities [8]. This study is imperative in that it provides information about the morphology of human vaginal mucosa

that had been xenografted into athymic nude mice. It is hoped that information obtained from this study will facilitate future research application, particularly in cases where mice models are used to identify efficacious agents for various infections.

1.3 PURPOSE OF THE STUDY

1.3.1 Aim

The aim of this study was to analyze and compare morphological characteristics of normal human vaginal mucosa and human vaginal mucosa that had been xenografted into athymic nude mice.

1.3.2 Objectives

- Firstly, we used immunohistochemistry to investigate expression profiles of cytokeratin 1, 5, 13 and 14, collagen type IV, laminin, elastin, fibronectin, Langerhans cells, VEGFR-2 and VEGFR-3 in normal vaginal tissues and xenografted vaginal tissues.
- Based on the outcome of the first objective, the staining intensity of all vaginal tissues was assessed semi-quantitatively and scored according to a specified scoring system.
- Staining intensities reported were statistically compared. Staining intensities reported by Kok were also included in statistical tests.
- The nature of the epithelium, basement membrane and stromal layer were ultimately determined based on the expression patterns of human and mouse markers as well as on statistical data.

1.3.3 Research Question

The research question was, ‘Are morphological characteristics of human vaginal tissue retained after transplantation into athymic nude mice?’

1.4 RESEARCH METHODOLOGY

The study was undertaken in an academic research environment at the University of Stellenbosch and the University of the Western Cape. An experimental prospective research design consisting of two phases was used. The first phase involved preparation of human vaginal tissues whereas the second phase entailed immunohistochemical profiling of human vaginal tissues. In the first phase, cysts were constructed from human vaginal mucosae, xenografted into athymic nude mice and retrieved 9-weeks post transplantation. In the second phase, expression patterns of human and murine markers were investigated immunohistochemically. Tissue sections were then scored according to a semi quantitative scoring system. Mean staining intensities of normal and xenografted vaginal tissues were statistically analyzed using GraphPad Prism 5.0 (GraphPad Software, Inc).

1.5 ORGANIZATION OF CHAPTERS

- Chapter 1 – Introduction
- Chapter 2 – Literature Review
- Chapter 3 – Materials and Methods
- Chapter 4 – Results
- Chapter 5 – Discussion and Conclusion
- Chapter 6 – Limitations of the Study and Future Prospects

1.6 CONCLUDING REMARKS

Chapter 1 gave an overview of the research project. The background, aim and objectives as well as the significance of the project were outlined to present the rationale of conducting this study. Chapter 2 will review the literature of human vaginal mucosa and athymic nude mouse models. The markers under investigation and immunohistochemistry will also be reviewed in the next chapter.

CHAPTER TWO

LITERATURE REVIEW

Human vaginal mucosa is the first part of the female genital tract that encounters commensal bacteria and pathogenic micro-organisms [9]. Knowledge of the histological distribution of proteins in the extracellular-matrix (ECM) of human vaginal mucosa is scarce, although a better understanding of this may lead to improved protection of vaginal mucosa. Moreover, for several decades, the laboratory mouse has been the primary species in which experimental treatments for various conditions have been tested [1, 2, 8, 10]. However, the predictive value of a mouse model has been and still remains the subject of detailed investigations. This chapter will review human vaginal mucosa and athymic nude mice. The focus of this chapter will also be on some aspects of biochemistry and molecular biology of human and murine markers under investigation. The chapter will be concluded by briefly discussing immunohistochemistry, a technique that was used to analyze expression profiles of the markers under investigation.

2.1 ORGANIZATION OF HUMAN VAGINAL MUCOSA

The human vagina is a muscular tube that extends from the ectocervix to the vestibule [11]. The vagina serves as a conduit for menstrual flow, receives the erect penis during sexual intercourse and acts as a birth canal. Under normal conditions, the length of the vagina is approximately 6-7.5 cm across the anterior wall and 9 cm across the posterior wall. The vagina extends upwards and back into the pelvic cavity. It is posterior to the urinary bladder and urethra, anterior to the rectum and is attached to these structures by connective tissues. The vaginal wall comprises three layers namely, adventia, muscularis and mucosa. Adventia,

the outer fibrous layer, consists of a dense connective tissue interlaced with elastic fibers. This outer layer attaches the vagina to the surrounding organs. The middle muscular layer is predominantly composed of smooth muscle fibers. The inner mucosal layer consists of stratified squamous epithelium [12]. This layer lacks mucous glands and vaginal mucus is therefore provided by cervical and vestibular glands [12]. The key role of vaginal tissue is to provide protection from strain during copulation [13]. Since the mucosa is the subject of this study, its constituents, the epithelium, the basement membrane and connective tissue will be briefly discussed.

2.1.1 Epithelium: A Protective Barrier

The epithelium serves as one of the primary tissues that cover and protect the exterior surface and the interior cavities of the body [14]. The epithelium is classified according to certain characteristics such as the number of cell layers, the shape and distinct functions of the cells. As already stated above, the human vaginal mucosa consists of stratified squamous epithelia [12, 14, 15]. It is a highly flexible structure commonly referred to as non-keratinized epithelium and consists mainly of squamous cells [14]. The epithelium rests on both the lamina propria and an underlying sub-mucosa [15]. It is differentiated in a manner that allows it to fulfill certain demands such as protecting the underlying tissues from mechanical, chemical and microbial stress. The surface epithelial layers act as permeability barriers that regulate movement of substances across the mucosa, thereby protecting the underlying deeper tissues. If the barrier is compromised, then potentially lethal substances may adhere to the surface of the mucosa, penetrate it and induce pathologic changes which could present as local or systemic diseases. The permeability barrier of the epithelium is influenced by the composition and organization of lipids found on superficial cell layers of the tissue. This barrier is relatively inert due to terminally differentiated cells of the epithelium. These properties are factors that enable the mucosa to remain functional for extensive periods

during *ex-vivo* studies. The intermediate cell layers of the epithelia comprise small membrane coated granules (mcg), which extrude their contents into the intercellular space [14].

2.1.2 Basement Membrane: A Specialized ECM

The extracellular matrix (ECM) is a diverse and dynamic protein network that plays a critical role in cell and tissue function [16-20]. Originally, the ECM was perceived as a physical scaffold that provides mechanical support and strength to cells and tissues [17, 18]. However, it has now been established that the ECM does not only promote the interaction between cells and tissues, but also elicits biochemical signaling [17]. Physical and chemical features of the ECM are essential for development and for responses to physiological and pathological signals [21].

The basement membrane (BM) is a 50-100 nm complex and highly organized layer of the ECM and is commonly referred to as specialized extracellular matrix (sECM) [21, 22]. BMs are found in every tissue of the human body [22, 23] and their formation is necessary for normal tissue development and function [21]. Although BMs of different tissues are heterogeneous [23], they all provide structural integrity and regulate vital cellular signaling cues from the microenvironment [21, 22, 24]. BMs separate cell monolayers from the underlying connective tissue [22, 24-26]. BMs are divided into lamina lucida, lamina densa and the sublamina densa [25, 27-29]. The lamina densa defines the electron dense region of the BM. This region is mainly composed of collagen and laminin networks crosslinked by nidogen/entactin and percelan [28]. These components are essential for BM stability [22, 28, 30]. BM components interact with cell-surface receptors and non-integrin receptors to monitor biological activities which include development, proliferation, differentiation, growth and migration of cells [21]. A detailed discussion of the structure and roles of collagen IV and laminin is included in subsequent sections.

2.1.3 Connective Tissue: A Supportive Component

The connective tissue is the most abundant type of tissue that binds cells which occur in tissues throughout the body. This fibrous tissue consists of relatively few cells which synthesize connective tissue matrix. Physical properties of the matrix promote functions of the connective tissue. Connective tissues provide mechanical support by inducing strength, stability, protection and tissue repair. Moreover, connective tissues provide a surface area for intercellular exchange. Such an exchange is critical for a continuous supply of essential substances and removal of waste products [31].

2.2 ANIMAL MODELS

Animal models have been used extensively to study biological behavior of human tissues. This has led to the development of various animal models of malignant diseases. The majority of these models can be grouped into two. The first group which consists of grafts of tumor material can be categorized into immune-competent or immune-deficient animals. The second group consists of genetically engineered mice that replicate a specific cancer genotype [1]. Although these two groups both possess unique qualities, the ability of the second group in illustrating significant clinical activities remains unclear [1]. Since this study entails using immune-deficient mice, the significance of athymic nude mice will thus be briefly reviewed in the following sub-section.

2.2.1 Significance of Athymic Nude Mice in the Medical World

A nude mutant mouse was discovered more than four decades ago [2, 8, 32]. It was named athymic nude mouse because it lacks a functionally active thymus. A nude mouse is a timid and genetically odd animal that is hairless due to a single autosomal recessive gene [32, 33]. Since the first successful hetero-transplantation of human colonic adenocarcinoma into nude

mouse by Rygaard and Povlsen, several laboratories have been using these nude mice [1]. Athymic nude mice are therefore regarded unique due to their lack of cell-mediated immune response [32].

Athymic nude mouse (NM) model has now become an established tool to investigate the biology and pathophysiology of human diseases [2, 8, 32], and to develop diagnostic and therapeutic strategies [8]. For instance, the model allows routine and efficient transplantation and propagation of human tumor tissues into mice [1]. Since NMs have an ability to host cancer cells without rejection, the effects of therapeutic drugs or radiation are determined using these strains of mice [8]. In addition, it has been reported that in general, xenografts in NMs retain their original morphology and biology and show a high degree of genetic integrity. Nonetheless, in some cases, original morphology and biology is not retained. It has been reported that changes in cell growth and morphology of xenografts could result from immunological and local factors including, cell-to-cell or cell-to-matrix interactions, growth factors, cytokines, hormones and locally active enzymes [8]. For instance, some studies have demonstrated that although tumor xenografts normally retain the phenotype of the original tumor, the metastatic potential is lost [8]. This clearly indicates that there are biological and morphological changes that occur when human tissues are transplanted into a murine environment. Therefore, if therapeutic approaches to treating conditions of the female genital tract using NM models are to be achieved, it is important to determine which morphological properties of human vaginal tissues change after transplantation into NMs.

2.3 CYTOKERATINS

Cytokeratin (CK) is a cytoskeletal intermediate filament protein expressed in various human epithelial cells. The expression of CKs is specific for each epithelial cell type. At least 20 CK subtypes are known with molecular weight ranging from 40 to 70 kD. Acidic type I CKs are

designated CK9 to CK19 whereas Basic Type II CKs are designated CK1 to CK8 [34, 35]. It has been reported that CKs are involved in the formation of cellular frameworks and can serve as markers of malignancies associated with the epithelium [36].

2.4 COLLAGEN TYPE IV

Collagens constitute 30% of the total protein mass in humans, which makes collagens the main components of the ECM. Predominantly expressed collagen types include interstitial matrix type I and basement membrane type IV [17]. This section provides a brief overview of the structure and expression of collagen. The involvement of collagen IV in BM assembly is also summarized.

2.4.1 The α -Chains of Collagen IV

Type IV collagen is a non-fibrillar collagen that constitutes approximately 50% of all BMs [22, 37, 38]. Studies have shown that non-fibrillar collagen occurs at embryonic stage day 4.5 (E4.5) in mice. Non-fibrillar collagens can be distinguished from connective tissue fibrillar collagens by the presence of globular non-collagenous (NC) domains [22]. Collagen IV consists of six distinct chains referred to as α -chains ($\alpha 1$ - $\alpha 6$) [21, 22, 39, 40]. Each α -chain is 400 nm long and consists of three domains namely, Amino (N)-terminal 7S domain, triple collagenous domain and carboxyl (C)-terminal non-collagenous (NC) globular domain [22, 41]. The triple collagenous domain has repetitive Gly-X-Y amino acid sequence where X and Y represent proline and hydroxyproline respectively. The sequence of amino acids is crucial for structural integrity of collagen IV protomer and suprastructure. Short sequence interruptions of the collagenous domain provide a sufficient degree of flexibility. The 7S and NC1 domains are essential for type IV collagen network formation [22]. Although the six α -chains are homologous, their NC1 domains are not the same. Cells secrete Type IV collagen as protomers [22], which are essentially three distinct heterotrimers termed $\alpha 1\alpha 1\alpha 2$, $\alpha 3\alpha 4\alpha 5$

and $\alpha 5\alpha 5\alpha 6$ [21, 22]. Protomers serve as the building blocks of type IV collagen networks [22]. Assembled protomers are distributed on tissues in a specific manner and ultimately define the structure and function BMs [21].

2.4.2 Expression and Interaction of Collagen IV

Collagen IV exists as $\alpha 1\alpha 1\alpha 2$ heterotrimer during development [21], where it is evenly distributed in BMs [17, 21, 42]. However, during maturation, the $\alpha 1\alpha 1\alpha 2$ heterotrimer gets partially displaced by another heterotrimer such as $\alpha 3\alpha 4\alpha 5$. This has been observed in the kidney glomeruli, the skin, oesophagus and smooth muscle cells [21]. Mechanical stability of BMs is mainly influenced by collagen IV scaffold [3, 21, 43, 44]. This protein provides mechanical support to tissues and is actively involved in tissue function [45]. Collagen IV interacts with various cells including platelets, hepatocytes, hepatocytes, and keratinocytes. Endothelial cells (ECs), pancreatic cells as well as tumor cells have also been reported to interact with collagen IV. Collagen IV interactions are regulated by integrins and non-integrin receptors. Integrins that have been identified in collagen IV interactions include $\alpha 1\beta 1$, $\alpha 2\beta 1$, $\alpha 3\beta 1$, $\alpha 6\beta 1$, $\alpha 10\beta 1$, $\alpha 11\beta 1$, $\alpha v\beta 3$, and $\alpha v\beta 5$. Non-integrin receptors that have been reported in such interactions include CD44 and discoidin domain receptor-1 (DDR-1). Moreover, it has been indicated that DDR-1-collagen IV interactions are critical for the structural integrity and filtration function of BMs in the kidney [21].

2.4.3 Collagen IV Assembly

Self-assembly of collagen IV suprastructure is responsible for BM assembly [22]. Collagen IV together with laminin are enmeshed to form the basic framework of BMs. Protomers and NC1 domains, which induce triple helix formation are both formed in the Golgi apparatus. These protomers are then secreted and self-assembled into collagen IV suprastructure. Four protomers interact through their 7S domains which are then covalently stabilized. This

interaction has been shown to have a structure that resembles a ‘spider shape’. In addition, two protomers interact through NC1 trimers to form NC1 hexamer, which is also stabilized by a covalent bond. Both these types of protomer interaction establish a unique scaffold which plays a critical role in the formation of BMs [22].

2.5 LAMININ



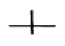

The laminin family of glycoproteins was first discovered as a product of mouse Engelbreth-Holm Swarm (EHS) sarcoma cells almost three decades ago [18, 27, 28]. This non-collagenous glycoprotein is significantly implicated in various biological activities such as BM assembly and regulation of cellular differentiation, adhesion and migration [28, 46]. In this section, the structure and distribution of laminin as well as the role it plays in BM formation and tumor invasion shall be briefly explored.

2.5.1 Family of Laminin Glycoproteins

Laminins are extracellular heterotrimeric glycoproteins composed of different combinations of chains designated α -, β -, and γ -chains [18, 21, 22, 28, 30, 47, 48], depending on sequence identity and protein domain organization [22]. These large molecules are 400-900 kDa in weight and exhibit a cross-like structure [28, 48]. To date, five α , four β , and three γ chains [28, 47-49], including splice variants [28] have been identified. In vertebrates, these subunits assemble into at least sixteen laminin isoforms termed laminin 1-15 [21, 28, 48]. Each laminin chain is composed of rodlike, globular and coiled regions. The separate chains are linked by disulphide bonds at the coiled coil regions. The 400 kDa α -chain is the largest [22, 28], and comprises of long and short arms at the carboxyl-terminal and amino-terminal ends respectively. The C-terminal end of the long arm consists of domains named LG 1-5 [28]. The β - and the γ -chains are approximately 200 kDa and differ from the α -chain by the absence of the G domains [22]. The C-terminal end of the α -chain interacts with integrin

receptors and dystroglycans. Moreover, the N-terminal end also binds to integrin receptors, although it is more implicated in laminin polymerization. The β and γ chains associate with other components of the ECM [28].

Table 2.1: Functional Domains of Laminin

	Molecule or fragment	Structural features	Biologic functions
A. Whole laminin		Short arms 35 nm Long arms 76 nm Rich in α -D-mannopyranosyl residues	Promotes attachment, spreading, migration, growth, morphogenesis, and metastasis
B. Short arm domain		Globular end regions rich in α -D-galactosyl end groups May be composed of more than one type of chain	Binds to Type IV collagen Promotes cell attachment and spreading
C. Protease-resistant region of short arms		Disulfide bonded "knot" Rich in mannose-terminated oligosaccharide units	Contains laminin receptor-binding domain
D. Long arm		May contain alpha helix structure Protease labile	Binds heparin sulfate proteoglycan Promotes neurite growth

Adapted from [50]

2.5.2 Tissue Distribution of Laminin Isoforms and Receptors

Laminin, one of the major constituents of the BM [51-54] has been implicated in various ECM-regulated activities. Such activities include interaction with epithelial cells, stimulation and maintenance of tumor initiation and development [49]. All 15 laminin isoforms are constituents of BMs. Expression patterns of laminin isoforms are modulated both temporally and spatially within organisms [28]. This leads to distinct distribution of the different laminin isoforms during development and in adult tissues [21, 22, 28, 48]. Therefore the laminin isoforms fulfill precise key roles in modulating tissue structure and cell behavior [21, 28, 48].

Laminin 1 (111), the isoform that was first identified during development at E4.5 in mice, is the highly expressed type in the BM [22, 46]. Laminin-111 and laminin-511 are the main isoforms essential for embryonic development, whereas other isoforms are implicated during organ maturation and specific tissue functions [21]. The $\alpha 1$ chain, present in laminin 1 (111) and 3 (121), is highly expressed in epithelial cells during early embryogenesis. Its expression becomes more restricted during development and is then only found in adult reproductive organs, kidney and liver [28]. Laminin-111 has also been found in the chondrocytes of

healthy human cartilage [21]. Laminins 2 (211), 4 (221) and 12 (213) consist of the $\alpha 2$, which is mostly expressed in the neuromuscular system [21, 28], where they coordinate postsynaptic and presynaptic maturation [21]. The $\alpha 3$ chain, found in laminins 5 (332), 6 (311), and 7 (321), is localized to the skin and other epithelia. Laminin-332 plays a significant role in skin function. Furthermore, expression of this isoform has been observed in embryonic cartilage [21]. The $\alpha 4$ chain, found in laminins 8 (411), 9 (421), and 14 (423), is expressed in cells of mesenchymal origin. Laminin 8 together with laminin 10 (511), 11 (521) and 15 (523) are readily expressed throughout the body in adult epithelial, neuromuscular, and vascular tissues [28].

2.5.3 The Interaction of Laminin with Cell Surface Receptors

Integrins and non-integrin molecules are some of the major laminin cell surface receptors [28, 53]. More than eight integrins that have been identified include $\alpha 1\beta 1$, $\alpha 2\beta 1$, $\alpha 5v1$, $\alpha 3\beta 1$, $\alpha 6\beta 1$, $\alpha 6\beta 4$, $\alpha v\beta 3$, $\alpha v\beta 5$ and $\alpha 7\beta 1$ [28]. Each integrin is sequence-specific and thus recognizes and interacts with a specific set of isoforms. The recognition site located on the integrin receptor is formed by the combination of its α - and β -chains [28]. The G-domain at the C-terminal end serves as the major site for laminin cell adhesion [22]. Therefore, laminin-integrin interaction occurs substantially at the C-terminal end of the α -chain. However, such an interaction can also occur at the N-terminal end. The β - and γ -chains can also partake in laminin-integrin interaction [28]. Some of laminin interactions include α -dystroglycan with laminin $\alpha 1$ and $\alpha 2$ chains and the Lutheran blood group glycoprotein which interacts exclusively with laminin $\alpha 5$ chains [21]. Non-integrin cellular receptors for laminins include syndecans [21] and heparin sulphate proteoglycans [28]. Interaction of laminin with non-integrin receptors also occurs at the C-terminal of the α -chain [28].

2.5.4 Prominent Role of Laminins: Basement Membrane Assembly

Laminins play a critical role in providing structure to the ECM and adhesion of cells to the BM [22, 55, 56]. It has now been established that the precise manner in which alpha subunits interact with integrins or non-integrin receptors is essential for the self-assembly and polymerization of laminin networks [21]. This network assembling of laminin heterotrimeric laminins into oligomers is necessary for BM formation [21, 22, 57]. As already stated, the scaffold of enmeshed laminin and type IV collagen networks is the basic framework of BMs [22, 54, 58]. In the Golgi apparatus, ionic interactions enhance $\beta\gamma$ dimer formation, which is subsequently stabilized and secreted when the α -chain is included. Disulfide bridges provide stability for the three chains at their intersection point, thereby allowing laminin to self-assemble into a honeycomb-like polymer. The mechanism of self-assembly still remains elusive, but it appears to be calcium dependent and associated to the globular domain VI of each chain. It has also been proposed that the three-arm interaction model for laminin polymer self-assembly could be responsible for the honeycomb network [22, 28].

2.5.5 The Role of Laminin in Pathology: Tumor Invasion

Under physiological or pathological states, the ECM houses laminin fragments that are unable to polymerize into networks, consequently promoting cell migration as has been illustrated by laminin-332 [21]. Laminin 332 has been reported to partake in cell migration, and it has hence been implicated in tumor invasion [28, 50]. Highly expressed laminin $\gamma 2$ -chain has been noted in many epithelial human cancers such as lung and colon cancers. This high expression level of $\gamma 2$ -chain, particularly at the leading edges has been linked to cancer invasiveness. Moreover, the detection of this chain has been proposed to serve clinical diagnostic and prognostic purposes. Most of the $\gamma 2$ chains that were detected in tumor cells were positioned in the cytoplasm [28].

2.6 ELASTIN

Tissue flexibility and extensibility are critical properties in multicellular organisms [59]. Elastic fibers, the insoluble macromolecules of the ECM, are the key components of connective tissues [60, 61]. Elastic fibers provide resilience to connective tissues, which aids in long-range deformability. Moreover, passive-elastic recoil of connective tissues is another property provided by elastic fibers [59, 62]. These properties are essential for the long-term function of different forms of tissues. Elastic fibers comprise two morphologically and chemically distinct constituents namely elastin and microfibrils. About 90% of the fiber is constituted by elastin [62-64] which is on the internal core and is enclosed by microfibrils [59, 62]. The structure of elastin, with particular focus on the events that lead to formation of elastin are described in this section.

2.6.1 Elastin: A Protein Synthesized from Tropoelastin

Elastin is a chemically inert, highly insoluble polymer synthesized from a precursor molecule tropoelastin [60, 62, 63, 65]. Tropoelastin, a soluble, non-glycosylated and hydrophobic protein provides stability to elastin through its covalently cross-linked molecules. Tropoelastin is about 60-70 kDa and can exist as either an open globular molecule or a distended polypeptide [62]. Expression of this precursor molecule with subsequent elastin formation appears in fibroblast, vascular smooth muscles cells, endothelial cells and chondrocytes [63]. Elastin is classified as a major ECM tissue protein that is critically involved in tissue elasticity and resilience [62, 63, 65, 66].

2.6.2 Structural Properties of Elastin

Several studies have been undertaken to establish structural properties of soluble elastin, however, a consensus has not yet been attained. Macroscopically, elastin appears as a pale

yellow amorphous mass. Transmission electron and atomic force microscopy (TEM and AFM) studies have indicated that elastin is a fibrillar substructure composed of approximately 5nm thick filaments that are parallel-aligned and resemble a twisted rope. Circular dichroism (CD) is another study that has been done to illustrate that human tropoelastin consists of 3% α -helix, 41% β -sheet, 21% β -turn and 33% of other structures [62].

2.6.3 Elastogenesis: From Tropoelastin to Elastic Fibers

Formation of elastic fibers is a highly organized process that entails a chain of events. The interaction of microfibrils and tropoelastin during formation of elastic fibers is a process limited to foetal and early neonatal development [64]. These critical events include control of intracellular transcription and translation of tropoelastin, intracellular processing and secretion of the protein into the ECM. Moreover, the transport and alignment of tropoelastin at elastogenesis sites and conversion of tropoelastin to insoluble elastin polymer form part of elastogenesis events [62]. The process of elastogenesis is summarized in Figure 2.2.

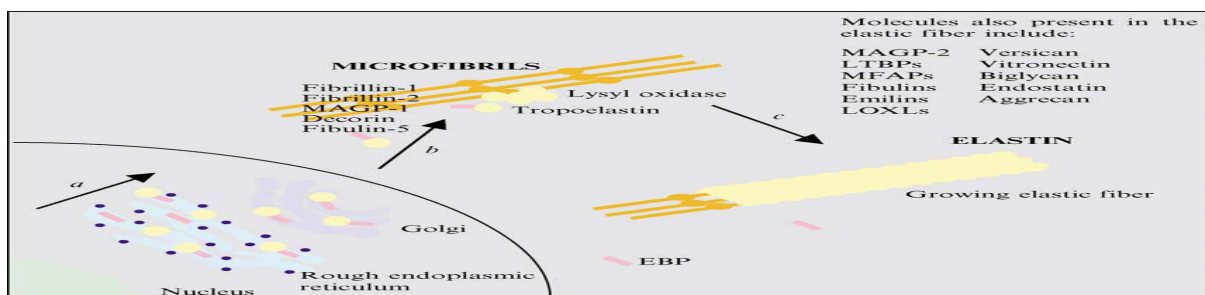


Figure 2.1: Classical Model of Elastogenesis. Tropoelastin is transcribed from a single gene and alternatively spliced in the nucleus. (A) Subsequent to translation and signal sequence cleavage, tropoelastin associates with EBP and FKBP65 in the rough endoplasmic reticulum. The tropoelastin-EBP complex then moves through the Golgi and gets secreted to the cell surface. (B) Secreted tropoelastin gets oxidized by a lysyl oxidase family member and tropoelastin associates with microfibrils and other tropoelastin molecules through coacervation to generate the nascent elastic fiber. (C) Continued secretion, oxidation and deposition of tropoelastin occupy the bulk of elastin synthesis. EBP-elastin binding protein; FKBP65-65-kDa FK506 binding protein; MAGP-microfibril associated glycoprotein; LTBP-latent transforming growth factor β -binding protein; MFAP-microfibril associated protein; LOXL-lysyl oxidase like. Source: [62].

2.7 FIBRONECTIN

Fibronectin (FN) is a complex glycoprotein associated with cellular interactions which involve inter-communication between cells and the extracellular material [67]. The active form of FN is an elongated protein assembled into an insoluble fibril [68]. The transformation of the FN molecule into a fibril is an extensively regulated cell-mediated process [68]. This section details biological and structural characteristics of fibronectin. The role fibronectin plays in cellular interactions and in tumorigenesis is also outlined.

2.7.1 Fibronectin: Brief Overview

Fibronectin is widely expressed by multiple cell types and it has been demonstrated that it is essential for development in vertebrates. Evidence of this has been provided in studies in which inactivation of the *FN* gene resulted in early embryonic lethality of mice [69]. This major ECM protein exists as an asymmetric dimer consisting of two identical subunits of approximately 250 kDa. These subunits are covalently bonded at a region close to the carboxyl-terminus by a pair of disulfide bonds [67-70]. Each monomer consists of three types of repeating units named type I, type II and type III [68-70]. The FN molecule contains 12; 2 and about 15 type I, type II and type III repeats, respectively. These repeats contribute to approximately 90% of the FN sequence [69]. Although FN molecules are derived from a single gene, the resulting protein can exist in multiple forms that arise from alternative splicing of a single pre-mRNA that can yield as many as 20 variants in human FN [68, 69].

2.7.2 Fibronectin: Constituent of the Plasma and the ECM

FN is an abundant soluble constituent of the plasma (300 µg/ml) and other body fluids. It also forms an insoluble constituent of the ECM [67, 69]. Moreover, the molecule is also scattered in the juxtacanalicular tissue (JCT) and in the trabecular beams [68]. Although FNs can be synthesized by a vast number of cells *in vitro*, fibroblasts and ECs appear to be the major

producers. Apart from fibroblasts and ECs, FNs can also be synthesized by chondrocytes, myoblasts, macrophages, hepatocytes, epithelial and amniotic cells [67]. Based on solubility traits, two types of FN termed plasma (pFN) and cellular (cFN) FNs have been identified. pFN exists as a soluble protein whereas cFN is a less-soluble form [67, 69, 70], that has the appearance of fibrillar extracellular matrix [69]. Although pFN and cFN can be distinguished, they have structural similarities [67]. pFN is synthesized predominantly in the liver by hepatocytes [67, 69], although ECs and macrophages could also contribute given their close association with the bloodstream [67]. Glucose, glucocorticoids, ascorbic acid and transforming growth factor beta-2 (TGF- β 2) are some of the factors that regulate FN expression in the trabecular meshwork (TM). TGF- β 2 also enhances cross-linking of FN to itself and the surrounding ECM through action of tissue transglutaminase. TGF-FN complex is resistant to degradation, and thus, self-cross-linking of FN may stimulate deposition and retention of FN in the ECM [68].

2.7.3 Fibronectin: A Mediator of Cellular Interactions

FNs have been implicated in a wide variety of cellular interactions with the ECM. Such interactions include cellular adhesion and morphology [18, 55, 67, 69, 70], cytoskeletal organization, cell migration, embryonic differentiation, oncogenic transformation, phagocytosis, chemotaxis and hemostasis or thrombosis [67]. Some of these cellular interactions are discussed below.

The adhesion of FNs to solid substrates is the most basic role of FNs that has been extensively studied [67]. Numerous studies have indicated that FNs promote the adhesion and spreading of cells to a variety of materials including plastic, collagen, gelatin, and fibrin [67, 69]. Cells that synthesize less or no FN often require additional exogenous FN to enhance adhesion and spreading. Inadequate synthesis of FN by these cells often results from their

oncogenic transformation. Concomitant with the spreading induced by an addition of FN, cells usually acquire highly ordered intracellular microfilament bundles [67]. The role of FN in phagocytosis was initially suggested on the basis of *in vivo* results which indicated that there is an association between the levels of pFN and the ability of an organism to clear unwanted material from the circulatory system. It was suggested that FN operates as a ‘non-specific opsonin’ for the reticulo-endothelial system. This became even more intriguing when it became apparent that FN has a binding affinity for certain bacteria such as *Staphylococcus aureus*. Data from *in vitro* studies also presented evidence that FN stimulates phagocytosis of gelatin-coated beads by certain macrophages although heparin is required as a cofactor [67]. Hemostasis and thrombosis are additional biological processes that particularly involve pFN. FN is also involved in the regulation of several pathways. It has been reported that FN induces myogenesis and inhibits myoblast fusion, chondrogenesis and melanogenesis. In addition to this, FN has also been reported to stimulate adrenergic differentiation in explanted neural crest cells [67]. Extensive literature from other cell types suggests that FN and its receptors provide mechanical support for cell attachment and mediate a wide variety of biological processes that entail regulation of outflow resistance, including matrix production, ECM turnover, gene expression, growth factor signaling and cytoskeletal organization. Moreover, FN and its receptors regulate cellular mechano-responsiveness to physical forces such as stretch [68].

2.7.4 Functional Domains of Fibronectin

The most important characteristic of FN is its ability to precisely interact with a wide variety of macromolecules. The best-established interactions which have been reported are the interactions with gelatin, collagens, fibrin, heparin and proteoglycans [67]. The ability of this molecule to perform so many functions is chiefly due to their flexible structure and functional domains [67, 68]. It has been shown that polypeptide regions of FNs are somewhat

susceptible to attack by a number of proteases. Such proteases cleave these polypeptide regions to generate separate, structured domains. composed of specific ligand binding sites [67]. The domains are briefly summarized below.

2.7.4.1 Collagen-Binding Domain

The first FN domain to be isolated was collagen-binding domain. This FN region is approximately 30-40000 daltons [67] and is composed of repeats I and II [69]. This region can be produced from digestion of an intact FN with chymotrypsin, subtilisin, thermolysin or pronase. Although this region is still unable to mediate cell interactions, it does interact with collagen or gelatin affinity columns [67]. Interestingly, such interactions are more effective with denatured collagen (gelatin) than are with native collagen. The presence of collagen-triple helix appears to play a significant role in FN-collagen interactions [69]. In addition, larger fragments can be generated under various proteolytic conditions which allow mapping of the domain close to the amino-terminus [67].

2.7.4.2 Cell-Binding Domain

This cell-binding region can be generated from other FN fragments that do not bind to collagen affinity columns. This domain exists for provision of other cell-binding activities. The region has the ability to mediate interaction between cells and collagen. A fragment of 15 000 daltons still retains a significant amount of the cell-binding activity of the intact FN, but does not allow either collagen or heparin binding [67].

2.7.4.3 Fibrin and Transglutaminase Interaction Sites

FN is also composed of two major fibrin-binding sites termed fibrin I and fibrin II [69]. The major site is located at the N-terminal domain and it is generated from type I, type 4 and type 5 repeats. The interaction of FN with fibrin is essential for cell adhesion or cell migration into

fibrin clots [69]. Initial stages of wound healing may therefore require binding of FN to fibrin from blood [67].

2.7.4.4 Glycosaminoglycan-Binding Domain

The binding of FN to heparin and heparin-sulphate is involved in the uptake of foreign substances by macrophages and in structural organization of the ECM. *In vitro* studies have indicated the complex nature of FN-heparin interactions with more than two constituents of moderate binding affinity. The molecule can have either two or three distinct regions that bind to heparin. One binding site is located in the FN amino-terminal domain. A second binding site is located near the C-terminus of the molecule. The presence of these multiple heparin-binding domains with their respective sensitivities to divalent cations and salt concentrations indicates that FN interactions are indeed complex [67].

2.7.4.5 Disulfides and Sulfhydryls

Analysis of FN fragments has indicated that its subunits are bound by inter-chain disulfides and are located near the carboxyl terminus of the molecule. Both the amino-terminal and the collagen-binding domains have a high degree of intra-chain disulfides. The amino-terminal domain has roughly 10% half cysteine and possibly 10 intra-chain disulfides. The intra-chain disulfides may be liable for the compact protease-resistant structure of this domain. The intra-chain disulfides of the collagen-binding domain are vital for collagen binding. In addition, every FN subunit is composed of more than one sulfhydryl group with one group located approximately 170 000 daltons from the amino-terminus and the other close to the carboxyl-terminus. Inhibition of FN interaction with the cell surface matrix often results if sulfhydryl groups are alkylated. There are possibilities that these sulfhydryls partake in inter-molecular disulphide bonding of FN to other FN molecules or to other cell surface components such as proteoglycans [67].

2.7.4.6 Heparin-Binding Domain

FN contains two major heparin-binding domains that have a binding affinity for heparin sulphate proteoglycans. Heparin II, the stronger heparin-binding domain is located at the C-terminus whereas the weaker binding domain, Heparin I, is positioned at the amino-terminal end of the protein. Heparin II has a high binding affinity for glycosaminoglycan and chondroitin sulphate, whereas Heparin I domain contains a *Staphylococcus-aureus*-binding site that mediates FN interactions with the bacterium. Heparin-binding domains of other cell types can induce cell adhesion [69].

2.7.5 Fibronectin Depletion: The Association with Tumorigenicity

Oncogenic transformation leads to pleiotropic changes in cellular properties. Such changes include decreased adhesion, rounded morphology and loss of cytoskeletal organization [67]. Studies have indicated that loss of FN is also concomitant with this oncogenic transformation [67, 71]. In some instances, an addition of FN can be used to revert such changes, thus it is possible that they reflect a common effect of the transforming agent. Reduced synthesis, reduced binding and increased rates of degradation are some of the factors that have been linked to loss of FN. Moreover, *in vivo* studies have indicated a relation between FN depletion and tumorigenesis [67]. These reports suggest that a correlation between FN depletion and acquisition of metastatic potential may exist. Given that FN is involved in the adhesion of cells to ECMs, tumor invasion and metastasis may induce a shift in the cellular function of FN [67].

2.8 LANGERHANS CELLS

In 1868 from a study of the human skin, dendritic leukocytes of the epidermis were first identified by a German clinician, Paul Langerhans [13, 72-74]. The study demonstrated that cells, which now bear his name, Langerhans, are non-pigmented cells with a dendritic

morphology [73, 74]. As time passed, it became apparent that Langerhans cells (LCs) do not only reside in the epidermis, but are also present in many other tissues, including the female genital tract. In electron microscopy, Birbeck granules contained within LCs serve as the key identifying feature of the cells [13, 73-75]. Initially, physiological knowledge of LCs was limited. However, culture systems that permit *in vitro* generation of mouse and human LCs are now enabling researchers to gain more insight on the physiology of LCs. *In vitro* production of Human LCs is currently obtained using either bone marrow progenitors cultured in granulocyte-macrophage colony-stimulating factor (GM-CSF), tumor necrosis factor (TNF) or blood monocytes cultured with GM-CSF [72, 76, 77].

2.8.1 Langerhans Cells: Regulators of Immune Responses

LCs are the principal cells that regulate immune surveillance [13, 77-79] of various mucosal barriers, including that of the reproductive tract [13]. In the female reproductive tract, LCs are hormonally controlled and their role is tightly regulated. LCs play an integral role in antigen acquisition and immune effector mechanisms. Moreover, the cells are involved in detection and response of the reproductive tract to invading pathogens such as causative agents of sexually transmitted infections [13]. Pathogen detection is made possible by the presence of Toll-like receptors and C-type lectins on LCs. Such receptors and lectins identify pathogen-associated molecular patterns such as constituents of the bacterial wall, or bacterial and viral nucleic acid motifs [77]. Conversely, LCs may also present a negative effect on the immune system. In one study, a reconstructed vaginal mucosa integrating Langerhans cells was developed to provide evidence that Langerhans cells support transmission of HIV-1 strains to peripheral blood mononuclear cells [80].

2.9 VASCULAR ENDOTHELIAL GROWTH FACTOR RECEPTOR

A closed circulatory system consists of a network of blood vessels essential for the development and maintenance of all tissues in the body [81]. Normal vasculature is architecturally structured to bring oxygen and nutrients to cells, allow for specific exchange of contents, and remove waste such as a urea and lactic acid in a streamlined, efficient manner [7, 81-83]. Vasculogenesis, the emergence of these blood vessels, is one of the earliest events in embryogenesis during which mesodermal cells differentiate into hemangioblasts [83, 84]. Vasculogenesis is completed with the formation of the primary vascular plexus, and all further transformations and maturation of the vascular network proceed during angiogenesis [83].

2.9.1 Angiogenesis: Modulator for Physiological and Pathological Processes

Angiogenesis, a complex process of new blood vessel formation from pre-existing vascular networks [81, 83, 85-88], is critical for the development and maintenance of any living tissue [7]. Angiogenesis is closely regulated by a balance between factors that stimulate and factors that inhibit the development of new vasculature [87, 89]. Angiogenesis is essential for both physiological and pathological processes [87, 90]. In healthy adults, the levels of angiogenic factors are in equilibrium and ECs are mostly quiescent [85, 87]. Under such circumstances, angiogenesis is restricted to certain processes such as wound healing, development and reproduction. Nonetheless, under pathologic states such as tumor growth, progression and metastasis [81, 82, 87, 89], rheumatoid arthritis, and atherosclerosis [81, 87], pathologic angiogenesis comes into play [81, 82, 87]. During pathologic angiogenesis, the balance of pro- and anti-angiogenic factors is shifted such that the production of pro-angiogenic factors outweighs anti-angiogenic factors, resulting in new blood vessel formation [85, 87, 89]. Increased blood vessel formation provides tumors with oxygen and nutrients which enable

the growth and progression of tumors [81, 87]. Angiogenic factors responsible for this shift include hypoxia, activated oncogenes and metabolic stress [86].

During the past two decades, extensive studies have indicated that several factors including vascular endothelial growth factor (VEGF), angiopoietin and ephrins are major contributors of blood vessel formation [91]. Among these pro-angiogenic factors, the VEGF family proteins and receptors have been the center of interest. They have thus, been extensively characterized due to their prominent role as angiogenesis mediators [7, 81, 85]. This section proceeds by describing VEGF-VEGFRs and their role in angiogenesis and vasculogenesis

2.9.2 VEGF Family and Receptors

Vascular endothelial growth factor (VEGF) is a homodimeric glycoprotein with a molecular weight of 34-45 kDa [85, 86]. VEGF, also known as vascular permeability factor (VPF) [7], undergoes alternative splicing to yield mature proteins of 121, 165, 189 and 206 amino acids [85]. The VEGF family consists of 7 secreted glycoproteins: VEGF-A, VEGF-B, VEGF-C, VEGF-D, VEGF-E, VEGF-F and placental growth factor (PlGF) [81, 85, 86]. All members except VEGF-E and svVEGF are encoded in the mammalian genome [81]. Three high-affinity VEGF tyrosine kinase receptors that have been identified include VEGF receptor (VEGFR)-1 (flt-1), VEGFR-2 (flk-1/KDR) and VEGFR-3 (flt-4) [81, 83, 86, 91]. These receptors belong to the superfamily of receptor tyrosine kinases (RTKs) [83]. Based on structural features, these receptors are highly homologous to each other [83, 85, 87, 91]. VEGFR-1 and VEGFR-2 consist of 1338 and 1356 amino acids in humans, respectively [91]. Furthermore, VEGFR-1 and VEGFR-2 consist of 7 extracellular immunoglobulin-like domains (Ig 1-VII) [81, 83, 85, 91], a single transmembrane protein, and a consensus tyrosine kinase (TK) domain, which is interrupted by an inter-kinase insert to yield TK-1 and TK-2 fragments [83, 85, 87]. VEGFRs have an additional downstream carboxy terminal region

[87, 91]. The different VEGF family members have distinct binding affinities for their respective receptors [84, 85]. All VEGF-A isoforms bind to VEGFR-1 and VEGFR-2, whereas PIGF1, PIGF2 and VEGF-B have a binding affinity for only VEGFR-1. VEGF-C and VEGF-D bind to VEGFR-2 and VEGFR-3, whereas VEGF-E has a specific binding affinity for VEGFR-2 [85].

2.9.3 Expression and Differential Roles of VEGFs and VEGFRs

2.9.3.1 VEGF-A: A Key Mediator for Angiogenesis

In vivo experiments have demonstrated that VEGFs play a crucial role in physiologic vasculogenesis and angiogenesis [85]. Moreover, VEGFs are also involved in inflammatory processes [83] and other pathologic conditions such as arthritis, diabetic retinopathy and psoriasis [83, 85]. VEGF expression is triggered by hypoxia. This has been demonstrated by a highly expressed VEGF mRNA under conditions of low oxygen in pathological cases. Furthermore, VEGF expression is enhanced by a wide range of factors that include epidermal growth factor (EGF), transforming growth factors (TGF α and TGF β), insulin-like growth factor 1 (IGF-1), fibroblast growth factors (FGF) and platelet derived growth factors (PDGF) [83].

VEGF-A is a major regulator for angiogenesis that interacts and stimulates two tyrosine kinase receptors VEGFR-1 and VEGFR-2 [84]. It has been reported that VEGF-A is over-expressed in many human solid tumors [83, 85], which ultimately induces new blood vessel formation in the growing tumor [83]. Tumor vessels are readily permeable, and this allows tumor cells to penetrate their surrounding vascular networks and metastasize to other organs [83]. This is associated with tumor progression and poor prognosis [85].

2.9.3.2 The Initial Expression of the VEGF Receptors

During murine development, the expressions of both VEGFR-1 and VEGFR-2 are initially detected at E7.5 in mesodermal cells of the tail region [91]. At E7.5-8.0, VEGFR-2 positive cells migrate to the head region and yolk sac, and differentiate into primitive ECs [91]. Hematopoiesis is initiated when ECs create blood islands at yolk sac [91]. Interestingly, VEGFR-1 and VEGFR-2 have also been detected in both liquid and solid tumor cells [84]. Gene targeting studies in mice have indicated that VEGFs and VEGFRs play a role in development of a vascular system [84]. In these studies, VEGF appears particularly important because loss of even a single *Vegf* allele results in embryonic lethality at days 11 to 12 [84]. *Vegfr2^{-/-}* mice die at embryonic days 8.5 to 9.5 due to defect in the development of hematopoietic and ECs resulting from impaired vasculogenesis [84]. Moreover, members of the VEGF family are involved in other biological processes, including lymphangiogenesis, vascular permeability, and hematopoiesis [84].

2.9.3.4 VEGFR-1: A Negative Regulator for Angiogenesis and a Positive Regulator of Macrophage Functions

Initially, VEGFRs were reported to be expressed exclusively on various ECs [85]. However, emerging evidence indicates that VEGFRs are also expressed by other cell types including tumor cells [85]. In addition to ECs, VEGFR-1 is also expressed by macrophages, monocytes, hematopoietic stem cells and certain non-endothelial cells [81, 84]. VEGFR-1 and VEGFR-2 play a role in physiological and pathological angiogenesis [84]. In early embryogenesis, the soluble form of VEGFR-1 acts as a negative regulator of VEGF-A by inhibiting VEGF-A and VEGFR-2 interaction [84]. This antagonistic action is essential to maintain equilibrium for an appropriate level of angiogenesis [84, 91]. The role of VEGFR-1 as a negative regulator of VEGF-A has been established from data of gene activation experiments in which *Flt1^{-/-}* mice died between 8.5 and 9.5 days of embryonic development

due to excessive growth and disorganization of blood vessels [84]. VEGFR-1 induces tumor growth, metastasis, and inflammation in partly a macrophage-dependent manner [91]. This receptor interacts with its ligands to initiate dimerization followed by trans/autophosphorylation of tyrosine residues at the cytoplasmic kinase domain. However, autophosphorylation of VEGFR-1 by VEGF-A is weak [83]. It has been suggested that VEGFR-1 is mainly a negative regulator of the activity of VEGF-A on vascular endothelial cells rather than mitotic signal transduction. This suggestion was based on structural peculiarity of VEGFR-1 as its soluble form produced by alternative splicing [83]. This form is not a transmembrane protein and has no tyrosine kinase domain, thus its inability to transduce a signal. VEGFR-1 also plays a role in blood vessel permeability [83]. VEGFR-1 mediates monocyte migration, recruitment of EC progenitors, hematopoietic stem cell survival and release of growth factors from liver ECs [84].

2.9.3.5 VEGFR-2: A Key Receptor for Angiogenesis

From the postnatal to adult stages, VEGFR-2 is readily expressed in ECs [84, 91]. In endothelial cells, VEGF-A stimulates VEGFR-2 gene expression via a positive feedback mechanism [91]. In addition to that, this receptor is expressed in a fraction of hematopoietic cells which may be the progenitor for ECs [84, 91]. However, the level of expression is significantly lower than that found in ECs, thus, it is inconclusive whether low VEGFR-2 levels in hematopoietic cells could have any biological impact [91]. A low VEGFR-2 expression is also observed in neuronal cells, osteoblasts, pancreatic duct cells, and progenitor cells. Biological role of VEGFR-2 in these non-endothelial cells remains unclear [91]. In tumor vasculature, VEGFR-2 expression is 3-5-fold higher than in normal vasculature [91].

VEGFR-2 has now been accepted as the main mediator of VEGF-A biological activity [83]. VEGFR-2 is actively involved in both embryonic angiogenesis and hematopoiesis [83]. Mice

with an inactive gene *flk1* die between 8.5 and 9.5 days of embryonic development [83]. The death of the animals results from disturbed vasculogenesis, as well as lack of EC differentiation and hematopoiesis [83]. Activation of VEGFR-2 stimulates a number of signal transduction pathways that induce mitogenesis, migration and survival of ECs [83]. This has been confirmed from *in vivo* studies in which inactivation of VEGFR-2 inhibited angiogenesis whereas activation of the receptor had an opposite effect [83]. In addition to that, VEGF-E, which interacts exclusively with VEGFR-2 induced cell proliferation and formation of tubular structures in endothelial cells *in vitro* and stimulated *in vivo* angiogenesis [83].

2.9.3.6 VEGFR-3: The Lymphangiogenesis Key Receptor

The expression of VEGFR-3 occurs during late stages of embryonic development. This receptor is mainly restricted to the lymphatic system endothelium [83, 84]. It regulates lymphangiogenesis [83, 84], a process that becomes selectively affected when the intracellular signaling pathways associated with this receptor are disturbed [83].

2.10 IMMUNOHISTOCHEMISTRY: A POWERFUL DIAGNOSTIC TOOL

The introduction of immunochemical techniques in routine pathology laboratories has enabled pathologists to improve their diagnostic abilities. Immunohistochemistry (IHC) is a crucial and powerful diagnostic tool that serves to identify and localize distinct antigens in tissues or cells based on antigen-antibody recognition [92-94]. Immunohistochemistry also termed immunocytochemistry seeks to exploit the specificity that occurs during the interaction of an antibody with its antigen-antigen at a light microscopic level [92]. This technique does not only enable detection of abnormal tissues, but it also enables pathologists to determine the immunophenotype of normal cells and neoplastic counterparts [93]. Immunohistochemistry is a critical tool in illustrating tumor cell lineage and metastasis.

Moreover, immunohistochemical semi-quantitative data is often used in the identification and illustration of prognostic and predictive markers [92]. This means that immunohistochemical staining may have therapeutic implications in various diseases.

2.10.1 Immunohistochemical Stain: More than just a special Stain

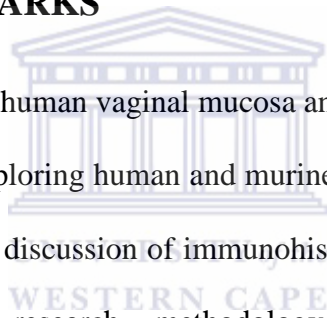
As emphasized by pioneers in the field of functional morphology, the primary objective of all staining techniques is to identify micro-chemically the existence and distribution of components that have already been identified macro-chemically. The basic critical principle of special stains, including immunohistochemical stains, is a sharp visual localization of target components in cells or tissues, based on satisfactory signal-to-noise ratio [92]. Over the years, several technical developments have led to the extensive use of immunohistochemistry today. In surgical pathology laboratories, antigens can now be successfully demonstrated in routinely processed formalin-fixed paraffin-embedded (FFPE) tissues [92, 95]. The enzymatic label (horseradish peroxidase) with a suitable chromogenic substrate allows visualization of the labelled antibody by light microscopy. A rapid growth of commercially available antibodies and the on-going refinement of immunohistochemical tools contribute towards the pivotal role of immunohistochemistry in medical diagnostic procedures. Moreover, demands for improved reproducibility and quantification have made researchers aware that immunohistochemistry can be 'more than just a special stain'. If all immunohistochemical processes are sufficiently monitored, the technique can provide tissue-based immune-assay with reproducibility and quantitative features similar to those of an enzyme-linked immunosorbent assay (ELISA) test. This means that not only will the protein or antigen be detected, but an accurate and reliable amount of that particular antigen will be measurable [92].

2.10.2 IHC Detection Systems

Various IHC methods have been established to achieve greater sensitivity during the staining of FFPE tissues. The methods range from a one-step direct conjugate detection system to multiple-step detection systems such as peroxidase anti-peroxidase (PAP), avidin-biotin conjugates (ABC) and biotin-streptavidin (B-SA). The main methods of immunostaining that are readily used include direct, indirect, alkaline phosphatase, peroxidase-anti-peroxidase and avidin-biotin methods [93]. In the study, the indirect conjugate (sandwich) method was used. It is a relatively simple modification of the direct conjugate method [92].

2.11 CONCLUDING REMARKS

Chapter 2 outlined the biology of human vaginal mucosa and the value of athymic nude mice. The chapter was continued by exploring human and murine markers under investigation. The chapter was concluded by a brief discussion of immunohistochemistry. Chapter 3 will give a detailed description of the research methodology, including a procedure for immunohistochemistry.



CHAPTER THREE

MATERIALS AND METHODS

3.1 ETHICAL APPROVAL

This study is a follow-up of two previous MSc research studies conducted separately by Wang [5] and Kok [6] for which prior ethical approval had been granted by the University of Stellenbosch and the University of the Western Cape (Reference Numbers N09/10/271 and N05/04/061). This study is partly a validation and partly a further investigation of the tissue characteristics of a novel in-vivo research model. It verifies the results and introduces enlightening statistics on the interpretation of the staining intensities of tissue preparations reported previously by Kok [6].

3.2 EXPERIMENTAL DESIGN – PART 1: TISSUE PREPARATION

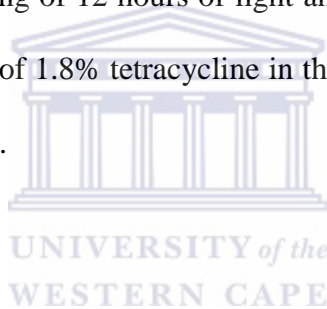
3.2.1 Cyst Production

Human vaginal mucosa was obtained from Tygerberg Hospital (Cape Town, South Africa) in a study conducted by Wang and Hille [5]. The vaginal mucosa had been removed during corrective procedures. A carrier medium containing 10% foetal calf serum (Delta Bioproducts, SA); minimum essential medium; streptomycin, penicillin and amphotericin- β was used to transport vaginal mucosa to the laboratory. In the laboratory, vaginal mucosa was divided twice, one portion served as a control for immunohistochemical examination whereas the other portion was used to produce experimental cysts. From the latter portion, the epithelium and its underlying connective tissue were separated with extreme caution in order to avoid injury to vaginal epithelium. Moreover, this was done to enhance successful separation of the epithelium from the connective tissue. Epithelial fragments of

approximately 8 X 4 mm in size were prepared. A glass ball of 2 mm in diameter was placed on each epithelial fragment and the tissue was sutured around the glass ball with DexonR (DG American Cyanamid Company, USA). A total of 24 cysts were prepared. Stringent infection control measures were also applied to reduce potential bacterial infection of vaginal epithelium.

3.2.2 Athymic Nude Mice

Male athymic mice aged 4-6 weeks were obtained from the Animal House at the University of Cape Town (Cape Town, South Africa). The animals were housed in pathogen-free isolators under controlled conditions of light and humidity. The temperature was maintained at 26°C and a light cycle consisting of 12 hours of light and 12 hours of darkness. The mice were provided with a suspension of 1.8% tetracycline in their drinking water. Sterilized mice feed was also provided *ad libitum*.



3.2.3 Cyst Xenografts

The cysts were xenografted into the dorsal neck region of immune-deficient mice using a trocar. Only one cyst was implanted per animal. Successful integration of newly implanted experimental cysts in host nude mice was achieved 9-weeks post implantation. During the 9-week period, terramycin and/or gentamicin were administered to the animals to minimize the high risk of infection associated with xenografts.

3.2.4 Cyst Retrieval

After a 9-week period, the implanted cysts were harvested from the animals. The animals were anaesthetized with a mixture of fentanyl and hypnodil. Surgical procedures were performed under sterile conditions. The cysts were fixed in buffered formalin, routinely processed and embedded in paraffin wax for subsequent use. Cysts with a morphologically

intact vaginal epithelium, a conspicuous adjacent stroma and no illustrations of infection were used. Cysts that were ruptured with excessive inflammation and signs of infection were excluded. As a result of the above mentioned selection criteria, only 10 cysts were in conditions suitable for experimental purposes. In this study, the phrases 'normal vaginal tissues' and 'xenografted vaginal tissues' refers to original tissues and their paired implanted cysts, respectively.

3.3 EXPERIMENTAL DESIGN – PART 2: IMMUNOHISTOCHEMISTRY

3.3.1 Principle

As already stated in Chapter 2, immunohistochemistry is a technique used for localizing specific antigens in tissues or cells based on antigen-antibody recognition [92]. This method exploits the specificity provided by antibody-antigen interaction at a light microscopic level. The basic critical principle of immunohistochemistry is a sharp visual localization of target components in a cell and tissue, based on satisfactory signal-to-noise ratio [92]. In daily practice, satisfactory results are obtained by amplifying the signal while simultaneously reducing specific background staining. In this study, indirect conjugate (sandwich) detection system was used to localize human and murine markers in normal vaginal tissues and xenografted vaginal tissues. In this method, the primary antibody that has specificity against the antigen in question (e.g., rabbit anti-mouse antibody) was added to a vaginal tissue section, and excess antibody was rinsed off. The labeled secondary antibody, which has specificity against the antigen on the primary rabbit antibody, was then added. Adding a secondary antibody is important for labeling sites on the tissue that express the primary antibody, which, in turn, is bound to the antigen [92].

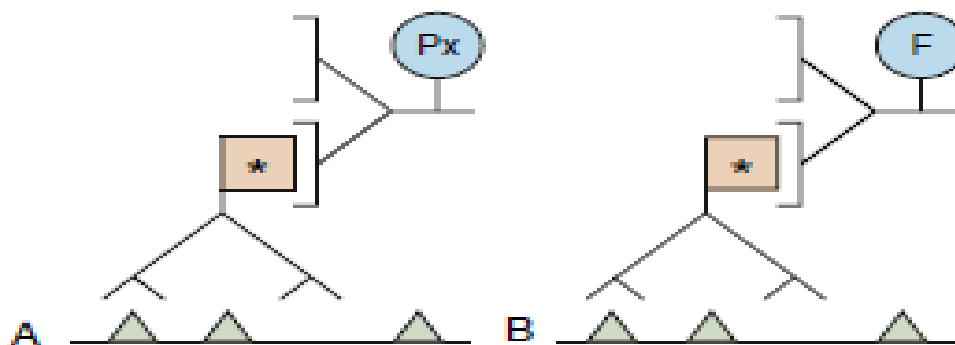


Figure 3.1: Indirect Conjugate (Sandwich) Method. The primary antibody is unlabeled. The method uses a labeled secondary antibody, having specificity against the primary antibody. Boxed-Antigen determinant on primary antibody; Px-Peroxidase label; F-Fluorescein label. Source: [92].

3.3.2 Antibodies

Mouse anti-human primary antibodies raised against 10 human antigens were used. Human primary antibodies used were; anti-cytokeratin 1, anti-cytokeratin 5, anti-cytokeratin 13, anti-cytokeratin 14, anti-collagen type IV, anti-laminin, anti-elastin, CD1a, anti-fibronectin and anti-VEGFR-3 (Leica Microsystems, SA). Rabbit anti-mouse primary antibodies raised against 6 mouse antigens were also used. The primary antibodies directed against mouse antigens included anti-collagen type IV, anti-laminin, Langerin, anti-fibronectin and anti-VEGFR-2 (Biocom Biotech CC, SA).

Table 3.1: Rabbit Anti-Mouse Antibodies used for Immunohistochemical Analysis of Murine Markers

Antibody Reference Code	Specificity	Dilution	Antigen Retrieval Method
C7510-50S	Collagen type IV	1:100	EDTA/Citrate Buffer Solution
LS-C25107	Laminin	1:100	EDTA/Citrate Buffer Solution
F4215-46	Fibronectin	1:100	EDTA/Citrate Buffer Solution
LS-C735	Langerhans cells	1:100	EDTA/Citrate Buffer Solution
V2100-17C2	VEGFR-2	1:50	EDTA/Citrate Buffer Solution

Table 3.2: Mouse Anti-Human Antibodies used for Immunohistochemical Analysis of Human Markers

Antibody Reference Code	Specificity	Dilution	Antigen Retrieval Method
NCL-CK1	Cytokeratin 1	1:20	EDTA Buffer Solution
NCL-CK5	Cytokeratin 5	1:100	EDTA/Citrate Buffer Solution
NCL-CK13	Cytokeratin 13	1:100	EDTA Buffer Solution
NCL-LL002 CK14	Cytokeratin 14	1:20	EDTA Buffer Solution
NCL-COLL-IV	Collagen type IV	1:100	Enzyme Digestion
NCL-LAMININ	Laminin	1:100	Enzyme Digestion
NCL-ELASTIN	Elastin	1:100	Enzyme Digestion
NCL-FIB	Fibronectin	1:100	Enzyme Digestion
NCL-CD1A-235	Langerhans cells	1:15	EDTA/Citrate Buffer Solution
NCL-L-VEGFR-3	VEGFR-3	1:50	EDTA/Citrate Buffer Solution

3.3.3 Procedure

Formalin-fixed, paraffin embedded blocks were cut into 3 μm sections. The sections were mounted on positively charged slides coated with Poly-L-Lysine solution (Sigma Aldrich, Pty Ltd, SA) and incubated overnight at 26°C. The first step involved dewaxing (deparaffinizing) tissue sections in xylene for 5 minutes, followed by immersing them in decreasing grades of alcohol for 2 minutes with each alcohol. 2X 100% alcohol, 2X 96% alcohol and 1X 70% alcohol were used. Sections were washed in water (H_2O) for 4 minutes and distilled water (dH_2O) for 2 minutes. Human antigen retrieval using anti-cytokeratin 1, anti-cytokeratin 13 and anti-cytokeratin 14 antibodies was performed using ethylene diamine tetracetic acid (EDTA) based buffer of pH 9.0 at 100°C for 10-15 minutes. Human antigen retrieval using anti-cytokeratin 5; CD1a and anti-VEGFR-3 antibodies was performed using citrate buffer of pH 6.0 at 100°C for 10-15 minutes. Human antigen retrieval using anti-collagen type IV; anti-laminin, anti-elastin and anti-fibronectin antibodies was performed using pepsin digestion method at 37°C for 30 minutes. All mouse antigens were retrieved using EDTA based buffer of pH 9.0 at 100°C for 10-15 minutes. A summarized version of the methods used for antigen retrieval is indicated on Table 3.1 and Table 3.2. Sections were washed in phosphate buffer solution (PBS), immersed in 3% hydrogen peroxide (H_2O_2) to block endogenous peroxidase activity, and washed again in PBS. Subsequent blocking was done with normal rabbit serum of 1:20 dilution for 20 minutes. Excess PBS was drained off and

tissue slides were dry-blotted to prevent further dilution of antibodies in PBS during incubation. Excess PBS was also removed to enhance optimum binding of antibodies. Sections were incubated with 250 μ l primary antibodies at room temperature for 30 minutes and rinsed in PBS for 2 minutes. Sections were then incubated with 300 μ l biotinylated secondary link antibodies at room temperature for 30 minutes and rinsed in PBS. Further incubation of sections was done with 300 μ l streptavidin horse radish peroxidase (HRP) at room temperature for 30 minutes. A chromogen substrate consisting of 1 ml substrate buffer and 50 μ l 3,3-diaminobenzidine (DAB) was added to each section. Sections were incubated at room temperature for 10 minutes, rinsed in water for 2 minutes and immersed in hematoxylin for 25 seconds. Sections were dehydrated using an increasing grade of alcohols by dipping sections 10 times per alcohol. Increasing grades of alcohol used were 1X 70% alcohol, 2X 96% alcohol and 2X 100% alcohol. Slides were rinsed with 2X xylene to ensure complete dehydration. A small drop of DPX mountant (glue) (Sigma Aldrich, Pty Ltd, SA) was placed on each cover slip and stained sections were subsequently mounted onto cover slips. Sections were left to air dry before being analyzed.

3.3.4 Light Microscopy

Tissue sections were analyzed by brightfield using 10X, 20X and 40X objectives of Nikon Eclipse 55! microscope (Nikon Instruments, Inc.). Images were taken using NIS Elements (Nikon Instruments, Inc.) software and Nikon Digital Sight DS-U2 camera (Nikon Corporation). Immunohistochemical structures of interest such as the epithelium, basement membrane and stromal layer were assessed on each tissue section. Sections were scored according to a scale explained in the next section.

3.3.5 Scoring Criteria

Following immunohistochemical staining of normal tissues and xenografted tissues, staining intensity of markers was assessed along the epithelium, the basement membrane and stromal layer. Staining intensity for each tissue was scored according to a semi-quantitative scoring system stipulated on Table 3.3 and Table 3.4. Semi-quantitative scoring procedure was performed in triplicate. Tissue sections were awarded a score of between 0 and 4 for all human and murine markers except for collagen IV and laminin which could only be awarded a maximum score of 3.

Table 3.3: Immunohistochemical Scoring Criteria for Human and Murine Markers

IHC Score	Description of the IHC Score
0	Negative Staining (No Positively Stained Cells)
1	Very Few Positively Stained Cells (10-25%)
2	Rare Positive Staining (25-50%)
3	Strong, Non-Uniform Positive Staining (50-75%)
4	Strong, Uniform Positive Staining (>75%)

Table 3.4: Immunohistochemical Scoring Criteria for Collagen IV and Laminin

IHC Score	Description of the IHC Score
0	Negatively Stained Basement Membrane
1	Rare Positively Stained Basement Membrane
2	Strong, Interrupted Stained Basement Membrane
3	Strong, Uniformly Stained Basement Membrane
4	

In selected cases, immunohistochemical scores staining scores were recorded by two independent observers before final scores could be established. This was done to ensure that optimum scores were used for statistical analysis.

3.4 STATISTICAL ANALYSIS

Staining intensities were statistically analyzed using GraphPad Prism5.0 (GraphPad Software, Inc). Firstly, Normality tests were performed to determine whether or not the data was sampled from a Gaussian distribution. Since the data was not normally distributed, repeated-measures one-way ANOVA with subsequent non-parametric Friedman's test was used to compare mean staining intensity of the paired vaginal tissues. Since Friedman's test ranks values in each row, it is not affected by sources of variability that may equally affect all values in a row. This matched test was therefore chosen to control experimental variability between tissue sections, and thus enhancing the power of the test statistic. Dunn's post-test was chosen to make further multiple comparisons between normal and xenografted vaginal tissues. Scores reported from Kok's study were also statistically assessed. A significance level of $P < 0.05$ was used for all tests and comparisons. All comparisons were conducted in triplicate to avoid statistical errors. Results were expressed in terms of mean \pm standard error of mean (SEM).

3.5 POSITIVE CONTROLS

In order to ascertain immunohistochemical staining results, positive controls that were processed in-house by Kok [6] were used in the current study.

3.5.1 Positive Human Tissue Controls

Seven human surgical tissues were used as positive controls (Table 3.5). The tissues had been obtained from the Division of Anatomical Pathology of the national health laboratory service (NHLS) (Tygerberg Hospital, Cape Town, South Africa).

Table 3.5: Positive Human Control Tissues Used for Validation of IHC Staining

Mouse Anti-Human Antibody	Antibody Reference Code	Positive Control Tissue
Cytokeratin 1	NCL-CK1	Human Skin
Cytokeratin 5	NCL-CK5	Human Prostate
Cytokeratin 13	NCL-CK13	Human Tonsil
Cytokeratin 14	NCL-LL002 CK14	Human Skin
Collagen Type IV	NCL-COLL-IV	Kidney/Basement Membrane
Laminin	NCL-LAMININ	Kidney/Small Intestine
Elastin	NCL-ELASTIN	Kidney/Small Intestine
Fibronectin	NCL-FIB	Normal Kidney
CD1a (Langerhans Cells)	NCL-CD1A-235	Human Skin
VEGFR-3	NCL-L-VEGFR-3	Human Placenta

3.5.2 Positive Mouse Tissue Controls

Two athymic nude mice obtained from the Animal House at the University of Cape Town (Cape Town, South Africa) had been used to process mouse tissues that served as positive controls. The mice had been dissected by Kok [6] at the division of Anatomical Pathology of the NHLS (Tygerberg Hospital, Cape Town, South Africa).

Subsequent tissue fixation had been performed at the division of Anatomy and Histology of the NHLS (Tygerberg Hospital, Cape Town, South Africa). Table 3.6 lists mice tissues that served as positive controls for IHC staining.

Table 3.6: Positive Mouse Control Tissues Used for Validation of IHC Staining

Rabbit Anti-Mouse Antibody	Antibody Reference	Positive Control Tissue
Collagen Type IV	C7510-50S	Mouse Kidney / Liver
Laminin	LS-C25107	Mouse Skin / Liver
Fibronectin	F4215-46	Mouse Skin / Liver
Langerhans Cells	LS-C735	Mouse Lung / Skin
VEGFR-2	V2110-17C2	Mouse Pancreas / Kidney

3.6 NEGATIVE CONTROLS

Negative tissue controls were included in the study to confirm the specificity of the immunohistochemical test and to assess the presence of non-specific background staining. Negative controls used had also been prepared in a previous study by Kok [6]. Normal human vaginal mucosa was used as a negative control. This step was important to substantiate the specificity of mouse antigen markers as well as to exclude cross reactivity with human antigens.

3.6.1 Negative Tissue: Control 1

The 1st negative control was a tissue section in which rabbit anti-mouse antibody was replaced with PBS. This was done to identify any false positive results.

3.6.2 Negative Tissue: Control 2

The 2nd negative control was incubated with a primary antibody and biotinylated secondary antibody and streptavidin HRP were replaced with PBS. The second control was included to verify negative staining of antigens.

3.7 ACCRONYMS USED IN THE STUDY

The acronyms NVT and XVT shall be used to denote normal vaginal tissues and xenografted vaginal tissues, respectively. NVT^a and XVT^a will denote normal and xenografted vaginal tissues of the previous study, respectively. The letters –h and –m will denote localization of human and mouse antigens (markers) respectively.

CHAPTER FOUR

RESULTS

4.1 HUMAN CYTOKERATIN 1 EXPRESSION PROFILE

4.1.1 Immunohistochemical Scores for Cytokeratin 1

Varied staining patterns of Cytokeratin 1 (CK1) were observed along the epithelium in both normal and xenografted vaginal tissues. All normal tissues displayed a moderate to strong positive staining of CK1. Weak reactivity patterns were seen in 6 of 10 xenografted tissues whereas the remaining 4 of 10 tissues stained negatively for CK1 (Table 4.1).

Table 4.1: Immunohistochemical Scoring of Human Vaginal Mucosa for Cytokeratin 1. Scores reflect the difference in the staining intensity between normal vaginal tissues and xenografted vaginal tissues. Mouse anti-human monoclonal antibody raised against cytokeratin 1 antigens was used in both tissues.

Tissue Reference No.	Immunohistochemical Score	
	<u>Normal Vaginal Tissue</u> NCL-CK1 Ab	<u>Xenografted Vaginal Tissue</u> NCL-CK1 Ab
15392/06	2	0
15396/06	4	0
16173/06	2	1
16175/06	4	1
16176/06	4	2
8960/06	3	0
8961/06	3	2
10156/06	4	1
17559/06	4	1
17560/06	4	0

*Scoring System; 0-Negative Staining; 1-Poor Staining (10-25%); 2-Rare Positive Staining (25-50%); 3-Some Positive Staining (50-75%); 4-Strong Uniform Positive Staining (>75%).

NCL-CK1 - Reference Code for Human Cytokeratin 1 Antibody; Ab - Antibody.

4.1.2 Statistical Comparisons of Cytokeratin 1 Staining Intensities

Mean staining intensities for cytokeratin 1 in NVT, XVT, NVT^α and XVT^α were 3.4±0.2667, 0.8±0.2494, 3.8±0.2000 and 1.3±0.3350, respectively. Repeated-measures one-way ANOVA with subsequent Friedman's test (Friedman Statistic=27.69) showed significant differences in the staining intensities between the tissue groups (P<0.0001). Dunn's post-test for multiple comparisons of the groups showed significant differences between NVT and XVT, NVT^α and XVT^α (P<0.05). A high significant difference was noted between NVT^α and XVT (P<0.05).

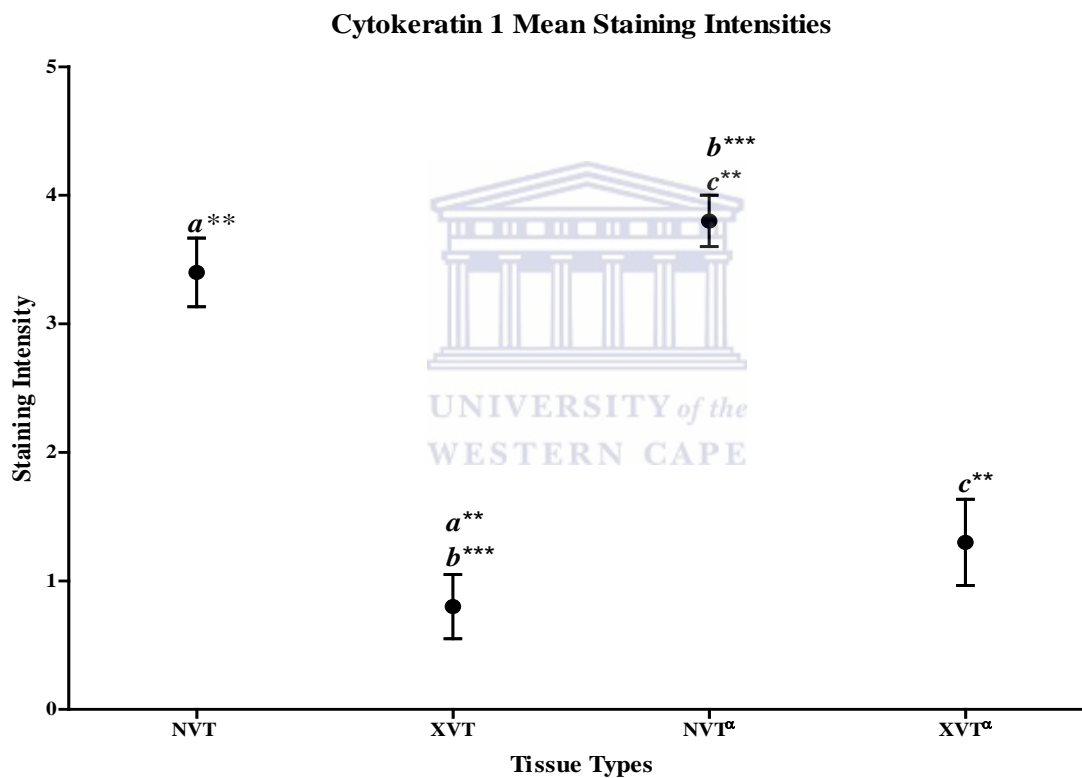


Figure 4.1: Mean Cytokeratin 1 Staining Intensity by Vaginal Mucosal Type. Data is expressed as mean ± standard error of mean (n=10). Friedman's test indicates that tissue types are significantly different (P<0.0001). Dunn's post test specifies tissue types that are significantly different (P<0.05) as denoted by similar alphabets.

NVT-Normal Vaginal Tissue; XVT-Xenografted Vaginal Tissue; ^αCorne Kok-Unpublished Work.

*Significant; **Very Significant; ***Extremely Significant

4.1.3 Photomicrographs of Vaginal Mucosae Stained for Cytokeratin 1

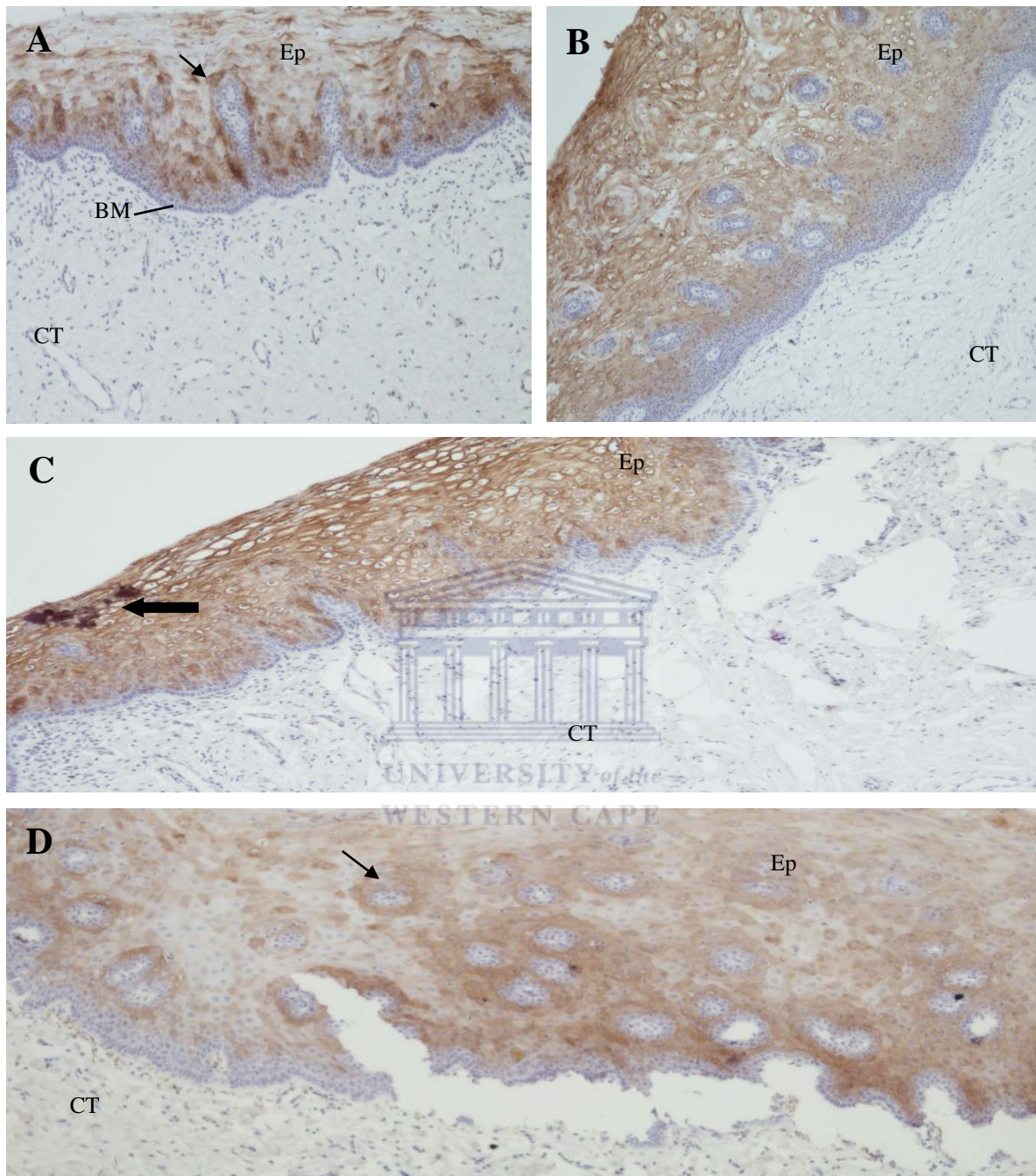


Figure 4.2. Immunohistochemical Staining of Cytokeratin 1 on Vaginal Mucosal Tissues. CK1 staining performed on (A) and (B) normal vaginal tissues. (C) and (D) xenografted vaginal tissues. Small arrows point to cells expressing CK1. Big arrow points to superficial and intermediate epithelial layers where CK1 is predominantly expressed. Ep-Epithelium; BM-Basement Membrane; CT-Connective Tissue. (*Magnifications X100*).

4.2 HUMAN CYTOKERATIN 5 EXPRESSION PROFILE

4.2.1 Immunohistochemical Scores for Cytokeratin 5

Cytokeratin 5 (CK5) was abundantly present in both normal and xenografted tissues. Positive staining was expressed along the epithelium, particularly on the basal layer (Figure 4.4). A strong, widespread distribution pattern was reported in 8 of 10 normal tissues and in 3 of 10 xenografted tissues (Table 4.2). Positive staining with rare interruptions was observed in 7 of 10 xenografted tissues.

Table 4.2: Immunohistochemical Scoring of Human Vaginal Mucosa for Cytokeratin 5. Scores reflect the difference in the staining intensity between normal vaginal tissues and xenografted vaginal tissues. Mouse anti-human monoclonal antibody raised against cytokeratin 5 antigens was used in both tissues.

Tissue Reference No.	Immunohistochemical Score	
	<u>Normal Vaginal Tissue</u>	<u>Xenografted Vaginal Tissue</u>
	NCL-CK5 Ab	NCL-CK5 Ab
15392/06	4	3
15396/06	4	3
16173/06	4	3
16175/06	4	4
16176/06	4	4
8960/06	3	3
8961/06	3	3
10156/06	4	4
17559/06	4	3
17560/06	4	2

*Scoring System; 0-Negative Staining; 1-Poor Staining (10-25%); 2-Rare Positive Staining (25-50%); 3-Some Positive Staining (50-75%); 4-Strong Uniform Positive Staining (>75%).

NCL-CK5 - Reference Code for Human Cytokeratin 5 Antibody; Ab - Antibody.

4.2.2 Statistical Comparisons of Cytokeratin 5 Staining Intensities

Mean staining intensities for cytokeratin 5 in NVT, XVT, NVT^a and XVT^a were 3.8 ± 0.1333 , 3.2 ± 0.2000 , 4.0 ± 0.0000 and 3.6 ± 0.1633 , respectively. Repeated-measures one-way ANOVA with subsequent Friedman's test (Friedman Statistic=13.35) indicated significant differences in the mean staining intensities between the tissues ($P=0.0039$). However, according to Dunn's multiple comparison test, there were no statistically significant differences in the staining intensities between all the tissue groups ($P>0.05$)

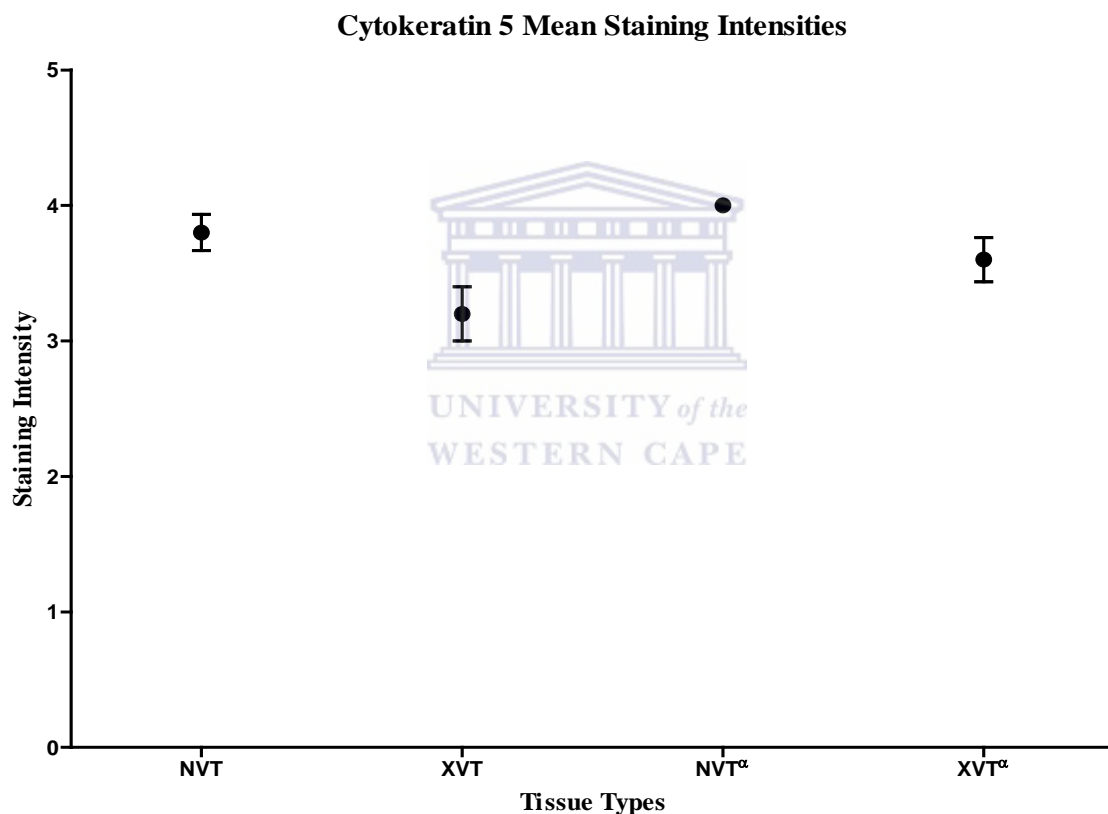


Figure 4.3: Mean Cytokeratin 5 Staining Intensity by Vaginal Mucosal Type. Data is expressed as mean \pm standard error of mean ($n=10$). Friedman's test indicates a significant difference between tissue types ($P=0.0039$). Conversely, Dunn's post test indicates that tissue types are not significantly different ($P>0.05$).

NVT-Normal Vaginal Tissue; XVT-Xenografted Vaginal Tissue; ^aCorne Kok-Unpublished Work.

4.2.3 Photomicrographs of Vaginal Mucosae Stained for Cytokeratin 5

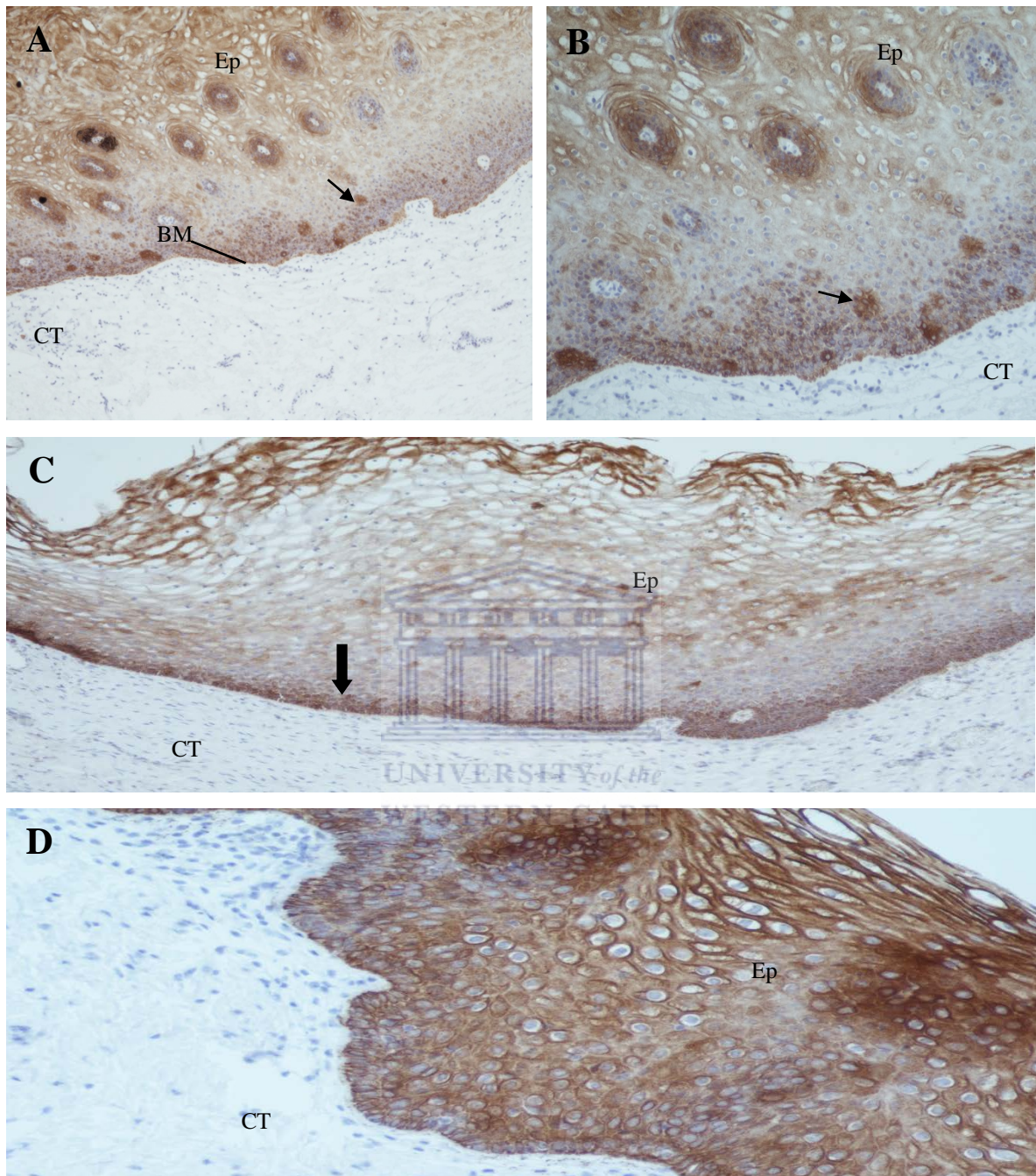


Figure 4.4. Immunohistochemical Staining of Cytokeratin 5 on Vaginal Mucosal Tissues. CK5 staining performed on (A) and (B) normal vaginal tissues. (C) and (D) xenografted vaginal tissues. Small arrows point to cells expressing CK5. Big arrow points to the basal epithelial layer where CK5 is mostly localized. Ep-Epithelium; BM-Basement Membrane; CT-Connective Tissue. (*Magnifications X100 for A, C, D and X200 for B*).

4.3 HUMAN CYTOKERATIN 13 EXPRESSION PROFILE

4.3.1 Immunohistochemical Scores for Cytokeratin 13

Normal and xenografted vaginal tissues displayed positive staining for cytokeratin 13 (CK13). CK13 was observed along the superficial, intermediate and parabasal layers of the epithelium (Figure 4.6) in both normal and xenografted tissues. A relatively similar strong staining pattern was reported in 9 of 10 normal tissues. A moderate to strong staining of CK13 was noted in 9 of 10 xenografted tissues while 1 xenografted tissue stained negatively (Table 4.3)

Table 4.3: Immunohistochemical Scoring of Human Vaginal Mucosa for Cytokeratin 13. Scores reflect the difference in the staining intensity between normal vaginal tissues and xenografted vaginal tissues. Mouse anti-human monoclonal antibody raised against cytokeratin 13 antigens was used in both tissues.

Tissue Reference No.	Immunohistochemical Score	
	<u>Normal Vaginal Tissue</u> NCL-CK13 Ab	<u>Xenografted Vaginal Tissue</u> NCL-CK13 Ab
15392/06	4	4
15396/06	4	0
16173/06	4	4
16175/06	4	3
16176/06	4	3
8960/06	4	3
8961/06	4	3
10156/06	3	2
17559/06	4	3
17560/06	4	2

*Scoring System; 0-Negative Staining; 1-Poor Staining (10-25%); 2-Rare Positive Staining (25-50%); 3-Some Positive Staining (50-75%); 4-Strong Uniform Positive Staining (>75%).

NCL-CK13 - Reference Code for Human Cytokeratin 13 Antibody; Ab - Antibody.

4.3.2 Statistical Comparisons of Cytokeratin 13 Staining Intensities

Mean staining intensities for cytokeratin 13 in NVT, XVT, NVT^α and XVT^α were 3.9±0.1000, 2.7±0.3667, 4.0±0.0000 and 4.0±0.0000, respectively. Repeated-measures one-way ANOVA with subsequent Friedman's test (Friedman Statistic=22.76) indicated significant differences in the mean staining intensities between all tissue groups (P<0.0001). Further statistical analysis with Dunn's multiple comparison test showed significant differences between NVT^α and XVT and between XVT and XVT^α (P<0.05).

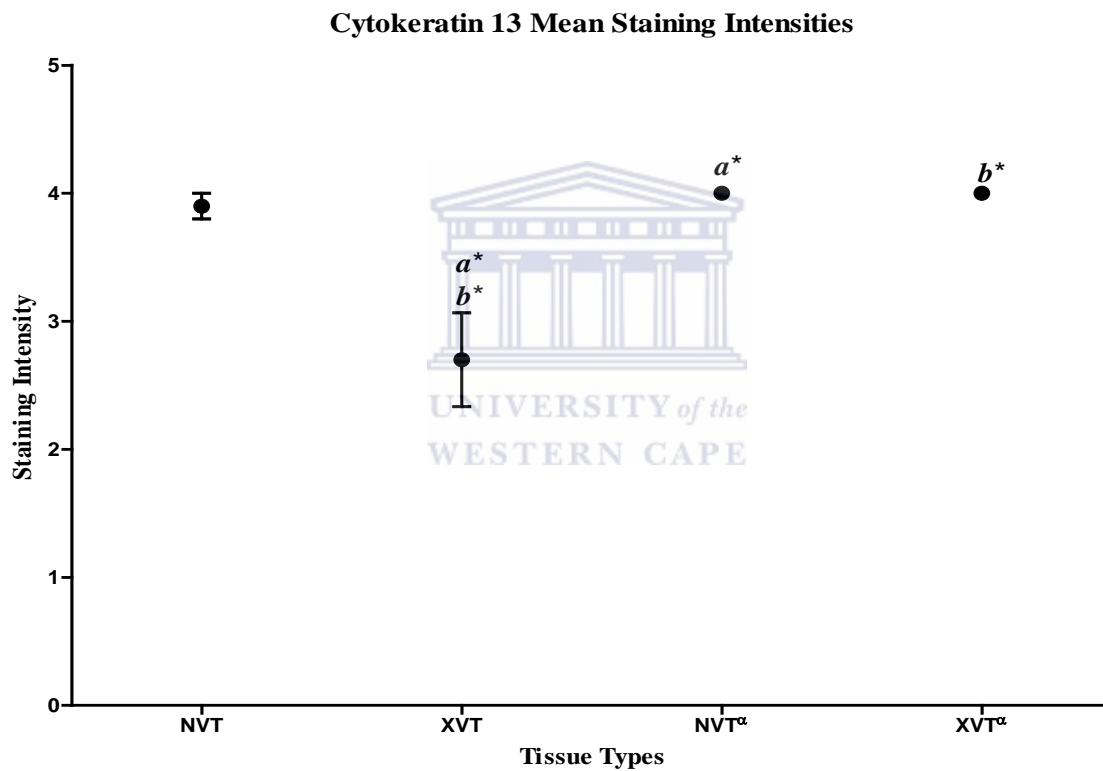


Figure 4.5: Mean Cytokeratin 13 Staining Intensity by Vaginal Mucosal Type. Data is expressed as mean ± standard error of mean (n=10). Friedman's test indicates a statistical difference between tissue types (P<0.0001). Further analysis with Dunn's post test shows tissue types that are significantly different (P<0.05) as denoted by similar alphabets.

NVT-Normal Vaginal Tissue; XVT-Xenografted Vaginal Tissue; ^αCorne Kok-Unpublished Work.

*Significant

4.3.3 Photomicrographs of Vaginal Mucosae Stained for Cytokeratin 13

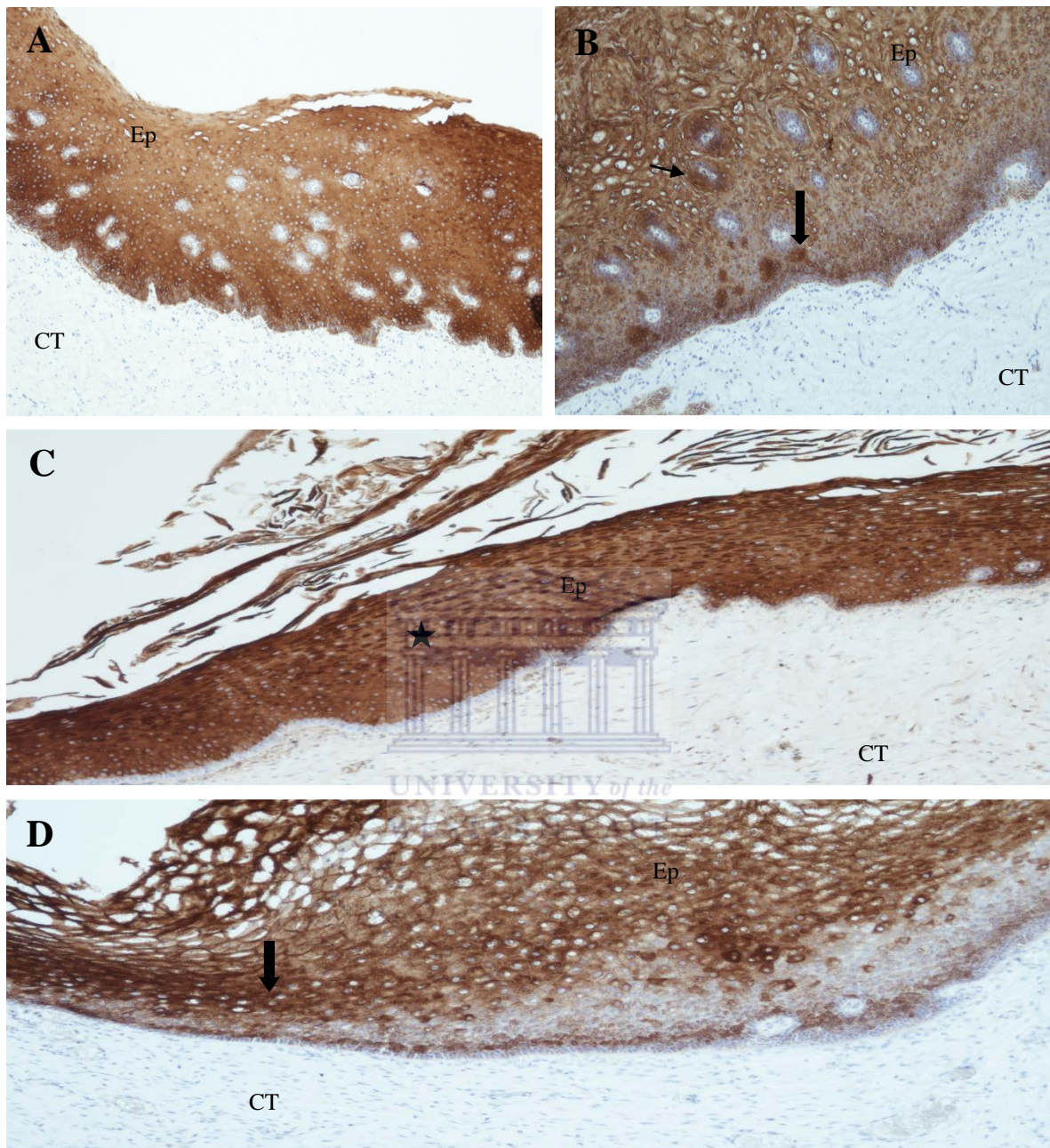


Figure 4.6. Immunohistochemical Staining of Cytokeratin 13 on Vaginal Mucosal Tissues. CK13 staining performed on (A) and (B) normal vaginal tissues. (C) and (D) xenografted vaginal tissues. Small arrow points to a cell expressing CK13. Big arrows point to the parabasal epithelial layer where CK13 is mostly localized. A star indicates diffusely expressed CK13 in all epithelial layers of this particular xenografted tissue. Ep-Epithelium; CT-Connective Tissue. (*Magnifications X100*).

4.4 HUMAN CYTOKERATIN 14 EXPRESSION PROFILE

4.4.1 Immunohistochemical Scores for Cytokeratin 14

Cytokeratin 14 (CK14) was demonstrated consistently in both normal and xenografted vaginal tissues. CK14 was predominantly localized to the basal epithelial layer (Figure 4.8). A strong, uniformly stained epithelium was observed in 9 of 10 normal tissues and in 3 of 10 xenografted tissues (Table 4.4). In most cases, xenografted tissues exhibited interrupted staining patterns.

Table 4.4: Immunohistochemical Scoring of Human Vaginal Mucosa for Cytokeratin 14. Scores reflect the difference in the staining intensity between normal vaginal tissues and xenografted vaginal tissues. Mouse anti-human monoclonal antibody raised against cytokeratin 14 antigens was used in both tissues.

Tissue Reference No.	Immunohistochemical Score	
	<u>Normal Vaginal Tissue</u> NCL-LL002CK14 Ab	<u>Xenografted Vaginal Tissue</u> NCL-LL002CK14 Ab
15392/06	4	3
15396/06	4	4
16173/06	3	3
16175/06	4	3
16176/06	4	4
8960/06	4	2
8961/06	4	3
10156/06	4	4
17559/06	4	1
17560/06	4	3

*Scoring System; 0-Negative Staining; 1-Poor Staining (10-25%); 2-Rare Positive Staining (25-50%); 3-Some Positive Staining (50-75%); 4-Strong Uniform Positive Staining (>75%).

NCL-LL002CK14 - Reference Code for Human Cytokeratin 14 Antibody; Ab - Antibody.

4.4.2 Statistical Comparisons of Cytokeratin 14 Staining Intensities

Mean staining intensities for cytokeratin 14 in NVT, XVT, NVT^α and XVT^α were 3.9 ± 0.1000 , 3.0 ± 0.3333 , 4.0 ± 0.0000 and 4.0 ± 0.0000 , respectively (Figure 4.7). Repeated-measures one-way ANOVA with subsequent Friedman's test (Friedman Statistic=18.55) indicated significant differences in the mean staining intensities between tissue groups ($P=0.0003$). Conversely, further analysis with Dunn's multiple comparison test, showed no statistical differences in the staining intensities between tissue groups ($P>0.05$)

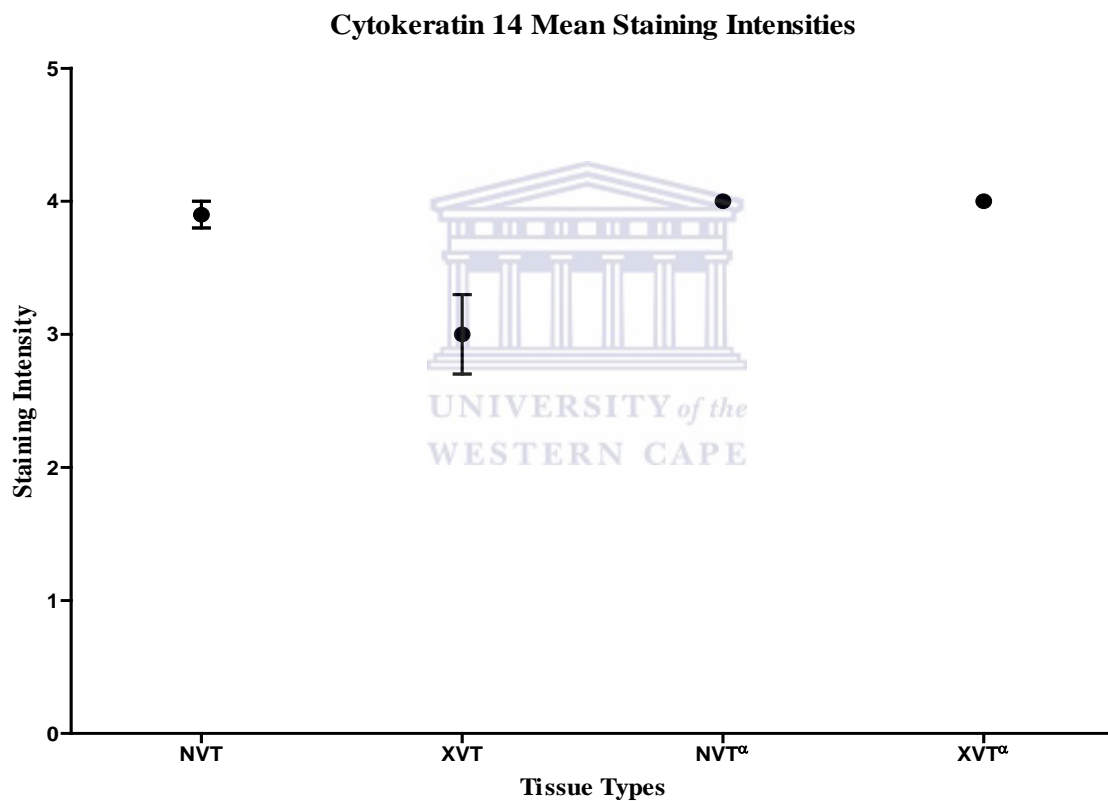


Figure 4.7: Mean Cytokeratin 14 Staining Intensity by Vaginal Mucosal Type. Data is expressed as mean \pm standard error of mean (n=10). Friedman's test indicates a statistical difference between tissue types ($P=0.0003$). On the contrary, Dunn's post test does not show any statistical difference between tissue types ($P>0.05$).

NVT-Normal Vaginal Tissue; XVT-Xenografted Vaginal Tissue; ^αCorne Kok-Unpublished Work.

4.4.3 Photomicrographs of Vaginal Mucosae Stained for Cytokeratin 14

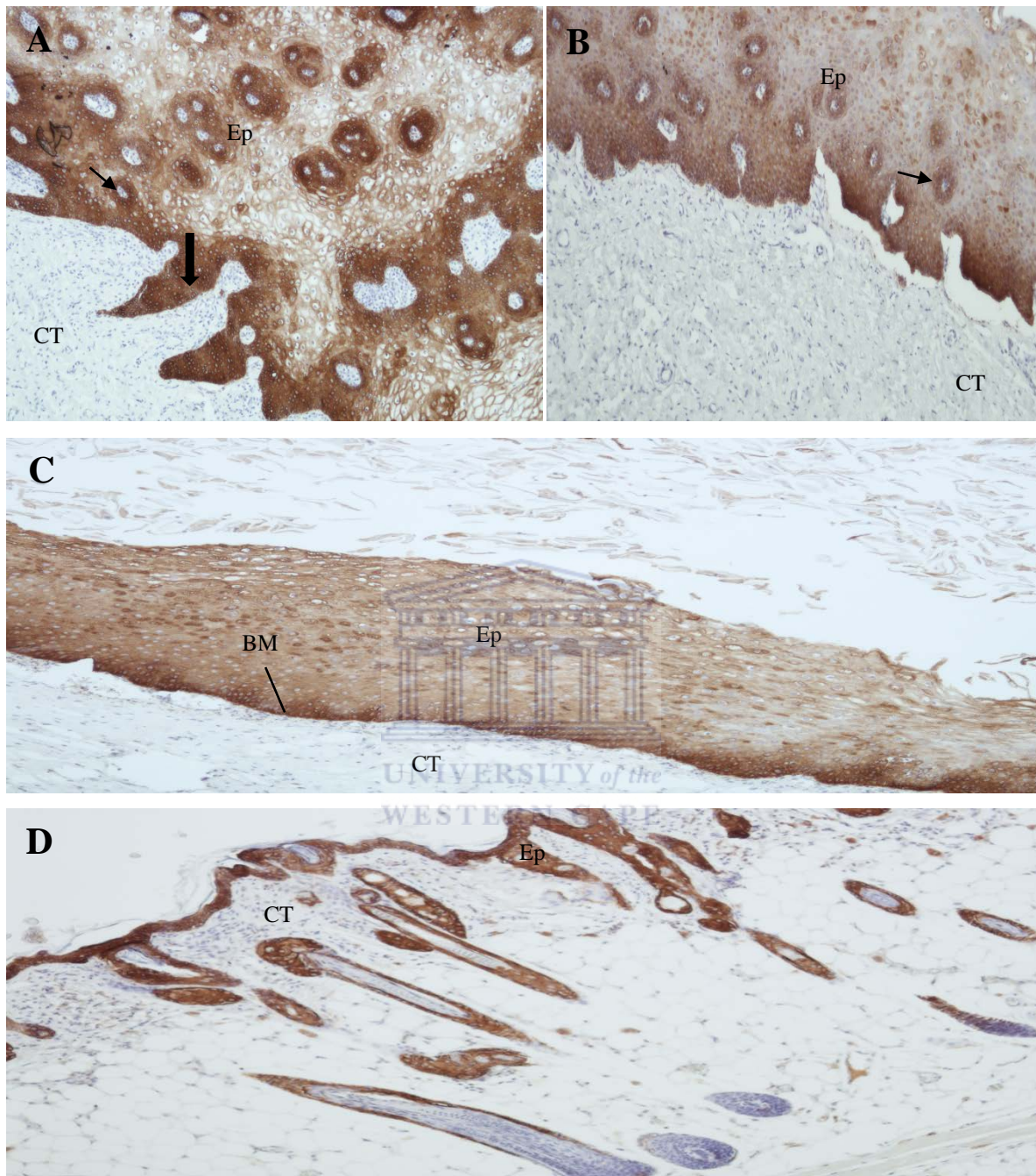


Figure 4.8. Immunohistochemical Staining of Cytokeratin 14 on Vaginal Mucosal Tissues. CK14 staining performed on (A) and (B) normal vaginal tissues. (C) and (D) xenografted vaginal tissues. Small arrows point to cells expressing CK14. Big arrow points to the basal epithelial layer where CK14 is mostly localized. Ep-Epithelium; BM-Basement Membrane; CT-Connective Tissue. (*Magnifications X100*).

4.5 COLLAGEN TYPE IV EXPRESSION PROFILE

4.5.1 Immunohistochemical Scores for Collagen IV

Human collagen IV was moderately expressed along the basement membrane in 8 of 10 normal tissues (Table 4.5). Limited or absent human collagen IV staining patterns were observed along the basement of xenografted tissues. In addition, positive staining was also noted around blood vessels in both normal and xenografted tissues (Figure 4.10). Only 3 of 10 xenografted tissues stained positively for mouse collagen IV whereas the other 7 tissues stained negatively (Table 4.5).

Table 4.5: Immunohistochemical Scoring of Human Vaginal Mucosa for Collagen IV. Scores reflect the difference in the staining intensity between normal vaginal tissues and xenografted vaginal tissues. The following collagen IV antibodies were used (a) Mouse anti-human monoclonal Ab; (b) Mouse anti-human monoclonal Ab; and (c) Rabbit anti-mouse monoclonal Ab.

Tissue Reference No.	Immunohistochemical Score		
	<u>Normal Vaginal Tissue</u>	<u>Xenografted Vaginal Tissues</u>	
	(A) NCL-COLL-IV Ab	(B) NCL-COLL-IV Ab	(C) C7510-50S Ab
15392/06	1	0	1
15396/06	1	1	0
16173/06	2	1	1
16176/06	2	1	0
8961/06	2	1	1
8926/06	2	1	0
10156/06	2	2	0
10159/06	2	0	0
17560/06	2	0	0
10501/06	2	1	2

*Scoring System; 0-Negative Staining; 1-Rare Positive Staining; 2-Rare Interrupted Positive Staining; 3-Strong Uniform Positive Staining.

NCL-COLL-IV - Reference Code for Human Collagen IV; C7510-50S - Reference Code for Mouse Collagen IV; Ab - Antibody.

4.5.2 Statistical Comparisons of Collagen IV Staining Intensities

Mean staining intensities for collagen IV in NVT, XVT-h and XVT-m were 1.8 ± 0.1333 , 0.8 ± 0.2000 and 0.5 ± 0.2236 , respectively. Mean staining intensities in NVT^α and XVT^α -h and XVT^α -m were 1.4 ± 0.1633 , 0.7 ± 0.1528 and 0.6 ± 0.1757 , respectively. Repeated-measures one-way ANOVA with subsequent Friedman's test (Friedman Statistic=16.79) indicated significant differences between the mean staining intensities between the tissue groups ($P \leq 0.0049$). Further statistical analysis with Dunn's multiple comparison test showed no statistical differences in the mean staining intensities between the tissue groups ($P > 0.05$).

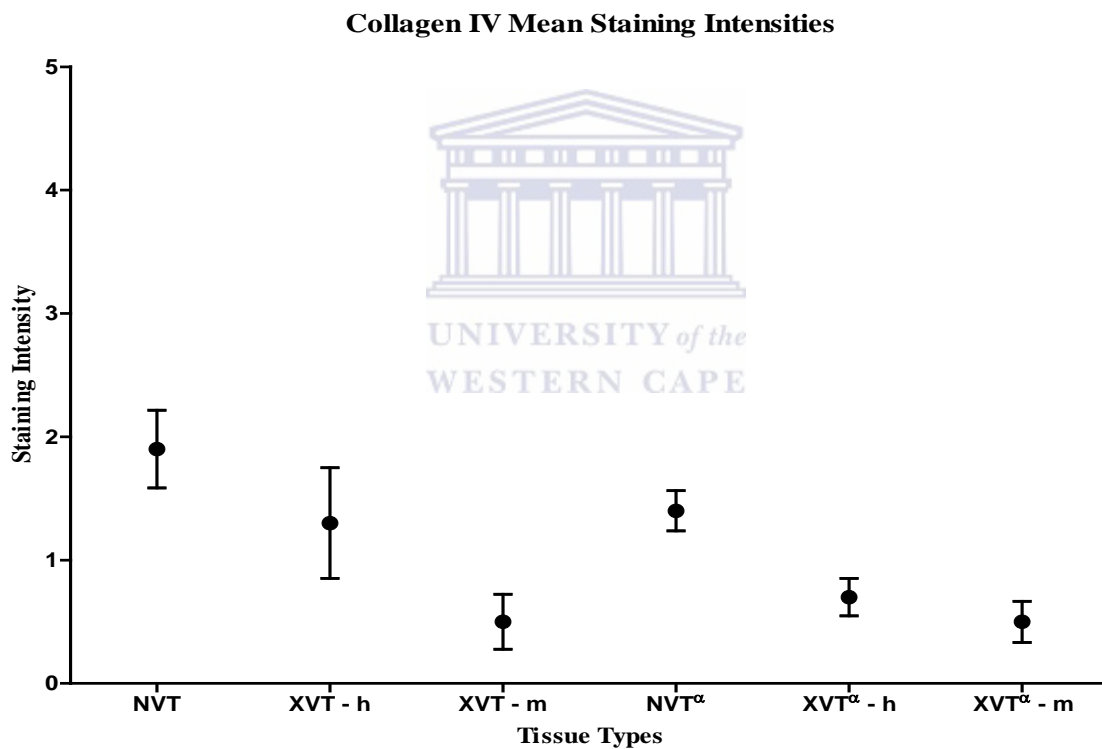


Figure 4.9: Mean Collagen IV Staining Intensity by Vaginal Mucosal Type. Data is expressed as mean \pm standard error of mean (n=10). Friedman's test indicates a statistical difference between tissue types ($P=0.0049$). Conversely, Dunn's post test does not show any statistical difference between tissue types ($P>0.05$).

NVT-Normal Vaginal Tissue; XVT-Xenografted Vaginal Tissue; $^\alpha$ Corne Kok-Unpublished Work; h- Human Antigen Localization; m-Mouse Antigen Localization.

4.5.3 Photomicrographs of Vaginal Mucosae Stained for Human Collagen IV

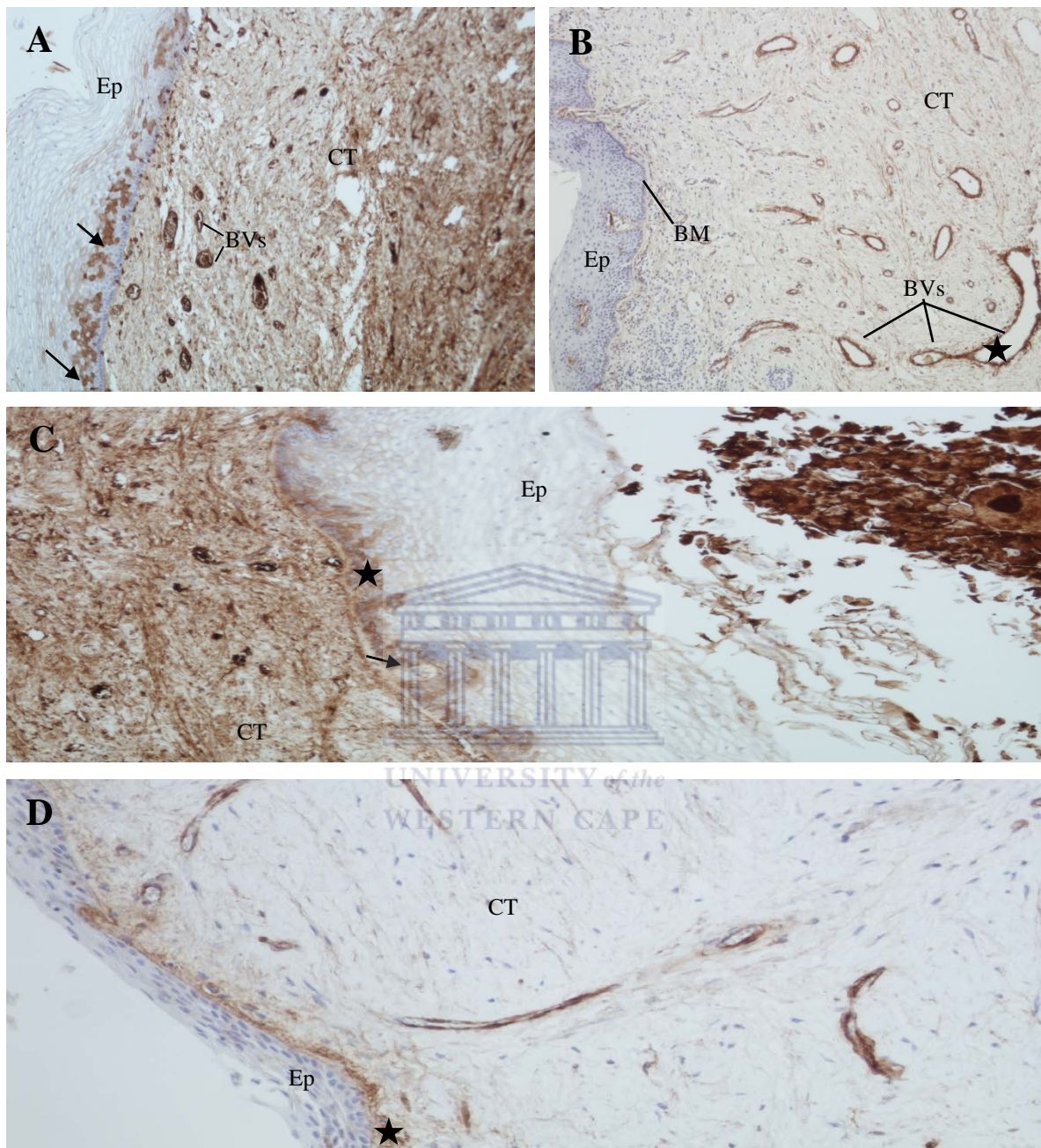


Figure 4.10. Immunohistochemical Staining of Human Collagen IV on Vaginal Mucosal Tissues. Collagen IV staining performed on (A) and (B) normal vaginal tissues. (C) and (D) xenografted vaginal tissues. Small arrows point to cells expressing collagen IV. Stars indicate that collagen IV is strongly expressed along the basement membrane and some blood vessels. Ep-Epithelium; BM-Basement Membrane; CT-Connective Tissue; BVs-Blood Vessels. (*Magnifications X100 for A, B, C and X200 for D*).

4.5.4 Photomicrographs of Human and Murine Tissues Stained for Mouse Collagen IV

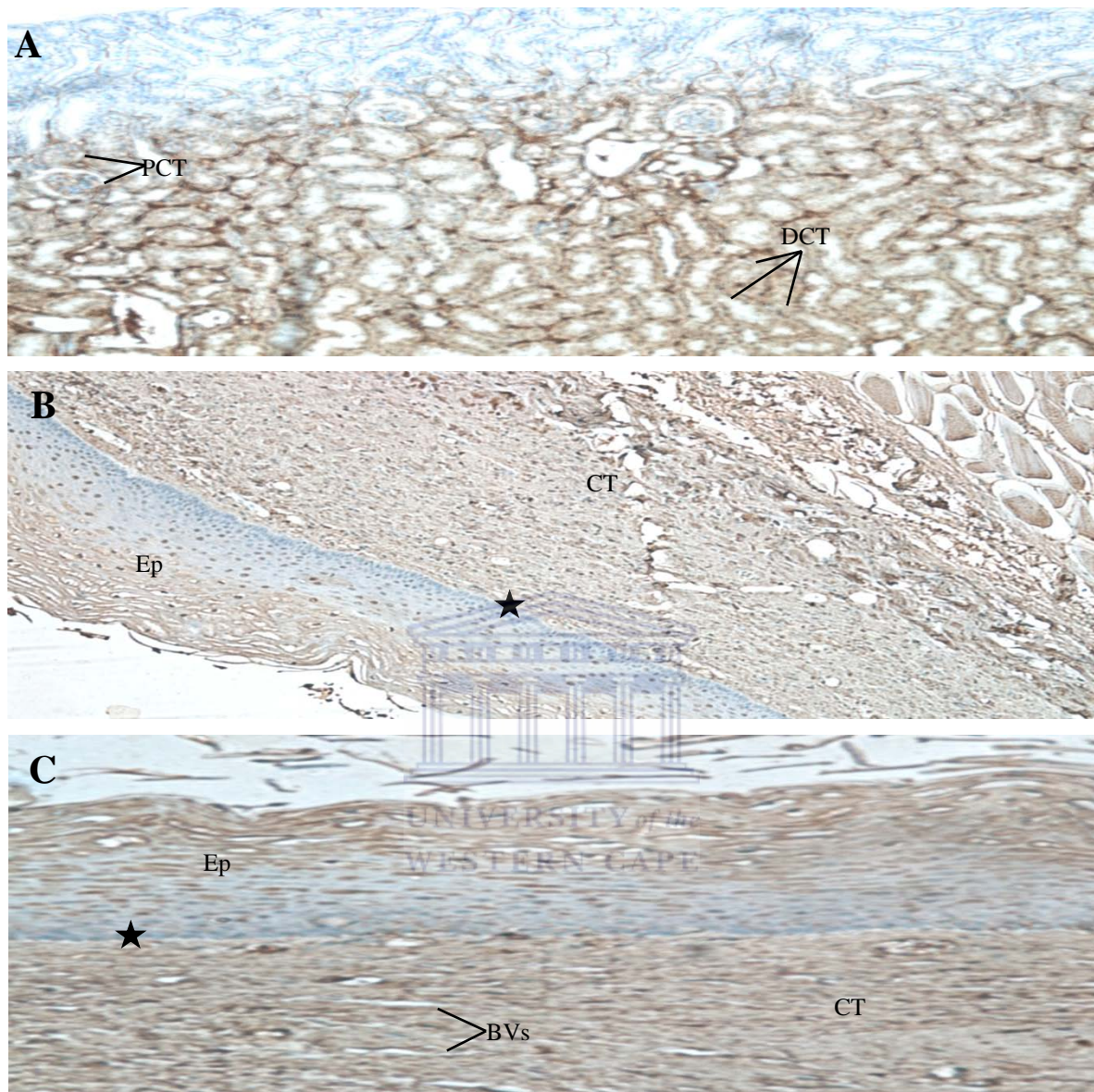


Figure 4.11. Immunohistochemical Staining of Mouse Collagen IV on Human and Murine Tissues. Collagen IV staining performed on (A) positive control - mouse kidney tissue (B) and (C) xenografted vaginal tissues. Stars indicate negative expression of mouse collagen IV along the basement membrane. PCT-Proximal Convoluted Tubules; DCT-Distal Convoluted Tubules; Ep-Epithelium; CT-Connective Tissue; BVs-Blood Vessels. (Magnifications X100 for A, B and X200 for C).

4.6 LAMININ EXPRESSION PROFILE

4.6.1 Immunohistochemical Scores for Laminin

Human laminin staining patterns were varied in both normal and xenografted vaginal tissues. The basement membrane and blood vessels exhibited positive staining of human laminin (Figure 4.13). Positive staining of human laminin was reported in 6 of 10 normal tissues and 7 of 10 xenografted tissues. A weak positive staining of mouse laminin was noted in only 2 of 10 xenografted tissues (Table 4.6).

Table 4.6: Immunohistochemical Scoring of Human Vaginal Mucosa for Laminin. Scores reflect the difference in the staining intensity between normal vaginal tissues and xenografted vaginal tissues. The following laminin antibodies were used (a) Mouse anti-human monoclonal Ab; (b) Mouse anti-human monoclonal Ab; and (c) Rabbit anti-mouse monoclonal Ab.

Tissue Reference No.	Immunohistochemical Score		
	Normal Vaginal Tissue	Xenografted Vaginal Tissues	
	(A) NCL-LAMININ Ab	(B) NCL-LAMININ Ab	(C) LS-C25107 Ab
15392/06	1	1	0
15396/06	2	1	0
16173/06	2	1	1
16176/06	0	0	0
8961/06	0	0	0
8926/06	0	0	0
10156/06	0	1	0
10159/06	2	1	1
17560/06	3	2	0
10501/06	3	1	0

*Scoring System; 0-Negative Staining; 1-Rare Positive Staining; 2-Rare Interrupted Positive Staining; 3-Strong Uniform Positive Staining.

NCL-LAMININ - Reference Code for Human Laminin Antibody; LS-C25107 - Reference Code for Mouse Laminin; Ab - Antibody.

4.6.2 Statistical Comparisons of Laminin Staining Intensities

Mean staining intensities for laminin in NVT, XVT-h and XVT-m were 1.3 ± 0.3958 , 0.8 ± 0.2000 and 0.2 ± 0.1470 , respectively. Mean staining intensities in NVT^a and XVT^a -h and XVT^a -m were 1.3 ± 0.3000 , 0.7 ± 0.2134 and 0.0 ± 0.0000 , respectively. Repeated-measures one-way ANOVA with subsequent Friedman's test (Friedman Statistic=22.59) indicated significant differences in the mean staining intensities between tissue groups ($P=0.0004$). Further statistical analysis with Dunn's multiple comparison test showed no statistical differences in the mean staining intensities between all tissue groups ($P>0.05$), with an exception for NVT and XVT^a ($P<0.05$).

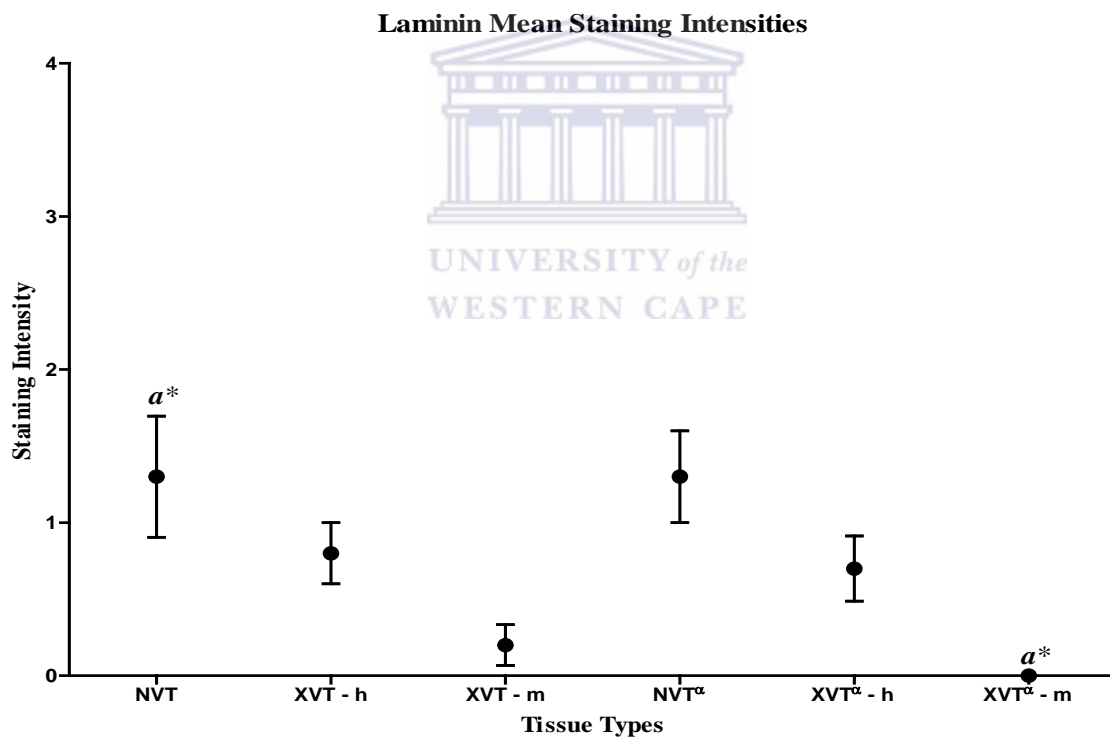


Figure 4.12: Mean Laminin Staining Intensity by Vaginal Mucosal Type. Data is expressed as mean \pm standard error of mean (n=10). Friedman's test indicates that tissue types are significantly different ($P=0.0004$). Dunn's multiple test specifies tissue types that are statistically different ($P<0.05$) as denoted by similar alphabets.

NVT-Normal Vaginal Tissue; XVT-Xenografted Vaginal Tissue; ^aCorne Kok-Unpublished Work; h-Localization of Human Antigens; m-Localization of Mouse Antigens.

*Significant

4.6.3 Photomicrographs of Vaginal Mucosae Stained for Human Laminin

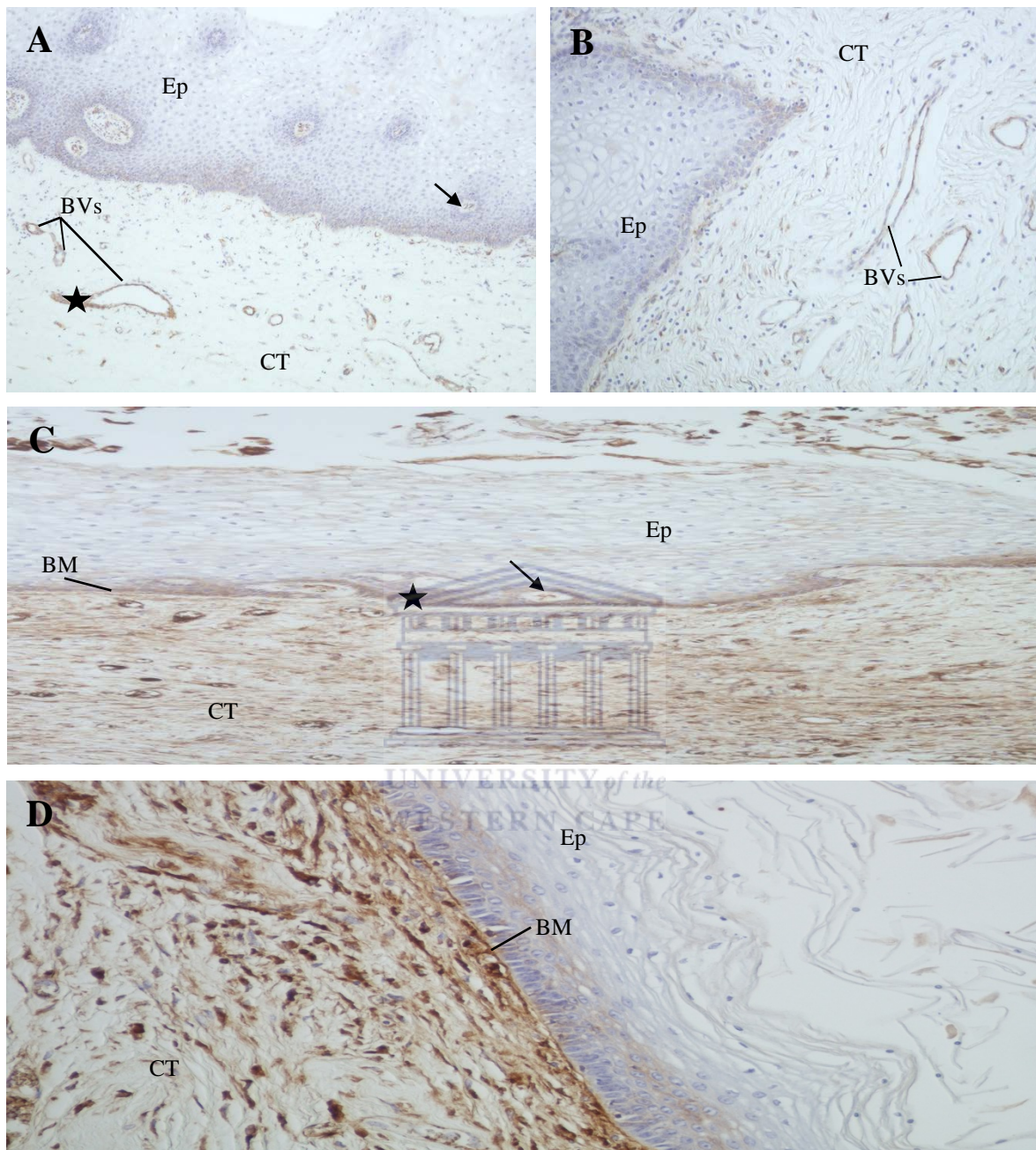


Figure 4.13. Immunohistochemical Staining of Human Laminin on Vaginal Mucosal Tissues. Laminin staining performed on (A) and (B) normal vaginal tissues. (C) and (D) xenografted vaginal tissues. Small arrows point to cells expressing laminin. Stars indicate that laminin is strongly expressed along the basement membrane and some blood vessels. Ep-Epithelium; BM-Basement Membrane; CT-Connective Tissue; BVs-Blood Vessels. (*Magnifications X100 for A, C and X200 for B, D.*)

4.6.4 Photomicrographs of Human and Murine Tissues Stained for Mouse Laminin

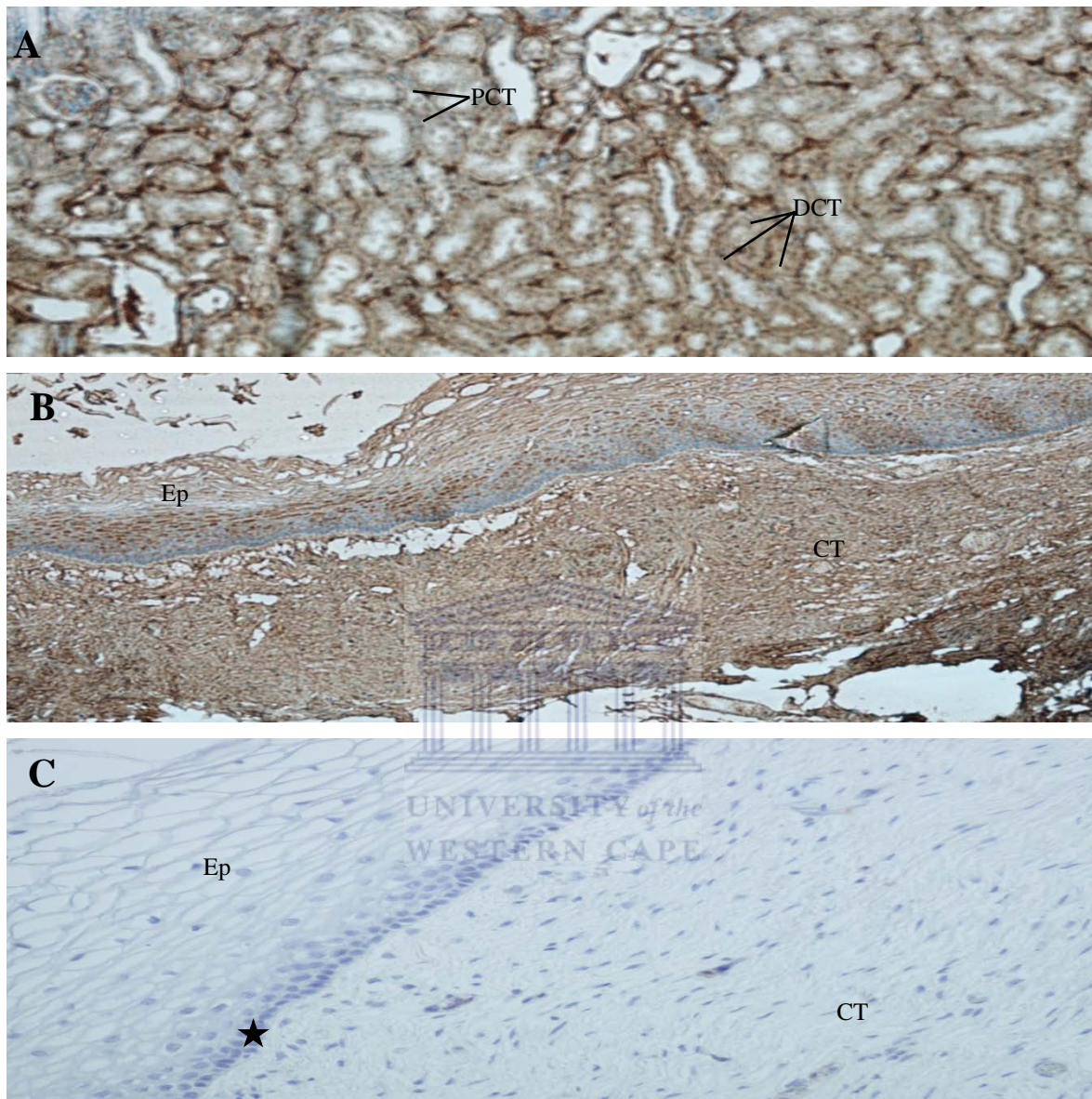


Figure 4.14. Immunohistochemical Staining of Mouse Laminin on Human and Murine Tissues. Laminin staining performed on (A) positive control - mouse kidney tissue (B) and (C) xenografted vaginal tissues. Stars indicate negative expression of mouse laminin along the basement membrane. PCT-Proximal Convoluted Tubules; DCT-Distal Convoluted Tubules; Ep-Epithelium; CT-Connective Tissue. (Magnifications X100 for A, B and X200 for C).

4.7 HUMAN ELASTIN EXPRESSION PROFILE

4.7.1 Immunohistochemical Scores for Elastin

A strong and well defined positive staining of elastin was seen across the stromal layer in both normal and xenografted vaginal tissues (Figure 4.16). Positive elastin staining was also observed along the basement membrane of some tissues. Interestingly, positive staining was reported in 8 of 10 normal tissues whereas 10 of 10 xenografted tissues stained positively (Table 4.7).

Table 4.7: Immunohistochemical Scoring of Human Vaginal Mucosa for Elastin. Scores reflect the difference in the staining intensity between normal vaginal tissues and xenografted vaginal tissues. Mouse anti-human monoclonal antibody raised against elastin antigens was used in both tissues.

Tissue Reference No.	Immunohistochemical Score	
	<u>Normal Vaginal Tissue</u> NCL-ELASTIN Ab	<u>Xenografted Vaginal Tissue</u> NCL-ELASTIN Ab
15392/06	4	3
15396/06	3	3
16173/06	4	4
16175/06	3	4
16176/06	3	3
8960/06	3	3
8961/06	3	4
10156/06	4	4
17559/06	0	4
17560/06	0	3

*Scoring System; 0-Negative Staining; 1-Poor Staining (10-25%); 2-Rare Positive Staining (25-50%); 3-Some Positive Staining (50-75%); 4-Strong Uniform Positive Staining (>75%).

NCL-ELASTIN - Reference Code for Human Elastin Antibody; Ab - Antibody.

4.7.2 Statistical Comparisons of Elastin Staining Intensities

Mean staining intensities for elastin in NVT, XVT, NVT^α and XVT^α were 2.7 ± 0.4726 , 3.5 ± 0.1667 , 4.0 ± 0.0000 and 3.9 ± 0.1000 , respectively. Repeated-measures one-way ANOVA with subsequent Friedman's test (Friedman Statistic=14.78) indicated significant differences in the mean staining intensities of the tissue groups ($P=0.0020$). Further statistical analysis with Dunn's multiple comparison test showed no statistical differences between the tissue groups ($P>0.05$).

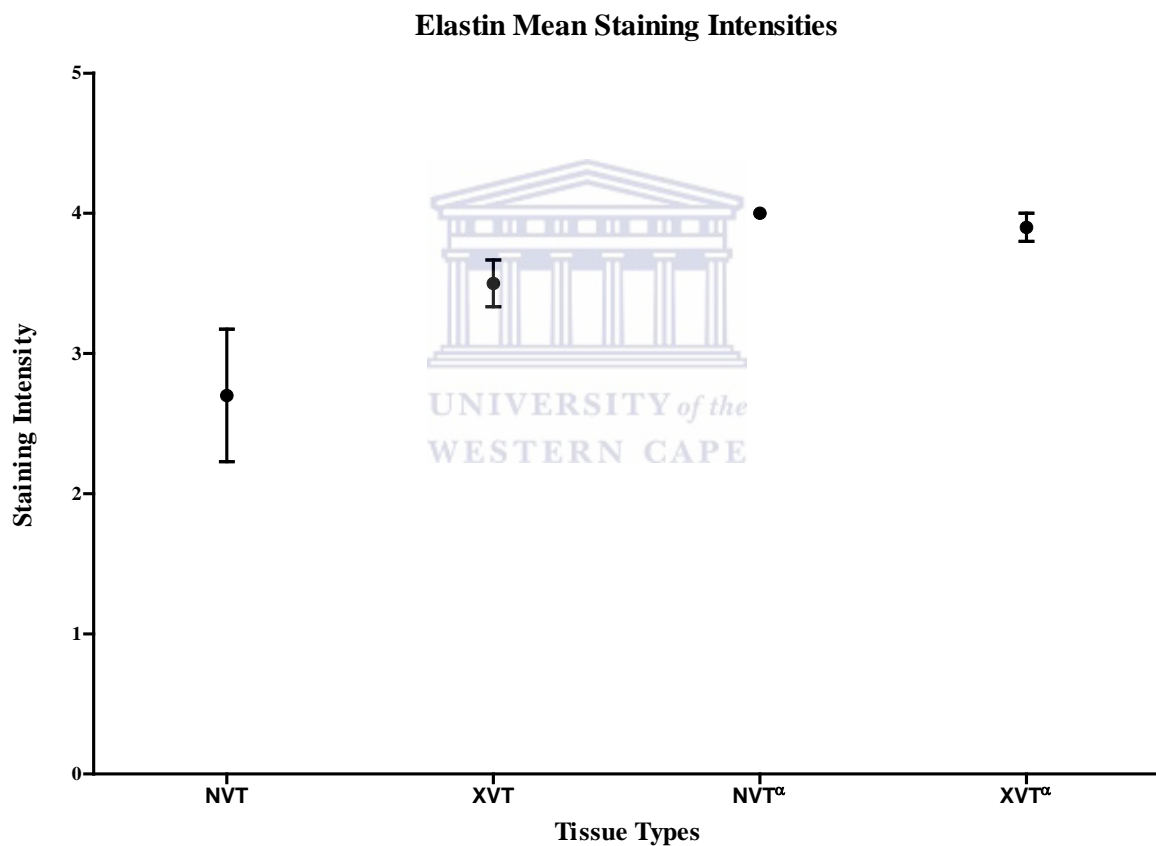


Figure 4.15: Mean Elastin Staining Intensity by Vaginal Mucosal Type. Data is expressed as the mean \pm standard error of mean ($n=10$). Friedman's test indicates that tissue types are significantly different ($P=0.0020$). However, Dunn's multiple comparison test indicates that tissue types are not significantly different ($P>0.05$).

NVT-Normal Vaginal Tissue; XVT-Xenografted Vaginal Tissue; ^αCorne Kok-Upublished Work.

4.7.3 Photomicrographs of Vaginal Mucosae Stained for Human Elastin

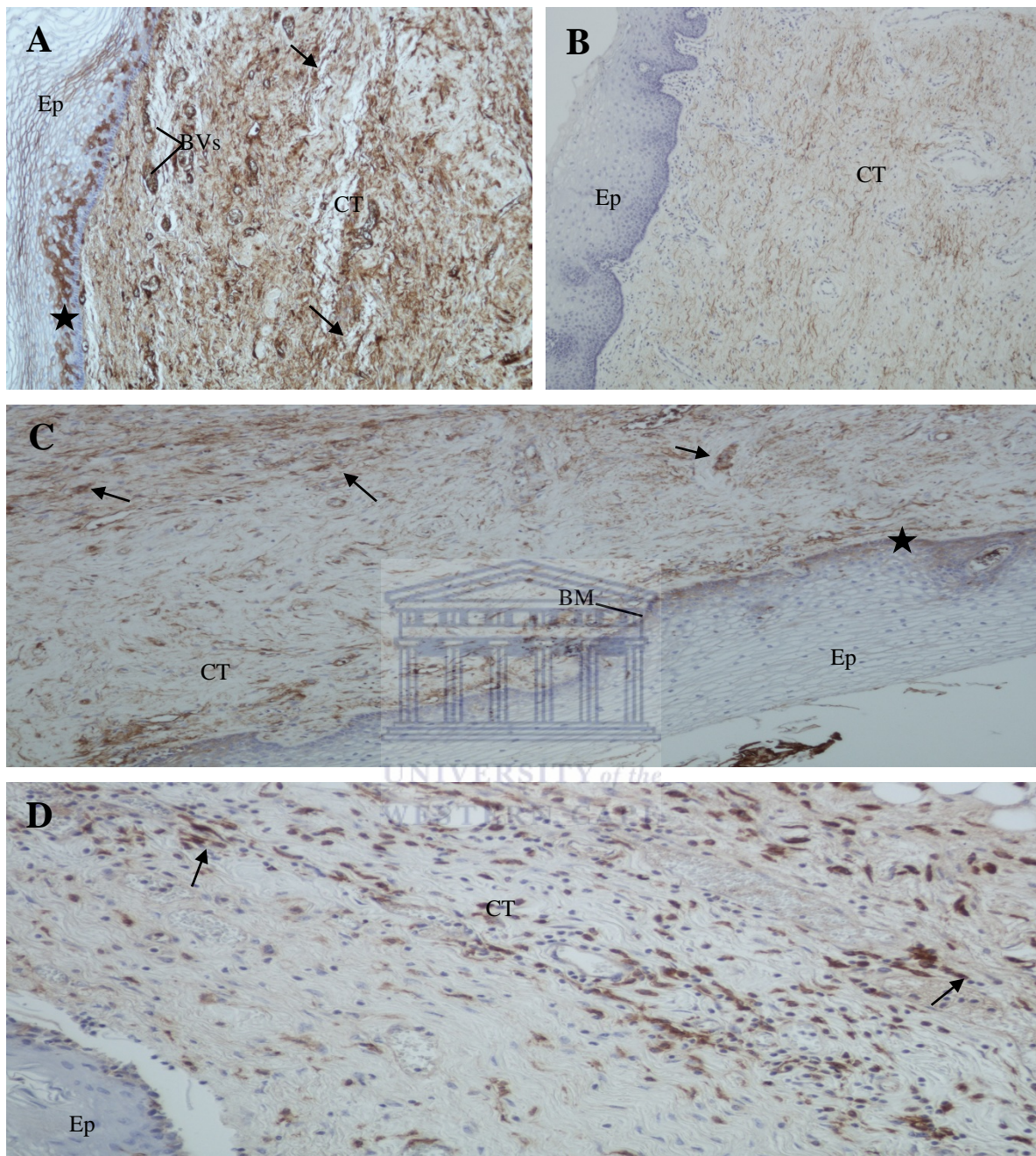


Figure 4.16. Immunohistochemical Staining of Human Elastin on Vaginal Mucosal Tissues. Elastin staining performed on (A) and (B) normal vaginal tissues. (C) and (D) xenografted vaginal tissues. Small arrows indicate a positive and uniformly stained connective tissue. Stars indicate that elastin is also expressed along the basement membrane of some vaginal tissues. Ep-Epithelium; BM-Basement Membrane; CT-Connective Tissue; BVs-Blood Vessels. (*Magnifications X100 for A, B, C and X200 for D*).

4.8 FIBRONECTIN EXPRESSION PROFILE

4.8.1 Immunohistochemical Scores for Fibronectin

A weak to moderate positive staining of human fibronectin was observed along the basement membrane and connective tissue in normal and xenografted tissues (Figure 4.18). Positive staining was reported in all normal tissues and in 7 of 10 xenografted tissues. Negative staining of mouse fibronectin was reported in 8 of 10 xenografted tissues whereas the other 2 tissues exhibited weak and moderate staining (Table 4.8).

Table 4.8: Immunohistochemical Scoring of Human Vaginal Mucosa for Fibronectin. Scores reflect the difference in the staining intensity between normal vaginal tissues and xenografted vaginal tissues. The following fibronectin antibodies were used (a) Mouse anti-human monoclonal Ab; (b) Mouse anti-human monoclonal Ab; and (c) Rabbit anti-mouse monoclonal Ab.

Tissue Reference No.	Immunohistochemical Score		
	<u>Normal Vaginal Tissue</u>	<u>Xenografted Vaginal Tissues</u>	
	(A) NCL-FIB Ab	(B) NCL-FIB Ab	(C) F4215-46 Ab
15392/06	1	0	0
15396/06	1	1	0
16173/06	2	1	2
16176/06	2	1	0
8961/06	2	1	0
8926/06	2	1	0
10156/06	2	2	1
10159/06	2	0	0
17560/06	2	0	0
10501/06	2	1	0

*Scoring System; 0-Negative Staining; 1-Poor Staining (10-25%); 2-Rare Positive Staining (25-50%); 3-Some Positive Staining (50-75%); 4-Strong Uniform Positive Staining (>75%).

NCL-FIB - Reference Code for Human Fibronectin Antibody; F4215-46 - Reference Code for Mouse Fibronectin Antibody; Ab - Antibody.

4.8.2 Statistical Comparisons of Fibronectin Staining Intensities

Mean staining intensities for fibronectin in NVT, XVT-h and XVT-m were 1.8 ± 0.1333 , 0.8 ± 0.2000 and 0.3 ± 0.2134 respectively. Mean staining intensities for NVT^α and XVT^α -h and XVT^α -m were 4.0 ± 0.0000 , 4.0 ± 0.0000 and 0.0 ± 0.0000 respectively. Repeated-measures one-way ANOVA with subsequent Friedman's test (Friedman Statistic=47.27) indicated significant differences in the mean staining intensities between tissue groups ($P < 0.0001$). Further statistical analysis with Dunn's multiple comparison test showed slight significant differences between NVT^α and XVT-h and between XVT-h and XVT^α -h ($P < 0.05$). A high statistical difference ($P < 0.05$) was reported between the following tissue groups; NVT^α and XVT-m, XVT-m and XVT^α -h, NVT^α and XVT^α -m as well as XVT^α -h and XVT^α -m.

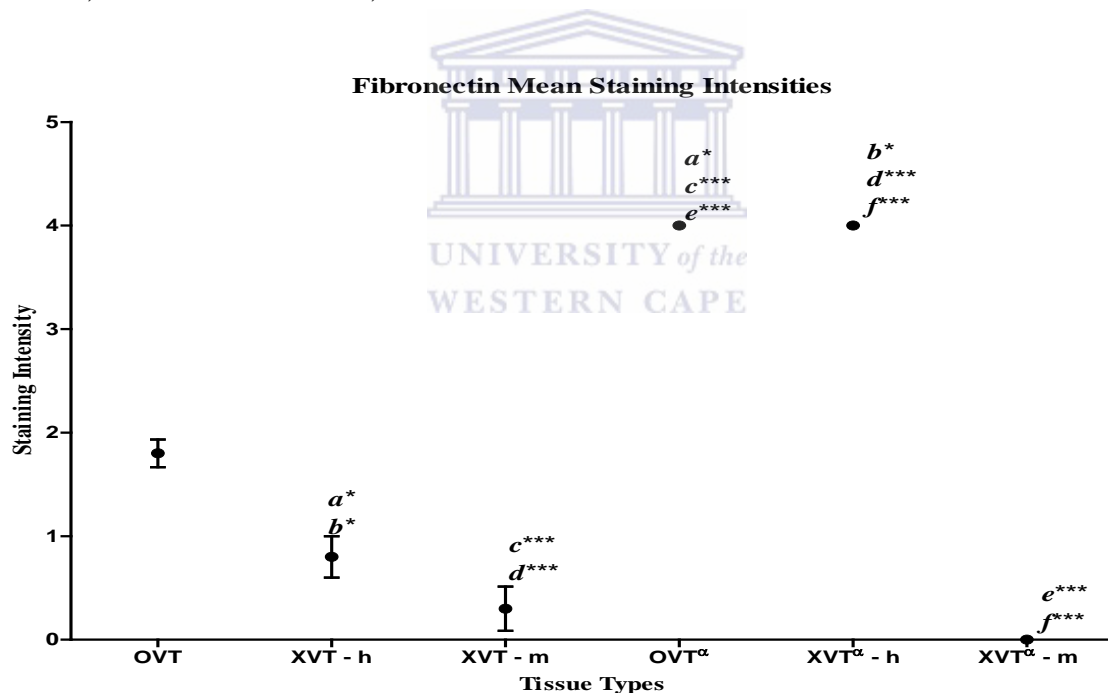


Figure 4.17: Mean Fibronectin Staining Intensity by Vaginal Mucosal Type. Data is expressed as mean \pm standard error of mean (n=10). Friedman's test indicates that tissue types are significantly different ($P < 0.0001$). Further analysis with Dunn's post test specifies tissue types that are significantly different ($P < 0.05$) as denoted by identical alphabets.

OVT-Original Vaginal Tissue; XVT-Xenografted Vaginal Tissue; ^aCorne Kok-Unpublished Work; h- Human Antigen Localization; m-Mouse Antigen Localization.

*Significant; **Very Significant; ***Extremely Significant

4.8.3 Photomicrographs of Vaginal Mucosae Stained for Human Fibronectin

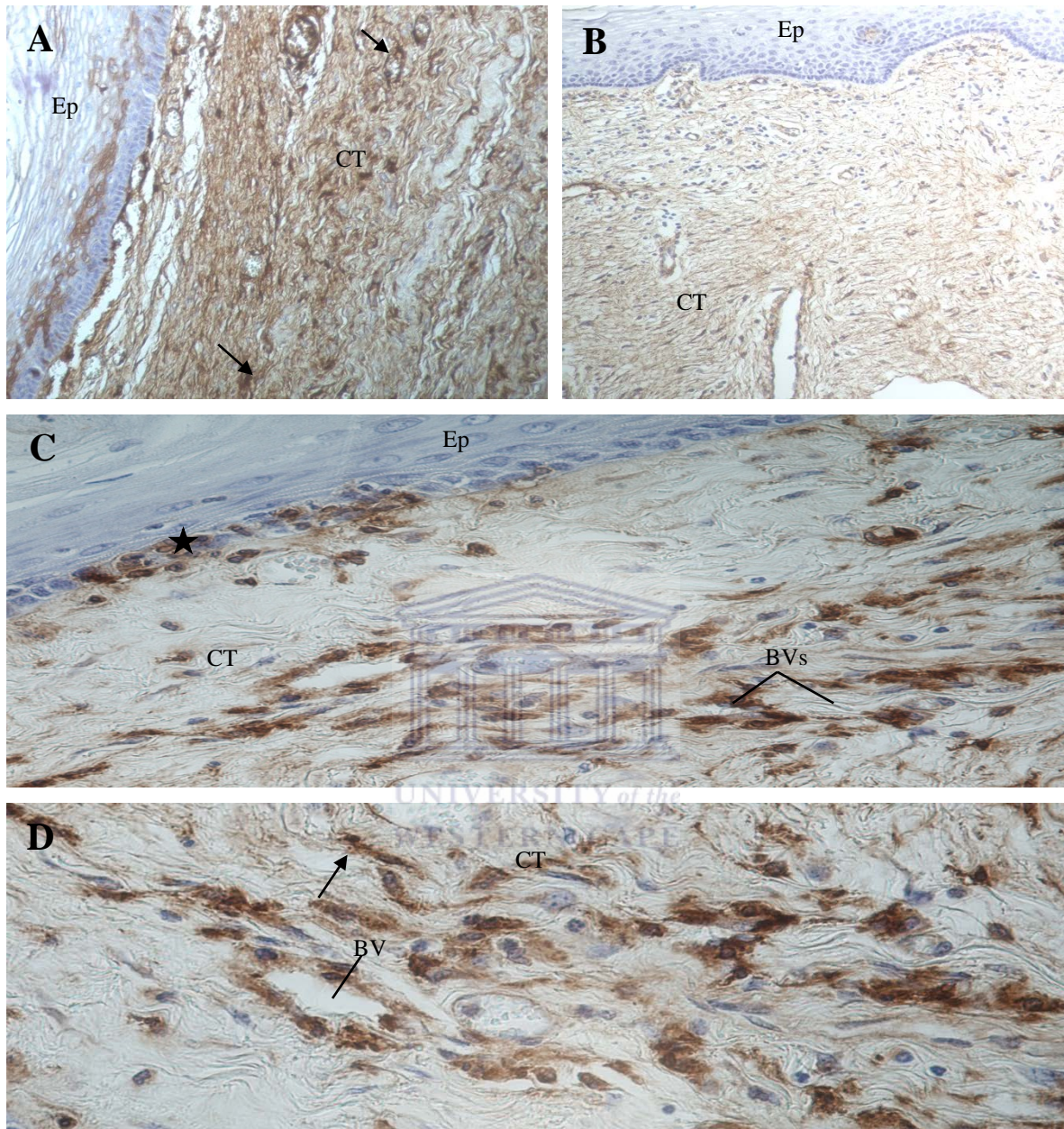


Figure 4.18. Immunohistochemical Staining of Human Fibronectin on Vaginal Mucosal Tissues. Fibronectin staining performed on (A) and (B) normal vaginal tissues. (C) and (D) xenografted vaginal tissues. Small arrows indicate positive and uniformly stained connective tissue. Blood vessels are also stained positively. A star denotes positive expression of fibronectin along the basement membrane of that particular vaginal tissue. Ep-Epithelium; CT-Connective Tissue; BVs-Blood Vessels. (*Magnifications X200 for A, B, and X400 for C, D*).

4.8.4 Photomicrographs of Human and Murine Tissues Stained for Mouse Fibronectin

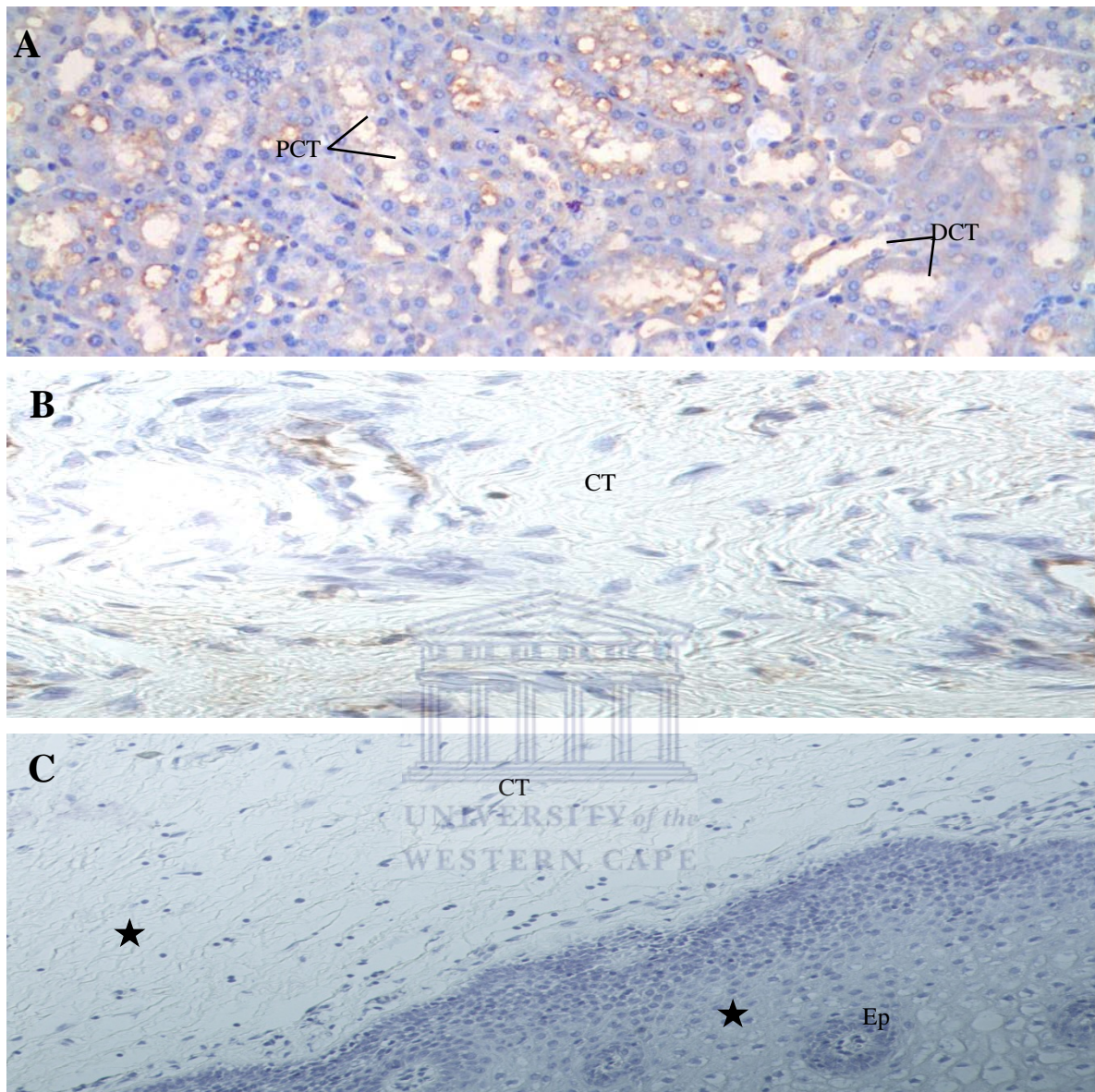


Figure 4.19. Immunohistochemical Staining of Mouse Fibronectin on Human and Murine Tissues. Fibronectin staining performed on (A) positive control - mouse kidney tissue (B) and (C) xenografted vaginal tissues. Stars indicate negative expression of mouse fibronectin throughout the connective tissue and the epithelium. PCT-Proximal Convoluted Tubules; DCT-Distal Convoluted Tubules; Ep-Epithelium; CT-Connective Tissue. (*Magnifications X200 for A, C and X400 for B.*)

4.9 LANGERHANS CELLS EXPRESSION PROFILE

4.9.1 Immunohistochemical Scores for Langerhans Cells

Staining patterns observed for human Langerhans cells (LCs) were varied in both normal and xenografted tissues. Positive staining of human LCs was scattered across the epithelium, particularly on the basal and parabasal layers (Figure 4.21). Human LCs were positively expressed in all normal tissues. In general, xenografted tissues stained positively for LCs, with only 3 of 10 tissues having stained negatively. Mouse LCs were negatively stained in 8 of 10 xenografted tissues (Table 4.9)

Table 4.9: Immunohistochemical Scoring of Human Vaginal Mucosa for Langerhans Cells. Scores reflect the difference in the staining intensity between normal vaginal tissues and xenografted vaginal tissues. The following antibodies were used (A) Mouse anti-human monoclonal Ab; (B) Mouse anti-human monoclonal Ab; and (C) Rabbit anti-mouse monoclonal Ab.

Tissue Reference No.	Immunohistochemical Score		
	Normal Vaginal Tissue	Xenografted Vaginal Tissues	
	(A) NCL-CD1A-235 Ab	(B) NCL-CD1A-235 Ab	(C) LS-C735 Ab
15392/06	4	0	0
15396/06	4	3	1
16173/06	4	2	1
16176/06	1	1	0
8961/06	1	1	0
8926/06	2	3	0
10156/06	2	0	0
10159/06	1	0	0
17560/06	1	3	0
10501/06	1	1	0

*Scoring System; 0-Negative Staining; 1-Poor Staining (10-25%); 2-Rare Positive Staining (25-50%); 3-Some Positive Staining (50-75%); 4-Strong Uniform Positive Staining (>75%).

NCL-CD1A-235 - Reference Code for Human Langerhans Cells Antibody; LS-C735 - Reference Code for Mouse Langerhans Cells Antibody; Ab - Antibody.

4.9.2 Statistical Comparisons of Langerhans Cells' Staining Intensities

Mean staining intensities for Langerhans cells in NVT, XVT-h and XVT-m were 2.1 ± 0.4333 , 1.4 ± 0.4000 and 0.2 ± 0.1333 , respectively. Mean staining intensities for NVT^α , XVT^α -h and XVT^α -m were 4.0 ± 0.0000 , 0.3 ± 0.1528 and 0.0 ± 0.0000 , respectively. Repeated-measures one-way ANOVA with subsequent Friedman's test (Friedman Statistic=40.55) indicated significant differences in the mean staining intensities between the tissue groups ($P < 0.0001$). Further statistical analysis with Dunn's multiple comparison test showed significant differences between NVT and XVT-m and between NVT and XVT^α -m ($P < 0.05$). A moderate significant difference was reported between NVT^α and XVT^α -h ($P < 0.05$). A high statistically significant difference was reported between; NVT^α and XVT-m, NVT^α and XVT^α -m ($P < 0.05$).

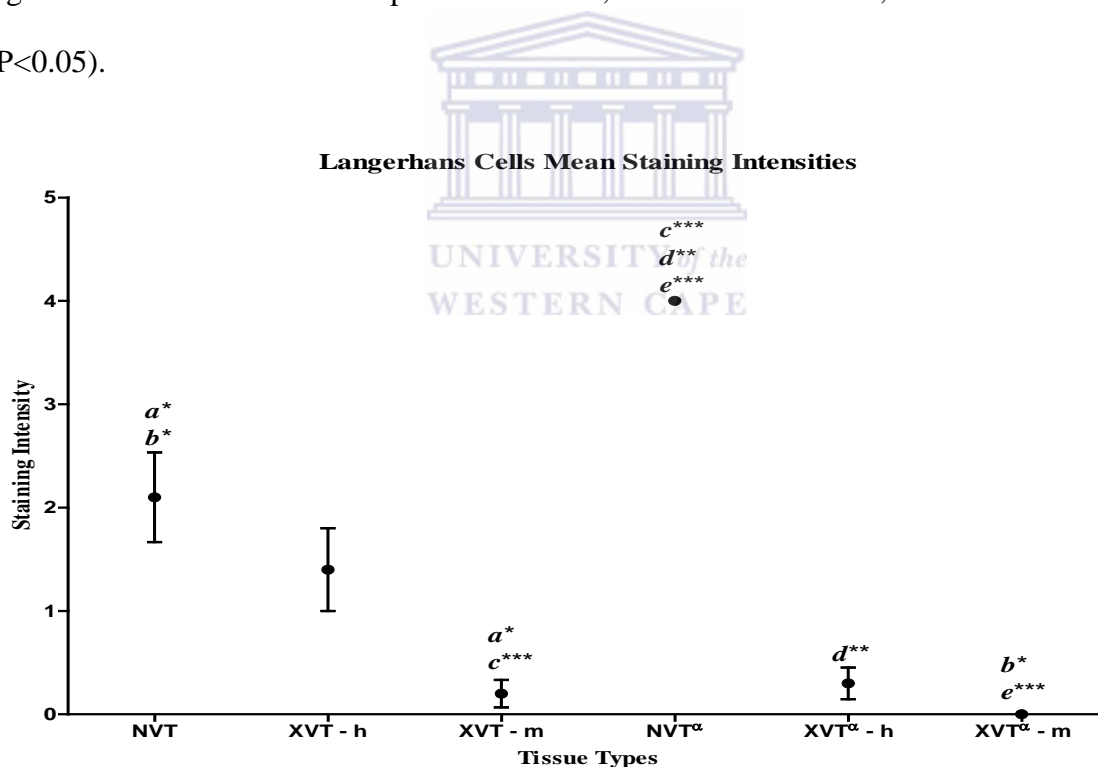


Figure 4.20: Mean Langerhans Cells Staining Intensity by Vaginal Mucosal Type. Data is expressed as mean \pm standard error of mean (n=10). Friedman's test indicates that tissue types are significantly different ($P < 0.0001$). Further analysis with Dunn's post test specifies tissue types that are significantly different ($P < 0.05$) as denoted by similar alphabets.

NVT-Normal Vaginal Tissue; XVT-Xenografted Vaginal Tissue; $^\alpha$ Corne Kok-Unpublished Work; h- Human Antigen Localization; m-Mouse Antigen Localization.

*Significant; **Very Significant; ***Extremely Significant

4.9.3 Photomicrographs of Vaginal Mucosae Stained for Human Langerhans Cells

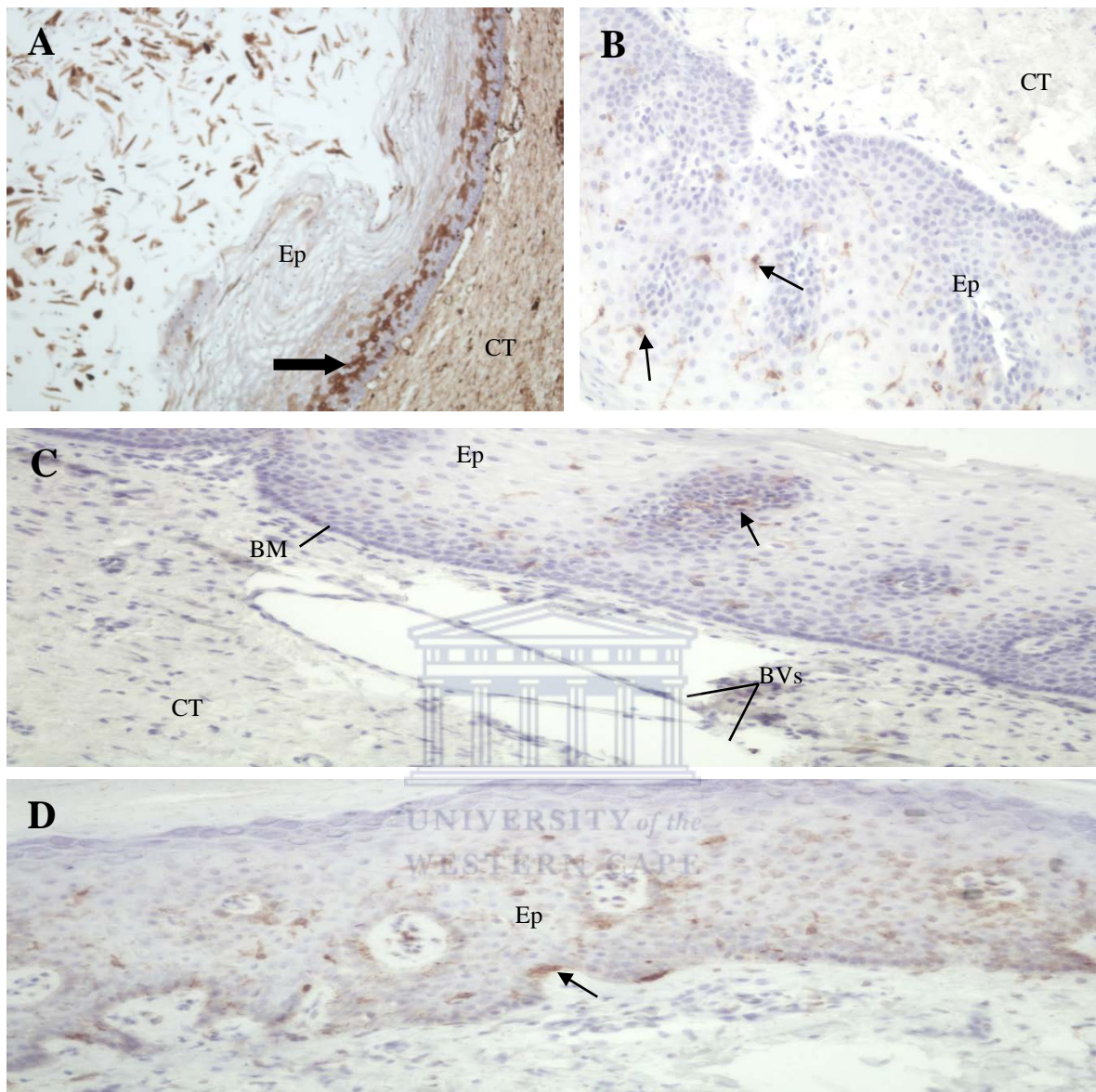


Figure 4.21. Immunohistochemical Staining of Human Langerhans Cells on Vaginal Mucosal Tissues. Langerhans cells staining performed on (A) and (B) normal vaginal tissues. (C) and (D) xenografted vaginal tissues. Small arrows point to positively expressed LCs along the epithelium. Big arrow points to a strong and uniformly stained basal epithelial layer of this particular normal tissue. Ep-Epithelium; BM-Basement Membrane; CT-Connective Tissue; BVs-Blood Vessels. (*Magnifications X100 for A and X200 for B, C, D*).

4.9.4 Photomicrographs of Human and Murine Tissues Stained for Mouse Langerhans Cells

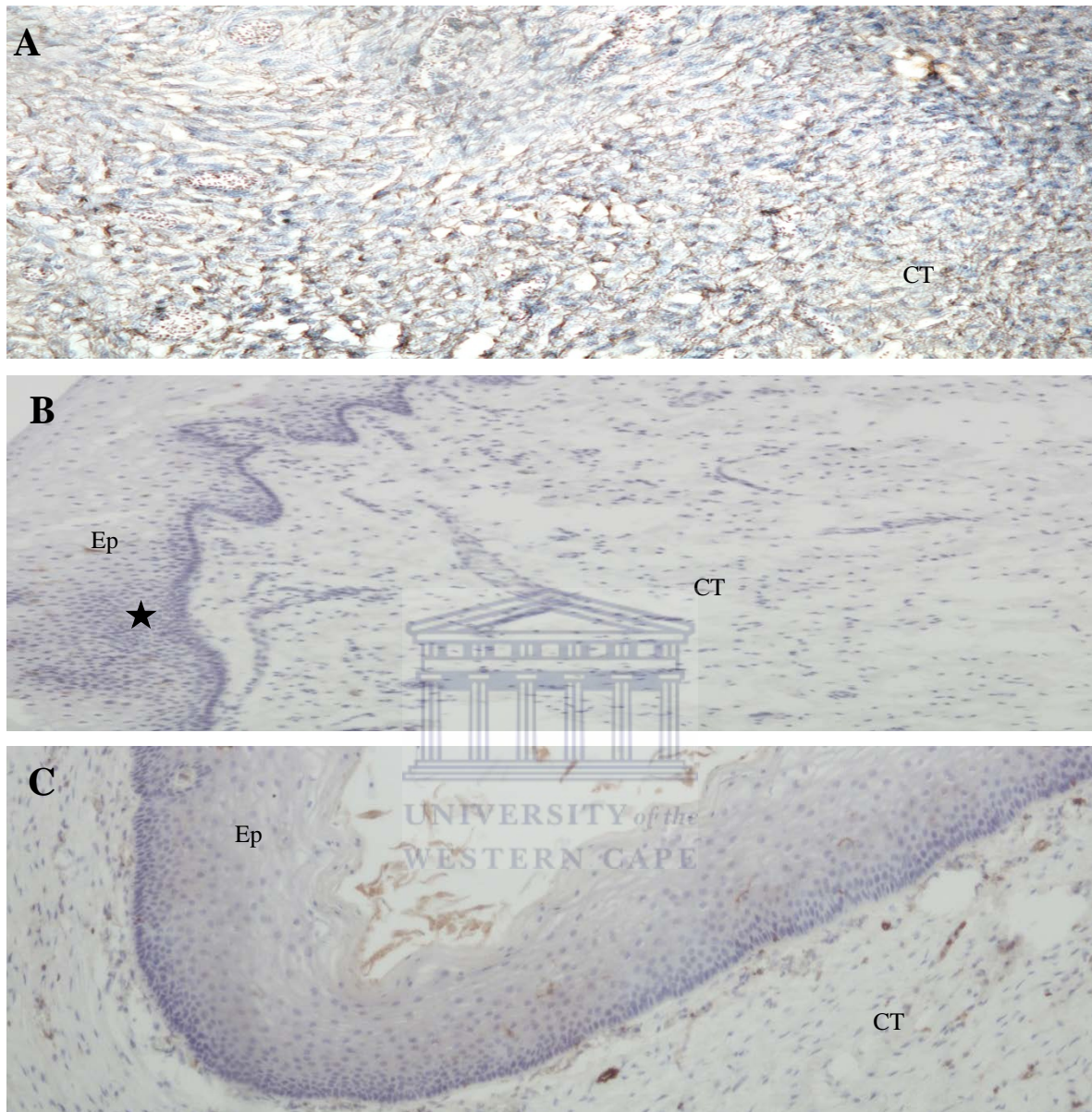


Figure 4.22. Immunohistochemical Staining of Mouse Langerhans Cells on Human and Murine Tissues. Langerhans cell staining performed on (A) and (B) normal vaginal tissues. (C) xenografted vaginal tissues. A star indicates that LCs are negatively expressed along the epithelium. Ep-Epithelium; CT-Connective Tissue. (*Magnifications X100 for B, C and X200 for A*).

4.10 VASCULAR ENDOTHELIAL GROWTH FACTOR RECEPTOR EXPRESSION PROFILE

4.10.1 Immunohistochemical Scores for VEGFR

Human VEGFR-3 did not show any obvious cytoplasmic staining reaction in all tissues. 5 of 10 normal tissues showed a very weak scattered positivity on some areas of the connective tissue whereas the other 5 normal tissues were completely negative. 9 of 10 xenografted tissues stained negatively for human VEGFR-3. All xenografted tissues displayed absolutely no reactivity for mouse VEGFR-2 (Table 4.10).

Table 4.10: Immunohistochemical Scoring of Human Vaginal Mucosa for VEGFR-3 and VEGFR-2. Scores reflect the difference in the staining intensity between normal vaginal tissues and xenografted vaginal tissues. The following antibodies were used (A) Mouse anti-human monoclonal Ab raised against VEGFR-3; (B) Mouse anti-human monoclonal Ab raised against VEGFR-3; and (C) Rabbit anti-mouse monoclonal Ab raised against VEGFR-2.

Tissue Reference No.	Immunohistochemical Score		
	<u>Normal Vaginal Tissue</u>	<u>Xenografted Vaginal Tissues</u>	
	(A) NCL-L-VEGFR-3 Ab	(B) NCL-L-VEGFR-3 Ab	(C) V2110-17C2 Ab
15392/06	1	0	0
15396/06	1	0	0
16173/06	1	0	0
16176/06	1	0	0
8961/06	1	0	0
8926/06	0	0	0
10156/06	0	1	0
10159/06	0	0	0
17560/06	0	0	0
10501/06	0	0	0

*Scoring System; 0-Negative Staining; 1-Poor Staining (10-25%); 2-Rare Positive Staining (25-50%); 3-Some Positive Staining (50-75%); 4-Strong Uniform Positive Staining (>75%).

NCL-L-VEGFR-3 - Reference Code for Human VEGFR-3 Antibody; V2110-17C2 - Reference Code for Mouse VEGFR-2 Antibody; Ab - Antibody.

4.10.2 Statistical Comparisons of VEGFR Staining Intensities

Mean staining intensities for VEGFR-3 in NVT, XVT-h, NVT^α and XVT^α-h were 0.5±0.1667, 0.1±0.1000, 0.0±0.0000 and 0.0±0.0000, respectively. Mean staining intensities for VEGFR-2 in XVT-m and XVT^α-m were both 0.0±0.0000. Repeated-measures one-way ANOVA with subsequent Friedman's test (Friedman Statistic=20.00) showed significant differences in the mean staining intensities between the tissue groups (P=0.0012). However, according to Dunn's multiple comparison test, there were no statistically significant differences between the tissue groups (P>0.05).

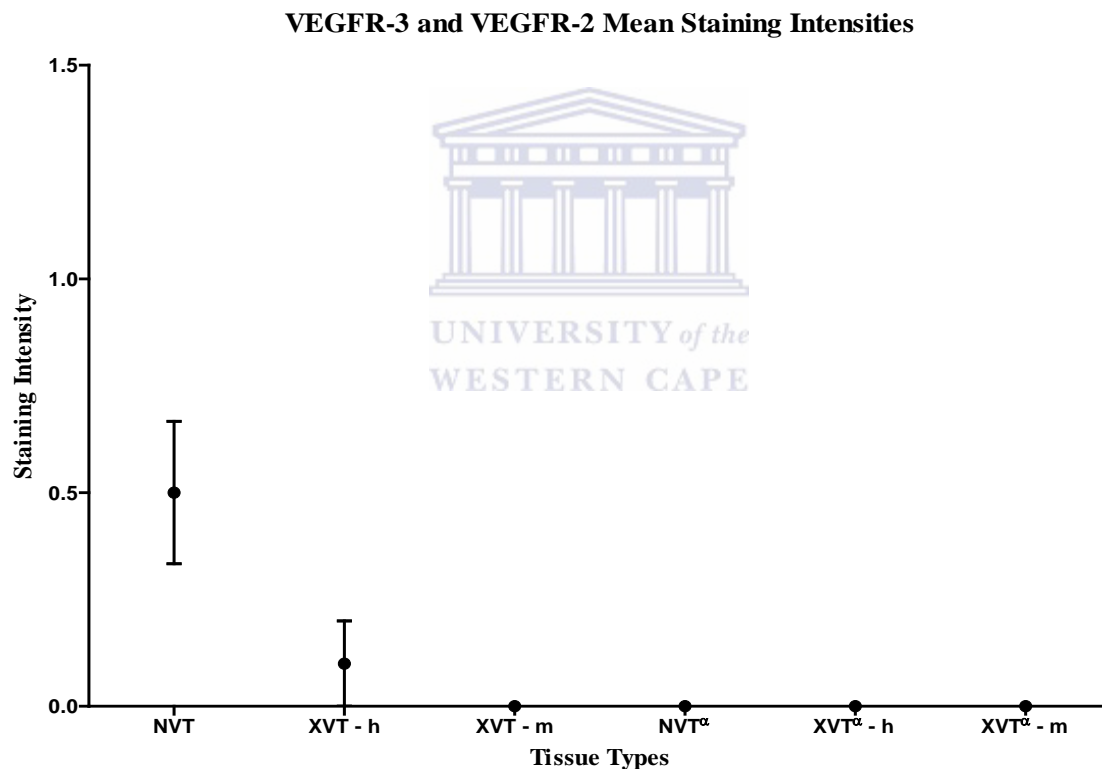


Figure 4.23: Mean VEGFR-3 and VEGFR-2 Staining Intensity by Vaginal Mucosal Type. Data is expressed as mean ± standard error of mean (n=10). Friedman's test indicates a statistical difference between tissue types (P=0.0012). Conversely, Dunn's post test does not show any statistical difference between tissue types (P>0.05).

NVT-Normal Vaginal Tissue; XVT-Xenografted Vaginal Tissue; ^αCorne Kok-Unpublished Work; h-Localization of Human VEGFR-3 Antigens; m-Localization of Mouse VEGFR-2 Antigens.

4.10.3 Photomicrographs of Vaginal Mucosae Stained for VEGFR

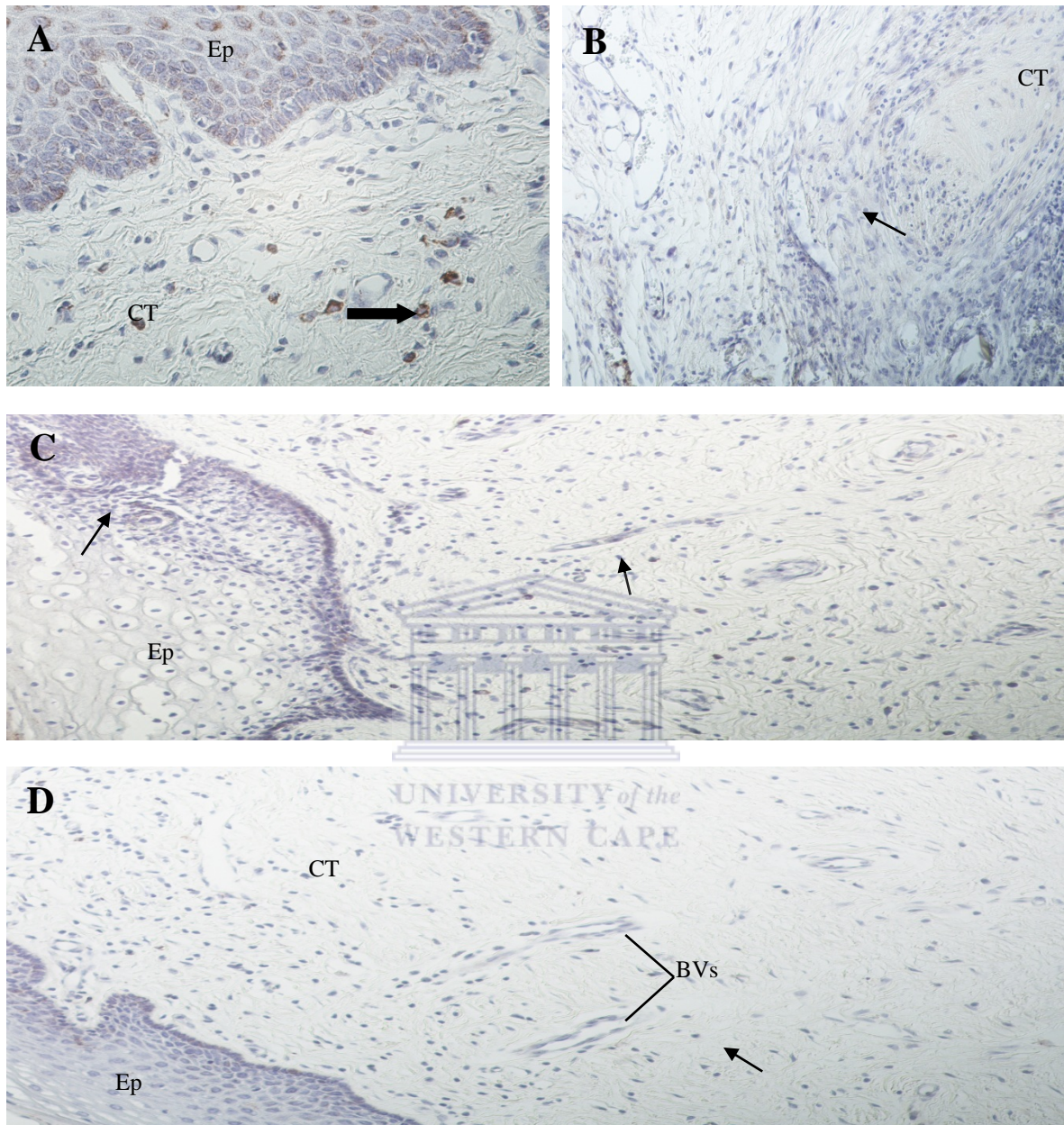


Figure 4.24. Immunohistochemical Staining of VEGFR-3 and VEGFR-2 on Human Vaginal Mucosal Tissues. VEGFR-3 staining performed on (A) normal and (B) xenografted vaginal tissues. VEGFR-2 staining performed on (C) normal and (D) xenografted vaginal tissues. Small arrows point to negatively expressed VEGFR along the epithelium, the connective tissue and around blood vessels. Big arrow points to a light positive staining of VEGFR-3 on the connective tissue. Ep-Epithelium; CT-Connective Tissue; BVs-Blood Vessels. (*Magnifications X200 for B, C, D and X400 for A.*)

CHAPTER FIVE

DISCUSSION AND CONCLUSION

As already stated, there is only one immunohistochemical study of the biocyst model proposed by Thompson *et al.*, [4] Therefore our results will be discussed in relation to that one immunohistochemical work done by Kok [6]. The ultimate goal of this chapter was to use data obtained to elucidate the nature of the epithelium, the basement membrane (BM) and stromal layer that had formed between the xenografted epithelial cyst and its surrounding mouse tissue.

5.1 INTERPRETATION OF RESULTS

5.1.1 Analysis of Cytokeratin 1 Expression Profile

Cytokeratin 1 (CK1) is a large keratin isotype of 68 kDa found in complex epithelia [96]. We firstly evaluated the expression pattern of human CK1 in NVTs and XVTs. CK1 was stained with mouse anti-CK1 primary antibody that reacts with squamous epithelia.

We observed in all NVTs, strong positively stained epithelial cells, particularly at the superficial and intermediate epithelial layers. In XVTs, the expression pattern of CK1 was either absent or moderate. Although our findings are consistent with those of the previous study, there is an interesting difference. Kok reported negative staining in most experimental cysts with a thin epithelium and positive staining in cysts with a thick epithelium [6]. In our study, the observed expression of CK1 was not well defined, nor was it different in XVTs with a thin or thick epithelium. Statistical analysis with Dunn's post test revealed significant differences between the staining intensity of NVTs, XVTs, NVT^α and XVT^α (P>0.05). It

therefore appears that a loss of CK1 occurred either during transplantation process or while xenografted vaginal tissues were in a mouse environment.

5.1.2 Analysis of Cytokeratin 5 Expression Profile

Cytokeratin 5 (CK5) is 58 kDa intermediate filament protein of the basal epithelial layer of various tissues [97, 98]. CK5 is considered a marker of basal epithelial cells and myoepithelial cells of normal breast tissue. In addition, it has been reported as a progenitor cell marker in neoplastic tissues [97, 99]. We evaluated the expression of human CK5 by staining tissues with mouse anti-CK5 monoclonal antibody.

The epithelium was considered positive when distinct cytoplasmic staining was present. The epithelium exhibited CK5 positive material in both NVTs and XVTs. Positive reaction of CK5 was localized to the parabasal and basal epithelial layers. CK5 staining was well defined and uniformly distributed in NVTs. Conversely, some XVTs exhibited occasional interruptions in the staining patterns observed. Similarly, Kok also reported even and uneven staining in NVTs and XVTs respectively. Despite qualitative differences in the staining patterns between NVTs and XVTs, statistical analysis with Dunn's post test revealed no significant differences between NTVs, XVTs, NVT^a and XVT^a ($P>0.05$).

5.1.3 Analysis of Cytokeratin 13 Expression Profile

Cytokeratin 13 (CK13) is an acidic intermediate filament protein of 54 kDa. It is the primary constituent of squamous, non-keratinized epithelium, transitional epithelium and pseudostratified epithelium. CK13 is often used as a marker of various epithelium-derived cancers [100]. Human CK13 was stained with mouse anti-CK13 monoclonal antibody.

Data presented herein indicates positive staining of CK13 in both NVTs and XVTs (Table 4.3). Positive staining was predominantly localized to the parabasal epithelial layer. In some tissues, positive staining of the BM was also noticed. Moreover, the staining intensity seen in

NVTs was greater than that exhibited by XVTs. This contradicts findings of previous work, in which a similar strong uninterrupted staining was reported in all vaginal tissues. Nevertheless, further statistical comparisons demonstrate no significant differences in the mean staining intensities between NVTs, XVTs, NVT^α and XVT^α (P>0.05). Therefore, we can confidently state that, although slight differences in the expression patterns between NVTs and XVTs were observed, human CK13 was indeed retained in a murine environment.

5.1.4 Analysis of Cytokeratin 14 Expression Profile

Cytokeratin 14 (CK14) is a member of the family of acidic type I cytokeratins [101] expressed by myoepithelial cells [102]. CK14 is expressed in the basal layer of stratified squamous and non-squamous epithelia [101, 103]. Human CK14 was stained with LL002, a sensitive monoclonal antibody that can distinguish stratified epithelial cells from simple epithelial cells.

CK14 was detected as cytoplasmic staining in the basal epithelial layer of vaginal tissues. Intense positive expression of CK14 was reported in all NVTs and XVTs. Statistical comparisons revealed no significant differences between NVTs, XVTs, NVT^α and XVT^α (P>0.05). A relatively strong expression of CK14 in both NVTs and XVTs reflects that this human marker is entirely maintained in a murine environment.

5.1.5 Analysis of Collagen Type IV Expression Profile

The ECM plays a critical role in cell migration, proliferation and differentiation [21, 45]. Degradation of the ECM is implicated in many physiological and pathological conditions. ECM degradation is characterized by several factors, including a reduction of collagen and elastin fiber networks. In this section, we also explored whether or not transplantation leads to a loss of collagen IV, the major constituent of BMs. Tissues were stained with mouse anti-

human antibodies and rabbit anti-mouse antibodies that recognize human and mouse collagen IV respectively. The antibodies react positively with the BM.

We report diffuse positive expression of human collagen IV along the BM and blood vessels in 10/10 NVTs and 7/10 XVTs (Table 4.5). Strong staining with occasional interruptions was noted in NVTs whereas XVTs presented thin staining patterns of human collagen IV. This coincides with data of Kok's study. Limited human collagen IV staining in XVTs could be due to injury incurred by the BM when the epithelium was separated from the underlying connective tissue during construction of cysts. Although mice that were used to host tissues were immune-deficient, they may still be other murine factors that contributed to a loss of human collagen IV in XVTs. Limited or absent staining of mouse collagen IV was also observed along the BM of XVTs. Interestingly, mouse collagen IV staining was not evident around blood vessels of XVTs that had stained positively along the BM. Statistical analysis shows no significant differences in the expression patterns of human collagen IV and mouse collagen IV in all vaginal tissues. Our statistical data therefore suggests no significant loss of human collagen IV after transplantation.

5.1.6 Analysis of Laminin Expression Profile

Like collagen IV, laminin is also one of the major constituents of the BM [21, 22, 48]. This large disulphide-bonded glycoprotein also occurs in the ECM, at sites other than the BM during early stages of development. Several studies have demonstrated that laminin is highly expressed in BMs of different human tissues [55]. In this section, we also examined the extent to which laminin is expressed by the BM of vaginal tissues.

As expected, human laminin was present along the BM of NVTs and XVTs. Blood vessels along the stromal layer also exhibited laminin positive material. Expression patterns of human laminin in NVTs and XVTs were relatively low to moderate. A very weak staining of

mouse laminin was observed in only 2 XVTs. Similarly, Kok also reported low to moderate expression of human laminin and negatively expressed mouse laminin. It also appears that damage to the BM could be responsible for these findings. Furthermore, our data is not consistent with published studies in which a high expression of laminin was reported [55]. This contrast could be that human tissues assessed in those studies were different from vaginal tissues and had neither been xenografted into mice. The statistical test revealed no significant differences in the staining intensities between all tissues ($P>0.05$).

5.1.7 Analysis of Elastin Expression Profile

Elastin is a polymeric protein and a major constituent of the ECM. It is a principal protein of elastic fibers that imparts elasticity to several tissues. Several literature reports indicate that elastin can change its morphology during ageing and different disease states [62, 63, 65, 66]. Here, we also investigated whether or not elastic fibers of vaginal tissues remain unchanged after transplantation.

Data presented herein indicates an intense positive staining of elastic fibers in both NVTs and XVTs. Positive staining was densely distributed across the stromal layer. In some tissues, positive staining of the BM was also noted. Interestingly, positive staining occurred in all XVTs, but in 8/10 NVTs. In addition, the staining intensity seen in XVTs was higher than that exhibited by NVTs. It is therefore suggested that increased elastin may be a secondary or reactive production of elastin by stromal cells adjacent to the cyst. This contradicts findings of the previous study, in which strong uniform staining was reported in all NVT^α and XVT^α. This discrepancy could not be explained. Nevertheless, further statistical comparisons demonstrate no significant differences between NVTs, XVTs, NVT^α and XVT^α ($P>0.05$). Therefore, we can confidently state that, elastic fibers do indeed remain the same after transplantation.

5.1.8 Analysis of Fibronectin Expression Profile

Fibronectin (FN) is a major adhesion glycoprotein that promotes interaction between epithelial cells and the ECM [67]. Vaginal tissues were stained with mouse anti-human antibodies and rabbit anti-mouse antibodies that recognize human and mouse FN respectively. The antibodies react positively with the connective tissue matrix.

Positive FN reaction was identified as brown cordlike and reticular structures along the BM, the stromal layer and around blood vessels. A moderate positive reaction of human FN was detected in NVTs and XVTs. None of the tissues reacted positively for mouse FN. These data are consistent with Kok's findings. The staining patterns reported for NVTs, XVTs, NVT^α and XVT^α were statistically different ($P < 0.05$).

5.1.9 Analysis of Langerhans Cells Expression Profile

Langerhans cells (LCs) are a group of antigen presenting cells of bone marrow origin which mainly reside on basal and suprabasal epithelial layers [104]. LCs are highly effective and play a vital role in the regulation of immune surveillance of mucosal barriers [13, 78]. Epidermal LCs can be identified using a number of markers. Accurate identification of LCs requires stable markers that are uniquely expressed on LCs [105]. Such markers include OKT6, Leu6 and CD1a. A positive staining reaction with such markers is regarded as the 'gold standard' for the identification of LCs [106]. CD1a is considered an exceptional marker, because unlike other markers, it stains both the dendrites and Birbeck granules contained within a cell body [105]. Several studies often use CD1a for the quantification of LCs in various human tissues. Therefore, in this study, human LCs were stained with CD1a. Mouse LCs were stained with Langerin (CD207).

Human LCs were detected as CD1a-positive brown stained cells in all NVTs and XVTs. Positively expressed human LCs with defined dendrites were localized to the basal and

suprabasal epithelial layers. Mouse LCs were negatively expressed in 8/10 tissues. Strikingly, when mouse skin was used as a positive control and stained with Langerin, the result remained negative despite attempts to optimize the experiment. Such an observation raises the question why mouse LCs were not functional. A weak positive staining observed in 2 XVTs may have been a false-positive result. Statistical comparisons revealed significant differences between the staining intensities of NVTs, XVTs, NVT^α and XVT^α (P<0.05). It appears that human LCs are not entirely sustained in a murine environment because their expression was greater in NVTs than XVTs. A well-defined dendritic morphology of human LCs observed in NVTs could reflect optimal immune surveillance of vaginal tissue prior to transplantation.

5.1.10 Analysis of Vascular Endothelial Growth Factor Receptor Expression Profile

Lymphatic vasculature plays a critical role in tumor metastasis, and as such, the mechanisms that regulate the growth of lymphatic vessels have become an attractive field in cancer research. VEGFR-3 is a key receptor for lymphangiogenic factors VEGF-C and VEGF-D. Emerging data indicates that VEGFR-3 contributes to angiogenesis, and hence its use as a marker for lymphatic vessels in several studies [107]. VEGFR-2 is a cell membrane receptor kinase expressed by endothelial cells and hematopoietic cells. VEGFR-2 is the main mediator of VEGF-A biological activity is actively involved in embryonic angiogenesis and hematopoiesis [83]. Human VEGFR-3 was stained with mouse anti-human primary antibody whereas mouse VEGFR-2 was stained with rabbit anti-mouse primary antibody.

We observed in 5/10 NVTs, small brown clusters of what appeared to be positively expressed VEGFR-3 along the stromal layer. In XVTs, VEGFR-3 was only expressed in one tissue. These findings contradict those of the previous study. Although brown clusters that were

observed in NVTs were reported as positive staining of VEGFR-3, further statistical analysis with Dunn's post test revealed no significant differences between the staining intensities of all tissues ($P>0.05$). We can therefore say the degree of positivity observed in those NVTs is not meaningful to postulate that VEGFR-3 marker was indeed expressed. Furthermore, since the staining did not occur around blood vessels as expected, it could have then been false-positive results. None of the tissues expressed mouse VEGFR-2, and this coincides with the immunohistochemical results of the previous study.

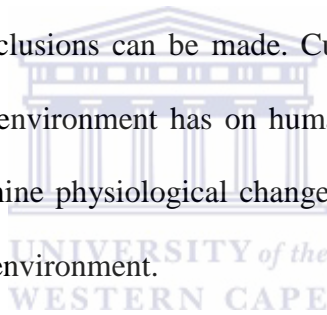
5.2 CONCLUSION

This study provides the basis for the characterization of human vaginal tissues that were xenografted into athymic nude mice. Immunohistochemical analysis of a panel of human and murine markers was performed to determine whether or not the morphology of human vaginal epithelium is retained after transplantation into a murine environment. The ultimate goal was to determine the nature of the stromal layer that had developed between xenografted cysts and mouse tissues.

Firstly, given that human cytokeratins were positively and strongly expressed on the epithelium of xenografted tissues, we can confidently state that the epithelium of the xenograft was still of human origin. Moreover, positively expressed human Langerhans cells and negatively expressed mouse Langerhans cells on the epithelium confirm this statement. Morphology of the epithelium is indeed retained despite transplantation into a murine environment, thus reaffirming findings of previous work. Secondly, although mouse collagen and mouse laminin were positively expressed in a few xenografted tissues, the degree of positivity was not as well defined as it was with human collagen IV and human laminin. However, there were no statistical differences in the staining intensities between human and mouse markers. These data are inconclusive and we can therefore only speculate that the BM

is mainly, but not entirely of human origin. Thirdly, human elastin and human fibronectin reacted positively with the stromal layer. Only one xenografted tissue reacted positively for human VEGRF-3. On the contrary, negative expression of mouse fibronectin and mouse VEGRF-2 was reported in most of the xenografted tissues. These expression patterns are very different from those of the previous study. According to our data, the stromal layer is of human origin. We therefore cannot agree with one of Kok's conclusions which suggested that the stromal layer is a combination of human and murine tissue. However, the fatty-tissue muscular layer interface at the periphery of the stroma is indeed a combination of human and murine tissue as suggested in the previous study.

In summary, the concept of 'cyst transplantation' is attractive, but it requires continued efforts before any definitive conclusions can be made. Currently, little is known about the effect that athymic nude mouse environment has on human vaginal cysts. Therefore, more information is required to determine physiological changes that occur when human vaginal tissues are subjected to a murine environment.



CHAPTER SIX

LIMITATIONS OF THE STUDY AND FUTURE PROSPECTS

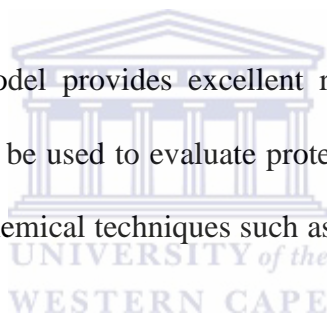
6.1 PROBLEMS ENCOUNTERED AND RECOMMENDATIONS

- The number of experimental cysts was not sufficient because cysts that had been ruptured and inflamed were excluded from the study. It is therefore important to construct a large number of cysts, to cover for any mishaps. In addition, a large number of cysts could provide a more comprehensive statistical data.
- Staining patterns with some rabbit anti-mouse primary antibodies could not be interpreted, making it difficult to award scores.
- Some slight background staining was noted in a few tissues. Since the antibodies used were monoclonal, we can disregard the fact that background staining could be due to non-specific antibody binding. We can therefore only suggest that the presence of endogenous enzymes was responsible for background staining. Working dilution of the antibodies could be increased to address this issue.

6.2 FUTURE DIRECTIONS

- We aim to gain further insight into the underlying mechanisms and factors that contributed to morphological changes that were observed in the xenografted human vaginal tissues.

- We intend to implement an *in vivo* biotest model integrating various human tissue types. The different tissues types will be xenografted to investigate whether their natural-tissue architecture is retained.
- Our future objective is to include a large panel of antibodies for each marker in order to determine any discrepancies in the expression patterns of human and murine markers.
- In a study by Sivard *et al.*, [80] an *in vitro* reconstructed vaginal mucosa incorporating Langerhans cells was developed. Such an *in vitro* culture model offers a great opportunity for a study that compares fresh human vaginal mucosa with reconstructed vaginal mucosa.
- Athymic nude mouse model provides excellent research opportunities for several studies. This model could be used to evaluate protein and gene expression of various human tissues using biochemical techniques such as polymerase chain reaction (PCR) and Western blot analysis.



REFERENCES

- [1] Morton CL, Houghton PJ: **Establishment of Human Tumor Xenografts in Immunodeficient Mice.** *Nature Protocols* 2007, **2**(2):247-250.
- [2] Yue W, Zhou D, Chen S, Brodie A: **A New Nude Mouse Model for Postmenopausal Breast Cancer Using MCF-7 Cells Transfected with the Human Aromatase Gene.** *Cancer Research* 1994, **54**:5092-5095.
- [3] Topley P, Jenkins DC, Jessup EA, Stables EN: **Effect of Reconstituted Basement Membrane Components on the Growth of a Panel of Human Tumour Cell Lines in Nude Mice.** *British Journal of Cancer* 1993, **67**:953-958.
- [4] Thompson IO, Van Wyk CW, Darling MR: **Human Vaginal Epithelium and the Epithelial Lining of a Cyst Model Constructed from it: A Comparative Light Microscopic and Electron Microscopic Study.** *South African Dental Journal* 2001, **56**(11):517-520.
- [5] Wang M: **Contamination, Infection and Inflammation Control in an Experimental Mucosal Cyst Model using Athymic Nude Mice.** *MSc Thesis.* University of the Western Cape; 2007.
- [6] Kok CW: **Molecular Characterization of Human Vaginal Mucosa obtained from Fresh Harvest and Implants in an Experimental Nude Mouse Model.** *MSc Thesis.* University of Stellenbosch; 2010.
- [7] Carroll AR, Coleman RL, Sood AK: **Therapeutic Advances in Women's Cancers.** *Front Bioscience* 2011, **3**:82-97.
- [8] Schmied BM, Ulrich AB, Matsuzaki H, El-Metwally TH, Ding X, Fernandes ME, Adrian TE, Chaney WG, Batra SK, Pour PM: **Biological Instability of Pancreatic Cancer Xenografts in the Nude Mouse.** *Carcinogenesis* 2000, **21**(6):1121-1127.
- [9] Johansson EL, Rudin A, Wassen L, Holmgren J: **Distribution of Lymphocytes and Adhesion Molecules in Human Cervix and Vagina.** *Immunology and Infectious Diseases* 1999, **96**:272-277.
- [10] Kerbel RS: **Human Tumor Xenografts as Predictive Preclinical Models for Anticancer Drug Activity in Humans.** *Cancer Biology and Therapy* 2003, **2**(4):134-139.
- [11] Abdul-Karim FW, Somrak TM, Yang B: **Chapter 11 - Vulva, Vagina and Anus.** In: *Comprehensive Cytopathology (3rd Edition).* Edinburgh: W.B. Saunders; 2008: 273-289.
- [12] Haschek WM, Rousseaux CG, Wallig MA: **Chapter 19 - Female Reproductive System.** In: *Fundamentals of Toxicologic Pathology (2nd Edition).* San Diego: Academic Press; 2010: 599-631.
- [13] Black CA, Murphy-Corb M: **Chapter 30 - Dendritic Cells in the Reproductive Tract.** In: *Dendritic Cells (2nd Edition).* London: Academic Press; 2001: 411-421.
- [14] Squier CA, Mantz MJ, Schlievert PM, Davis CC: **Porcine Vagina Ex Vivo as a Model for Studying Permeability and Pathogenesis in Mucosa.** *Pharmaceutical Sciences* 2008, **97**(1):9-21.
- [15] Miller CJ, Shattock RJ: **Target Cells in Vaginal HIV Transmission.** *Microbes and Infection* 2003, **5**:59-67.
- [16] Zeng Z, Cohen AM, Guillem JG: **Loss of Basement Membrane Type IV Collagen is Associated with Increased Expression of Metalloproteinases 2 and 9 (MMP-2 and MMP-9) during Human Colorectal Tumorigenesis.** *Carcinogenesis* 1999, **20**(5):749-755.

- [17] Egeblad M, Rasch MG, Weaver VM: **Dynamic Interplay between the Collagen Scaffold and Tumor Evolution.** *Current Opinion in Cell Biology* 2010, **22**(5):697-706.
- [18] Tanzer ML: **Current Concepts of Extracellular Matrix.** *Orthopaedic Science* 2006, **11**(3):326-331.
- [19] Sherwood DR: **Cell Invasion through Basement Membranes: An Anchor of Understanding.** *Trends in Cell Biology* 2006, **16**(5):250-256.
- [20] Schwarzbauer J: **Basement Membrane: Putting up the Barriers.** *Current Biology* 1999, **9**:242-244.
- [21] Kruegel J, Miosge N: **Basement Membrane Components are Key Players in Specialized Extracellular Matrices.** *Cellular and Molecular Life Sciences* 2010, **67**(17):2879-2895.
- [22] LeBleu VS, MacDonald B, Kalluri R: **Structure and Function of Basement Membranes.** *Experimental Biology and Medicine* 2007, **232**(9):1121-1129.
- [23] Chi C, Wang S, Prenter A, Cooper S, Wojnarowska F: **Basement Membrane Zone and Dermal Extracellular Matrix of the Vulva, Vagina and Amnion: An Immunohistochemical Study with Comparison with Non-Reproductive Epithelium.** *Australasian Journal of Dermatology* 2010, **51**:243-247.
- [24] Steukers L, Glorieux S, Vandekerckhove AP, Favoreel HW, Nauwynck HJ: **Diverse Microbial Interactions with the Basement Membrane Barrier.** *Trends in Microbiology* 2012, **20**(3):147-155.
- [25] Wetzels RHW, Robben HCM, Leigh IM, Schaafsma HE, Vooijs GP, Ramaekers FCS: **Distribution Patterns of Type VII Collagen in Normal and Malignant Human Tissues.** *American Journal of Pathology* 1991, **139**(2):451-459.
- [26] Kariya Y, Miyazaki K: **The Basement Membrane Protein Laminin-5 Acts as a Soluble Cell Motility Factor.** *Experimental Cell Research* 2004, **297**(2):508-520.
- [27] Guess CM, Quaranta V: **Defining the Role of Laminin-332 in Carcinoma.** *Matrix Biology* 2009, **28**(8):445-455.
- [28] Tzu J, Marinkovich MP: **Bridging Structure with Function: Structural, Regulatory, and Developmental Role of Laminins.** *International Journal of Biochemistry and Cell Biology* 2008, **40**(2):199-214.
- [29] Ray MC, Gately LE: **Basement Membrane Zone.** *Clinics in Dermatology* 1996, **14**:321-330.
- [30] Kramer JM: **Chapter 1 - Basement Membranes.** In: *The C elegans Research Community, WormBook*. Chicago: WormBook; 2005: 1-15.
- [31] Watkins J, Mathieson I: **Chapter 4 - Connective tissues.** In: *The Pocket Podiatry Guide: Functional Anatomy*. Edinburgh: Churchill Livingstone; 2009: 107-156.
- [32] Hadju SI, Lemos LB, Kozakewich H, Helson L, Beattie EJ: **Growth Pattern and Differentiation of Human Soft Tissue Sarcomas in Nude Mice.** *Cancer* 1981, **47**(1):90-98.
- [33] Sachs DH, Sykes M, Robson SC, Cooper DKC: **Xenotransplantation.** *Advances in Immunology* 2001, **79**:129-223.
- [34] Ikeda K, Tate G, Suzuki T, Mitsuya T: **Coordinate Expression of Cytokeratin 8 and Cytokeratin 17 Immunohistochemical Staining in Cervical Intraepithelial Neoplasia and Cervical Squamous Cell Carcinoma: An Immunohistochemical Analysis and Review of the Literature.** *Gynecologic Oncology* 2008, **108**:598-602.
- [35] Barrett AW, Cort EM, Patel P, Berkovitz BKB: **An Immunohistological Study of Cytokeratin 20 in Human and Mammalian Oral Epithelium.** *Archives of Oral Biology* 2000, **45**:879-887.

- [36] Bakhtiar Y, Hirano H, Arita K, Yunoue S, Fujio S, Tominaga A, Sakoguchi T, Sugiyama K, Kurisu K, Yasufuku-Takano K *et al*: **Relationship Between Cytokeratin Staining Patterns and Clinicopathological Features in Somatotropinomas**. *European Journal of Endocrinology* 2010, **163**:531-539.
- [37] Barnard K, Gathercole LJ, Bailey AJ: **Basement Membrane Collagen - Evidence for a Novel Molecular Packing**. *FEBS Letters* 1987, **212**(1):49-52.
- [38] Kefalides NA, Zahra Z: **Chapter 12 - Connective Tissues and Aging**. In: *Brocklehurst's Textbook of Geriatric Medicine and Gerontology (7th Edition)*. Philadelphia: W.B. Saunders; 2010: 73-81.
- [39] Ayad S, Boot-Handford R, Humphries MJ, Kadler KE, Shuttleworth A: **Chapter 15 - Collagen Type IV**. In: *The Extracellular Matrix Facts Book (2nd Edition)*. San Diego: Academic Press; 1998: 54-62.
- [40] Davidson B, Goldberg I, Gotlieb WH, Ben-Baruch G, Kopolovica J: **Expression of Matrix Proteins in Uterine Cervical Neoplasia using Immunohistochemistry**. *Obstetrics Gynecology* 1998, **76**:109-114.
- [41] Ghohestani RF, Li K, Rousselle P, Uitto J: **Molecular Organization of the Cutaneous Basement Membrane Zone**. *Clinics in Dermatology* 2001, **19**:551-562.
- [42] Kuhn K, Wiedemann H, Timpl R, Risteli J, Dieringer H, Voss T, Glanville RW: **Macromolecular Structure of Basement Membrane Collagens**. *FEBS Letters* 1981, **125**(1):123-128.
- [43] Ray JM, Stetler-Stevenson WG: **The Role of Matrix Metalloproteases and their Inhibitors in Tumour Invasion, Metastasis and Angiogenesis**. *European Respiratory* 1994, **7**:2062-2072.
- [44] Vazquez F, Palacios S, Aleman N, Guerrero F: **Changes of the Basement Membrane and Type IV Collagen in Human Skin during Aging**. *Climacteric and Postmenopause* 1996, **25**:209-215.
- [45] Indumathi S, Yin M, Taeyoung K, William K, Jacob R, Rong W: **Structural and Mechanical Profiles of Native Collagen Fibers in Vaginal Wall Connective Tissues**. *Biomaterials* 2012, **33**(5):1520-1527.
- [46] Hattori K, Mabuchi R, Fujiwara H, Sanzen N, Sekiguchi K, Kawai K, Akaza H: **Laminin Expression Patterns in Human Ureteral Tissue**. *Urology* 2003, **170**(5):2040-2043.
- [47] Hallmann R, Horn N, Selg M, Wendler O, Pausch F, Sorokin LM: **Expression and Function of Laminins in the Embryonic and Mature Vasculature**. *Physiological Reviews* 2005, **85**:976-1000.
- [48] Tsuruta D, Kobayashi H, Imanishi H, Sugawara K, Ishii M, Jones JCR: **Laminin-332-Integrin Interaction: A Target for Cancer Therapy?** *Current Medicinal Chemistry* 2008, **15**(20):1968-1975.
- [49] Cukierman E, Bassi DE: **Physico-Mechanical Aspects of Extracellular Matrix Influences on Tumorigenic Behaviors**. *Seminars in Cancer Biology* 2010, **20**:139-145.
- [50] Liotta LA: **Tumor Invasion and Metastases: Role of the Basement Membrane. Warner-Lambert Parke-Davis Award Lecture**. *American Journal of Pathology* 1984, **117**(3):339-348.
- [51] Botti J, Musset M, Moutsita R, Aubery M, Derappe C: **Two Laminin Receptors with N - Acetylglucosamine-Binding Specificity**. *Biochimie* 2003, **85**(1-2):231-239.
- [52] Macdonald PR, Lustig A, Steinmetz MO, Kammerer RA: **Laminin Chain Assembly is Regulated by Specific Coiled-Coil Interactions**. *Structural Biology* 2010, **170**(2):398-405.
- [53] Patarroyo M, Tryggvason K, Virtanen I: **Laminin Isoforms in Tumor Invasion, Angiogenesis and Metastasis**. *Cancer Biology* 2002, **12**(3):197-207.

- [54] Sanders EJ: **Chapter 5 - The Role of Extracellular Matrix during Development**. In: *Developmental Biology*. San Diego: Academic Press; 1998: 89-101.
- [55] Beliard A, Donnez J, Nisolle M, Foidart J: **Localization of Laminin, Fibronectin, E-cadherin and Integrins in Endometrium and Endometriosis***. *Fertility and Sterility* 1997, **67**(2):266-272.
- [56] Malinda KM, Kleinman HK: **The Laminins**. *Cell Biology* 1996, **28**(9):957-959.
- [57] Hamill KJ, Paller AS, Jones JCR: **Adhesion and Migration, the Diverse Functions of the Laminin α 3 Subunit**. *Dermatologic Clinics* 2010, **28**(1):79-87.
- [58] Ekblom P: **Receptors for Laminins During Epithelial Morphogenesis**. *Current Opinion in Cell Biology* 1996, **8**:700-706.
- [59] Kielty CM, Sherratt MJ, Shuttleworth CA: **Elastic Fibres**. *Cell Science* 2002, **115**(14):2817-2828.
- [60] Ross R: **The Elastic Fiber**. *Histochemistry and Cytochemistry* 1973, **21**(3):199-208.
- [61] Hushiki T: **Collagen Fibers, Reticular Fibers and Elastic Fibers. A Comprehensive Understanding from a Morphological Viewpoint**. *Archives of Histology and Cytology* 2002, **65**(2):109-126.
- [62] Mithieux SM, Weiss AS: **Elastin**. *Advances in Protein Chemistry* 2005, **70**:437-461.
- [63] Rodgers UR, Weiss AS: **Cellular Interactions with Elastin**. *Pathologie Biologie* 2005, **53**:390-398.
- [64] Sherratt MJ: **Tissue Elasticity and the Ageing Elastic Fibre**. *Age* 2009, **31**(4):305-325.
- [65] Keeley FW, Bellingham CM, Woodhouse KA: **Elastin as a Self-Organizing Biomaterial: Use of Recombinantly Expressed Human Elastin Polypeptides as a Model for Investigations of Structure and Self-Assembly of Elastin**. *The Royal Society* 2002, **357**(1418):185-189.
- [66] Gosline J, Lillie M, Carrington E, Guerette P, Ortlepp C, Savage K: **Elastic proteins: biological roles and mechanical properties**. *The Royal Society* 2002, **357**(1418):121-132.
- [67] Hynes RO, Yamada KM: **Fibronectins: Multifunctional Modular Glycoproteins**. *Cell Biology* 1982, **95**:369-377.
- [68] Faralli JA, Schwinn MK, Gonzalez JM, Filla MS, Peters DM: **Functional Properties of Fibronectin in the Trabecular Meshwork**. *Experimental Eye Research* 2009, **88**(4):689-693.
- [69] Pankov R, Kenneth MY: **Fibronectin at a Glance**. *Cell Science* 2002, **115**(20):3861-3863.
- [70] Romberger DJ: **Fibronectin**. *Cell Biology* 1997, **29**(7):939-943.
- [71] Liaw L, Crawford HC: **Functions of the Extracellular Matrix and Matrix Degrading Proteases during Tumor Progression**. *Brazilian Journal of Medical and Biological Research* 1999, **32**(1):805-812.
- [72] Blanco P, Palucka AK, Banchereau J: **Chapter 9 - Introduction to Dendritic Cells**. In: *Gene Therapy of Cancer (2nd Edition)*. San Diego: Academic Press; 2002: 167-177.
- [73] Abbott GF, Rosado-de-Christenson ML, Franks TJ, Frazier AA, Galvin JR: **From the Archives of the AFIP: Pulmonary Langerhans Cell Histiocytosis**. *Radiographics* 2004, **24**(3):821-841.
- [74] Maurer D, Stingl G: **Chapter 5 - Langerhans Cells**. In: *Dendritic Cells (2nd Edition)*. London: Academic Press; 2001: 35-51.
- [75] Romani N, Clausen BE, Stoitzner P: **Langerhans Cells and More: Langerin-Expressing Dendritic Cell Subsets in the Skin**. *Immunological Reviews* 2010, **234**(1):120-141.

- [76] Eggert AAO, Otto K, McLellan AD, Terheyden P, Linden C, Kämpgen E, Becker JC: **Chapter 12 - Generation of Human and Murine Dendritic Cells.** In: *Cell Biology (3rd Edition)*. Burlington: Academic Press; 2006: 103-112.
- [77] Villadangos JA, Young LJ: **Chapter 7 - Antigen-Presenting Cells and Antigen Presentation.** In: *Clinical Immunology (3rd Edition)*. Edinburgh: Mosby; 2008: 103-111.
- [78] Austyn JM: **Chapter 10 - Mobilization, Migration and Localization of Dendritic Cells.** In: *Dendritic Cells (2nd Edition)* London: Academic Press; 2001: 131-149.
- [79] Ueno H, Klechevsky E, Palucka AK, Banchereau J: **Chapter 19 - Human Dendritic Cell Subsets.** In: *Methods in Microbiology*. San Diego: Academic Press; 2010: 497-513.
- [80] Sivard P, Berlier W, Picard B, Sabido O, Genin C, Misery L: **HIV-1 Infection of Langerhans Cells in a Reconstructed Vaginal Mucosa.** *Infectious Diseases* 2004, **190**(2):227-235.
- [81] Shibuya M: **Vascular Endothelial Growth Factor-Dependent and -Independent Regulation of Angiogenesis.** *Biology and Molecular Biology Reports* 2008:278-286.
- [82] Ferrara N: **Vascular Endothelial Growth Factor.** *Arteriosclerosis, Thrombosis, and Vascular Biology* 2009, **29**(6):789-791.
- [83] Karamysheva AF: **Mechanisms of Angiogenesis.** *Biochemistry* 2008, **73**(7):751-762.
- [84] Kowanzetz M, Ferrara N: **Vascular Endothelial Growth Factor Signaling Pathways: Therapeutic Perspective.** *Clinical Cancer Research* 2006, **12**(17):5018-5022.
- [85] Moser C, Lang SA, Stoeltzing O: **The Direct Effect of Anti-Vascular Endothelial Growth Factor Therapy on Tumor Cells.** *Clinical Colorectal Cancer* 2007, **6**(8):564-571.
- [86] Murukesh N, Dive C, Jayson GC: **Biomarkers of Angiogenesis and their Role in the Development of VEGF Inhibitors.** *British Journal of Cancer* 2009, **102**(1):8-18.
- [87] Sullivan LA, Brekken RA: **The VEGF Family in Cancer and Antibody-Based Strategies for their Inhibition.** *Landes Bioscience* 2010, **2**(2):165-175.
- [88] Silva R, D'Amico G, Hodivala-Dilke KM, Reynolds LE: **Integrins: The Keys to Unlocking Angiogenesis.** *Arteriosclerosis, Thrombosis, and Vascular Biology* 2008, **28**(10):1703-1713.
- [89] Pennell NA, Lynch TJ: **Combined Inhibition of the VEGFR and EGFR Signaling Pathways in the Treatment of NSCLC.** *The Oncologist* 2009, **14**(4):399-411.
- [90] Nor JE, Christensen J, Mooney DJ, Polverini PJ: **Vascular Endothelial Growth Factor (VEGF)-Mediated Angiogenesis is Associated with Enhanced Endothelial Cell Survival and Induction of Bcl-2 Expression.** *American Journal of Pathology* 1999, **154**(2):375-384.
- [91] Shibuya M: **Differential Roles of Vascular Endothelial Growth Factor Receptor-1 and Receptor-2 in Angiogenesis.** *Biochemistry and Molecular Biology International* 2006, **39**(5):469-478.
- [92] Taylor CR, Shi SR, Barr NJ: **Chapter 1 - Techniques of Immunohistochemistry: Principles, Pitfalls, and Standardization.** In: *Diagnostic Immunohistochemistry (3rd Edition)*. Philadelphia: W.B. Saunders; 2011: 1-41.
- [93] Moreau A, Le Neel T, Truchaud A, Laboissee C: **Approach to Automation in Immunohistochemistry.** *Clinica Chimica Acta* 1998, **278**:177-184.
- [94] Hayat MA: **Chapter 1 - Comparison of Immunohistochemistry, in Situ Hybridization, Fluorescence in Situ Hybridization, and Chromogenic in Situ Hybridization.** In: *Handbook of*

Immunohistochemistry and in Situ Hybridization of Human Carcinomas. San Diego: Academic Press; 2004: 3-11.

- [95] Shi SR, Shi Y, Taylor CR: **Antigen Retrieval Immunohistochemistry: Review and Future Prospects in Research and Diagnosis over Two Decades**. *Histochemistry and Cytochemistry* 2011, **59**(1):13-32.
- [96] Attallah AM, El-Far M, Abdel CA, Zahran F, Farid K, Omran MM, Zagloul H, El-Deen MS: **Evaluation of Cytokeratin-1 in the Diagnosis of Hepatocellular Carcinoma**. *Clinica Chimica Acta* 2011, **412**(23-24):2310-2315.
- [97] Ramalho LNZ, Ribeiro-Silva A, Cassali GD, Zucoloto S: **The Expression of p63 and Cytokeratin 5 in Mixed Tumors of the Canine Mammary Gland Provides New Insights into the Histogenesis of These Neoplasms**. *Veterinary Pathology* 2006, **43**:424-429.
- [98] Lan Su D, Peter R, Morgan BDS, Lane BE: **Expression of Cytokeratin Messenger RNA Versus Protein in the Normal Mammary Gland and in Breast Cancer**. *Human Pathology* 1996, **27**:800-806.
- [99] Chu PG, Weiss LM: **Expression of Cytokeratin 5/6 in Epithelial Neoplasms: An Immunohistochemical Study of 509 Cases**. *Modern Pathology* 2002, **15**(1):6-10.
- [100] Raspollini MR, Fambrini M, Marchionni M, Baroni G, Taddei GL: **In Situ Adenocarcinoma and Squamous Carcinoma of Uterine Cervix Pathological and Immunohistochemical Analysis with Cytokeratin 13**. *Obstetrics and Gynecology* 2007, **134**:249-253.
- [101] Ravindranath RMH, Tam W, Bringas P, Santos V, Fincham AG: **Amelogenin-Cytokeratin 14 Interaction in Ameloblasts during Enamel Formation**. *Biological Chemistry* 2001, **276**:36586-36597.
- [102] Tse GMK, Tan PH, Lui PCW, Gilks CB, Poon CSP, Ma TKF, Law BKB, Lam WWM: **The Role of Immunohistochemistry for Smooth-Muscle Actin, p63, CD10 and Cytokeratin 14 in the Differential Diagnosis of Papillary Lesions of the Breast**. *Clinical Pathology* 2007, **60**:315-320.
- [103] Harnden P, Southgate J: **Cytokeratin 14 as a Marker of Squamous Differentiation in Transitional Cell Carcinomas**. *Clinical Pathology* 1997, **50**:1032-1033.
- [104] Se'guier S, Godeau G, Leborgne M, Pivert G, Brousse M: **Quantitative Morphological Analysis of Langerhans Cells in Healthy and Diseased Human Gingiva**. *Archives of Oral Biology* 2000, **45**:1073-1081.
- [105] Jacobs JJJ, Lehe C, Cammansa KDA, Yonedac K, Dasb PK, Elliotta GR: **An Automated Method for the Quantification of Immunostained Human Langerhans Cells**. *Immunological Methods* 2001, **247**:73-82.
- [106] Indrasingh I, Chandi G, Jeyaseelan L, Vettivel S, Chandi SM: **Quantitative Analysis of CD1a (T6) Positive Langerhans Cells in Human Tonsil Epithelium**. *Annals of Anatomy* 1999, **181**:567-572.
- [107] Petrova TV, Bono P, Holnthoner W, Chesnes J, Pytowski B, Sihto H, Laakkonen P, Heikkila P, Joensuu H, Alitalo K: **VEGFR-3 Expression Is Restricted to Blood and Lymphatic Vessels in Solid Tumors**. *Cancer Cell* 2008, **13**:554-556.

APPENDIXES

APPENDIX I

IMMUNOHISTOCHEMICAL STAINING PROTOCOL

Table I: Chronological Instructions Followed During IHC Staining

Step	Brief Description
Tissue Sectioning and Incubation	Mount paraffin-embedded tissues Incubate overnight at 26°C
Dewaxing	Deparaffinize sections in Xylene for 5 minutes Place in decreasing grades of alcohol (100%, 96% and 70%) for 2 minutes with each alcohol Rehydrate with distilled water for 2 minutes
Antigen Retrieval	Heat sections with the recommended unmasking solution (Citrate buffer, pH 6.0 for 10-15 minutes; EDTA buffer, pH 9.0 for 10-15 minutes; Pepsin for 30 minutes) Wash with PBS buffer
Peroxidase Blocking	Block sections using 3% hydrogen peroxide (H ₂ O ₂) for 5 minutes Wash with PBS buffer
Subsequent Blocking	Block with normal rabbit serum (1:20 diluted) and drain off excess without washing
Primary Antibody Incubation	Incubate sections with primary antibody at room temperature for 30 minutes Wash with PBS buffer
Biotinylated Secondary Antibody Incubation	Incubate sections with Biotinylated Secondary Link antibody at room temperature for 30 minutes Wash with PBS
Streptavidin-HPR Incubation	Incubate sections with Streptavidin-HPR at room temperature for 30 minutes Wash with PBS buffer
Chromogen Substrate	Add a solution of substrate buffer and DAB to each section Incubate at room temperature for 10 minutes
CuSO ₄ Addition	Incubate sections with CuSO ₄ at room temperature for 10 minutes
Rinsing	Rinse slides with water for 2 minutes
Counterstaining	Dip slides in Hematoxylin for 25 seconds
Rinsing	Rinse slides with water for 5 minutes

Dehydration

Rehydrate the sections by immersing in increasing grades of alcohol (70%, 96% and 100%)

Dip the sections in Xylene until clear

Mounting of Sections

Place DPX glue on the cover slips

Place the stained sections over the cover slips

Allow to air dry



APPENDIX II

IMMUNOHISTOCHEMISTRY WASHING BUFFERS

Table II: Different Concentrations of Phosphate Buffered Saline (PBS)

Concentration of the buffer	Measurement of the Constituents
10X Working PBS (0.1 M PBS, pH 7.2)	Na ₂ HPO ₄ (anhydrous) 10.9 g
	NaH ₂ PO ₄ (anhydrous) 3.2 g
	NaCl 90 g
	Distilled H ₂ O 1000 ml
20X Stock PBS Solution (0.2 M PBS, pH 7.2)	Na ₂ HPO ₄ (anhydrous) 21.8 g
	NaH ₂ PO ₄ (anhydrous) 6.4 g
	NaCl 180 g
	Distilled H ₂ O 1000 ml
Mix to dissolve the solution, adjust the pH to 7.2 using NaOH and HCl and store at room temperature.	
10X Working PBS – Tween 20 (0.1 M PBS, 0.5% Tween 20, pH 7.2)	Na ₂ HPO ₄ (anhydrous) 10.9 g
	NaH ₂ PO ₄ (anhydrous) 3.2 g
	NaCl 90 g
	Distilled H ₂ O 1000 ml
20X Stock PBS – Tween 20 Solution (0.2 M PBS, 1% Tween 20, pH 7.2)	Na ₂ HPO ₄ (anhydrous) 21.8 g
	NaH ₂ PO ₄ (anhydrous) 6.4 g
	NaCl 180 g
	Distilled H ₂ O 1000 ml
Mix to dissolve the solution, adjust the pH to 7.2 using NaOH and HCl. Add 5 ml of Tween 20 and store at room temperature.	

APPENDIX III

ANTIGEN RETRIEVAL BUFFERS

Table III: Constituents of the Unmasking Solutions used During IHC

Antigen Retrieval Buffer	Measurement of the Constituents
Sodium Citrate Buffer (10 Mm Sodium Citrate, 0.05% Tween 20, pH 6.0)	Tris-sodium citrate (dehydrate)..... 2.94 g
	Distilled H ₂ O 1000 ml
	Mix well to dissolve. Adjust the pH to 6.0 with 1 N HCl, add 0.5 ml Tween 20 and mix well. Store the solution at room temperature for up to 3 months or at 4°C for longer usage.
Citrate Buffer (10 Mm Citric Acid, 0.05% Tween 20, pH 6.0)	Citric acid (anhydrous) 1.92 g
	Distilled H ₂ O 1000 ml
	Mix well to dissolve. Adjust the pH to 6.0 with NaOH, add 0.5 ml Tween 20 and mix well. Store the solution at room temperature for up to 3 months or at 4°C for longer usage.
Tris EDTA Buffer (pH 9.0)	Tris (Hydroxymethyl) Aminomethane 6.055 g
	EDTA (Ethylenediaminetetra acetic acid 1.86 g
	Distilled H ₂ O 5000 ml
	Mix well to dissolve. Adjust the pH to 9.0 with 0.1 M NaOH or 0.1 N HCl. Store the solution at 4°C.

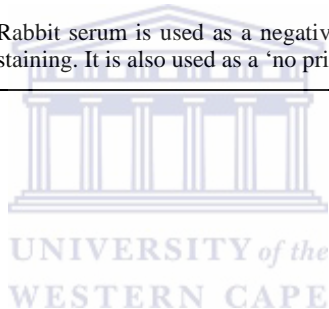
UNIVERSITY of the
WESTERN CAPE

APPENDIX IV

BLOCKING SOLUTIONS

Table IV: Constituents of the Blocking Solutions used During IHC

Blocking Solution	Measurement of the Constituents
Peroxidase Blocking Solution (3% H ₂ O ₂ in PBS)	30% H ₂ O ₂2 ml
	1X PBS18 ml
	Mix well and store at 4°C for up to 3 months.
Peroxidase Blocking Solution (0.3% H ₂ O ₂ in Methanol)	30% H ₂ O ₂0.2 ml
	Methanol 18 ml
	Mix well and store at 4°C.
Normal Rabbit Serum	NCL-R-Serum1 ml
	PBS Buffer 19 ml
	Rabbit serum is used as a negative control or as a blocking reagent in IHC staining. It is also used as a 'no primary' antibody control.



APPENDIX V

IMMUNOHISTOCHEMISTRY DILUENT SOLUTION

Novocastra IHC diluent is used to dilute primary antibodies, Biotinylated secondary antibodies and Streptavidin-HPR in immunohistochemical staining procedures.

Novocastra IHC Diluent – 500 ml

MANUAL POLYMER DETECTION SYSTEM

Biotinylated secondary antibody is applied for the detection of mouse IgG, mouse IgM and rabbit IgG primary antibodies.

RE7103 Biotinylated secondary antibody – 25 ml

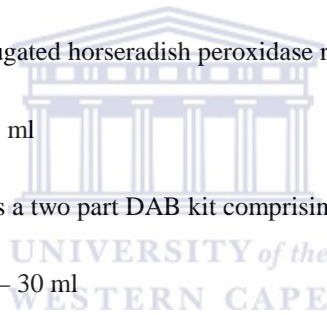
Streptavidin-HPR is a streptavidin-cojugated horseradish peroxidase reagent.

RE7104 Streptavidin-HPR – 25 ml

Novolink DAB (polymer), RE7230-K is a two part DAB kit comprising of:

RE7143 DAB Substrate buffer – 30 ml

RE7105 DAB Chromogen – 3 ml



APPENDIX VI

NOVOCASTRA™ LYOPHILIZED MOUSE MONOCLONAL ANTIBODIES

Cytokeratin 1

Product Code	NCL-CK1
Intended Use	Research only
Specificity	Human cytokeratin 1 intermediate filament protein (68kD)
Recommendations on Use	IHC: Working dilution of 1:20 – 1:40, incubation at 25°C for 60 minutes
Positive Controls	IHC: Normal skin
Staining Pattern	Cytoplasmic
Storage and Stability	Store unopened at 4°C, product performance is maintained up to expiry date
General Overview	Present in complex epithelium; reacts with all squamous epithelium

Cytokeratin 5

Product Code	NCL-CK5
Intended Use	In vitro diagnostic purposes
Specificity	Human cytokeratin 5 intermediate filament protein
Recommendations on Use	IHC: Working dilution of 1:100, incubation at 25°C for 30 minutes
Positive Controls	Prostate
Staining Pattern	Cytoplasmic
Storage and Stability	Store unopened at 2 - 8°C, product performance is maintained up to expiry date
General Overview	Present in the cytoplasm of many non-keratinized stratified squamous epithelia

Cytokeratin 13

Product Code	NCL-CK13
Intended Use	Research only
Specificity	Human cytokeratin 13 intermediate filament protein (54kD)
Recommendations on Use	IHC: Working dilution of 1:100 – 1:200, incubation at 25°C for 60 minutes
Positive Controls	IHC: Tonsil
Staining Pattern	Cytoplasmic staining of mucosa

Storage and Stability	Store unopened at 4°C, product performance is maintained up to expiry date
General Overview	Expressed as a major component of squamous, non-keratinized epithelium, transitional epithelium, pseudostratified epithelium and myoepithelium

Cytokeratin 14

Product Code	NCL-LL002
Intended Use	<i>In vitro</i> diagnostic purposes
Specificity	Human cytokeratin 14 intermediate filament protein
Recommendations on Use	IHC: Working dilution of 1:20, incubation at 25°C for 60 minutes
Positive Controls	IHC: Normal skin
Staining Pattern	Cytoplasmic
Storage and Stability	Store unopened at 2 – 8°C, product performance is maintained up to expiry date
General Overview	Stains the basal layer of stratified squamous and non-squamous epithelia

Collagen IV

Product Code	NCL-COLL-IV
Intended Use	Research only
Specificity	Human collagen type IV
Recommendations on Use	IHC: Working dilution of 1:100 – 1:200, incubation at 25°C for 60 minutes
Positive Controls	IHC: Kidney, basement membranes
Staining Pattern	Basement membranes
Storage and Stability	Store unopened at 4°C, product performance is maintained up to expiry date
General Overview	Major constituent of basement membranes

Laminin

Product Code	NCL-LAMININ
Intended Use	Research only
Specificity	Human laminin (850kD)
Recommendations on Use	IHC: Working dilution of 1:50 – 1:100, incubation at 25°C for 60 minutes
Positive Controls	IHC: Kidney, skeletal muscle, small intestine
Staining Pattern	Basement membranes of blood vessels, smooth muscle, ganglia and muscle fibers
Storage and Stability	Store unopened at 4°C, product performance is maintained up to expiry date

General Overview Organized within basement membranes such as those associated with epithelia, surrounding blood vessels, nerves and underlying pial sheaths of the brain

Elastin

Product Code NCL-ELASTIN

Intended Use Research only

Specificity Human insoluble elastin

Recommendations on Use IHC: Working dilution of 1:100 – 1:200, incubation at 25°C for 60 minutes

Positive Controls IHC: Kidney, small intestine, liver

Staining Pattern Extracellular

Storage and Stability Store unopened at 4°C, product performance is maintained up to expiry date

General Overview Present in connective tissue and imparts the property of elasticity to vertebrate elastic tissue

Fibronectin

Product Code NCL-FIB

Intended Use Research only

Specificity Cell-attachment domain of human fibronectin

Recommendations on Use IHC: Working dilution of 1:100 – 1:200, incubation at 25°C for 60 minutes

Positive Controls IHC: Normal kidney

Staining Pattern Extracellular staining of connective tissue matrix

Storage and Stability Store unopened at 4°C, product performance is maintained up to expiry date

General Overview Present in basement membranes and extracellular connective tissue matrix

CD1a

Product Code NCL-CD1a-235

Intended Use *In vitro* diagnostic purposes

Specificity Human CD1a molecule

Recommendations on Use IHC: Working dilution of 1:15 – 1:30, incubation at 25°C for 60 minutes

Positive Controls IHC: Normal skin

Staining Pattern Staining of Langerhans cells

Storage and Stability Store unopened at 2 - 8°C, product performance is maintained up to expiry date

General Overview Stains Langerhans cells and dendritic cells of skin and tonsil

Vascular Endothelial Growth Factor Receptor

Product Code	NCL-L-VEGFR-3
Intended Use	Research only
Specificity	Human vascular endothelial growth factor receptor-3
Recommendations on Use	IHC: Working dilution of 1:50 – 1:100, incubation at 25°C for 60 minutes
Positive Controls	IHC: Placenta
Staining Pattern	Cytoplasmic
Storage and Stability	Store liquid antibody at 4°C, product performance is maintained up to expiry date
General Overview	Present in many tissues including lung, intestine, brain and placenta



APPENDIX VII

STATISTICAL ANALYSIS DATA

Table VII - a: Statistical Comparisons of Cytokeratin 1 Staining Intensity

Parameter			
Table Analyzed	Cytokeratin 1		
Friedman test			
P value	< 0.0001		
Exact or approximate P value?	Gaussian Approximation		
P value summary	****		
Are means signif. different? (P < 0.05)	Yes		
Number of groups	4		
Friedman statistic	27.69		
Dunn's Multiple Comparison Test	Difference in rank sum	Significant? P < 0.05?	Summary
OVT vs XVT	20.50	Yes	**
OVT vs OVT [□]	-3.500	No	Ns
OVT vs XVT [□]	15.00	No	Ns
XVT vs OVT [□]	-24.00	Yes	****
XVT vs XVT [□]	-5.500	No	Ns
OVT [□] vs XVT [□]	18.50	Yes	**

Table VII - b: Statistical Comparisons of Cytokeratin 5 Staining Intensity

Parameter			
Table Analyzed	Cytokeratin 5		
Friedman test			
P value	0.0039		
Exact or approximate P value?	Gaussian Approximation		
P value summary	**		
Are means signif. different? (P < 0.05)	Yes		
Number of groups	4		
Friedman statistic	13.35		
Dunn's Multiple Comparison Test	Difference in rank sum	Significant? P < 0.05?	Summary
OVT vs XVT	10.50	No	ns
OVT vs OVT [□]	-4.000	No	ns
OVT vs XVT [□]	3.500	No	ns
XVT vs OVT [□]	-14.50	No	ns
XVT vs XVT [□]	-7.000	No	ns
OVT [□] vs XVT [□]	7.500	No	ns

Table VII - c: Statistical Comparisons of Cytokeratin 13 Staining Intensity

Parameter	
Table Analyzed	Cytokeratin 13
Friedman test	
P value	< 0.0001
Exact or approximate P value?	Gaussian Approximation
P value summary	****
Are means signif. different? (P < 0.05)	Yes

Number of groups	4		
Friedman statistic	22.76		
Dunn's Multiple Comparison Test	Difference in rank sum	Significant? P < 0.05?	Summary
OVT vs XVT	15.00	No	ns
OVT vs OVT [□]	-1.500	No	ns
OVT vs XVT [□]	-1.500	No	ns
XVT vs OVT [□]	-16.50	Yes	*
XVT vs XVT [□]	-16.50	Yes	*
OVT [□] vs XVT [□]	0.0	No	ns

Table VII - d: Statistical Comparisons of Cytokeratin 14 Staining Intensity

Parameter			
Table Analyzed	Cytokeratin 14		
Friedman test			
P value	0.0003		
Exact or approximate P value?	Gaussian Approximation		
P value summary	***		
Are means signif. different? (P < 0.05)	Yes		
Number of groups	4		
Friedman statistic	18.55		
Dunn's Multiple Comparison Test	Difference in rank sum	Significant? P < 0.05?	Summary
OVT vs XVT	12.00	No	ns
OVT vs OVT [□]	-2.000	No	ns
OVT vs XVT [□]	-2.000	No	ns
XVT vs OVT [□]	-14.00	No	ns
XVT vs XVT [□]	-14.00	No	ns
OVT [□] vs XVT [□]	0.0	No	ns

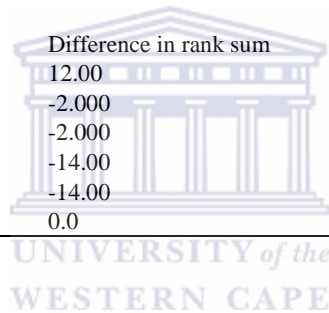


Table VII - e: Statistical Comparisons of Collagen IV Staining Intensity

Parameter			
Table Analyzed	Collagen IV		
Friedman test			
P value	0.0049		
Exact or approximate P value?	Gaussian Approximation		
P value summary	**		
Are means signif. different? (P < 0.05)	Yes		
Number of groups	6		
Friedman statistic	16.79		
Dunn's Multiple Comparison Test	Difference in rank sum	Significant? P < 0.05?	Summary
OVT vs XVT - h	12.50	No	Ns
OVT vs XVT - m	24.50	No	Ns
OVT vs OVT [□]	6.500	No	Ns
OVT vs XVT [□] - h	19.50	No	Ns
OVT vs XVT [□] - m	24.00	No	Ns
XVT - h vs XVT - m	12.00	No	Ns
XVT - h vs OVT [□]	-6.000	No	Ns
XVT - h vs XVT [□] - h	7.000	No	Ns
XVT - h vs XVT [□] - m	11.50	No	Ns
XVT - m vs OVT [□]	-18.00	No	Ns
XVT - m vs XVT [□] - h	-5.000	No	Ns
XVT - m vs XVT [□] - m	-0.5000	No	Ns
OVT [□] vs XVT [□] - h	13.00	No	Ns

OVT [□] vs XVT [□] - m	17.50	No	Ns
XVT [□] - h vs XVT [□] - m	4.500	No	Ns

Table VII - f: Statistical Comparisons of Laminin Staining Intensity

Parameter			
Table Analyzed	Laminin		
Friedman test			
P value	0.0004		
Exact or approximate P value?	Gaussian Approximation		
P value summary	***		
Are means signif. different? (P < 0.05)	Yes		
Number of groups	6		
Friedman statistic	22.59		
Dunn's Multiple Comparison Test	Difference in rank sum	Significant? P < 0.05?	Summary
OVT vs XVT - h	8.500	No	ns
OVT vs XVT - m	20.50	No	ns
OVT vs OVT [□]	0.5000	No	ns
OVT vs XVT [□] - h	11.50	No	ns
OVT vs XVT [□] - m	25.00	Yes	*
XVT - h vs XVT - m	12.00	No	ns
XVT - h vs OVT [□]	-8.000	No	ns
XVT - h vs XVT [□] - h	3.000	No	ns
XVT - h vs XVT [□] - m	16.50	No	ns
XVT - m vs OVT [□]	-20.00	No	ns
XVT - m vs XVT [□] - h	-9.000	No	ns
XVT - m vs XVT [□] - m	4.500	No	ns
OVT [□] vs XVT [□] - h	11.00	No	ns
OVT [□] vs XVT [□] - m	24.50	No	ns
XVT [□] - h vs XVT [□] - m	13.50	No	ns

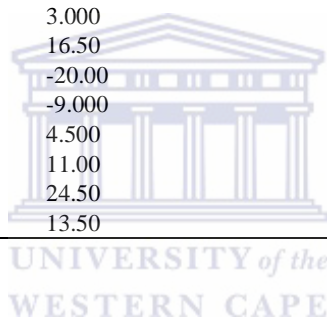


Table VII - g: Statistical Comparisons of Elastin Staining Intensity

Parameter			
Table Analyzed	Elastin		
Friedman test			
P value	0.0020		
Exact or approximate P value?	Gaussian Approximation		
P value summary	**		
Are means signif. different? (P < 0.05)	Yes		
Number of groups	4		
Friedman statistic	14.78		
Dunn's Multiple Comparison Test	Difference in rank sum	Significant? P < 0.05?	Summary
OVT vs XVT	-5.000	No	ns
OVT vs OVT [□]	-14.50	No	ns
OVT vs XVT [□]	-12.50	No	ns
XVT vs OVT [□]	-9.500	No	ns
XVT vs XVT [□]	-7.500	No	ns
OVT [□] vs XVT [□]	2.000	No	ns

Table VII - h: Statistical Comparisons of Fibronectin Staining Intensity

Parameter	
Table Analyzed	Fibronectin
Friedman test	

P value	< 0.0001
Exact or approximate P value?	Gaussian Approximation
P value summary	****
Are means signif. different? (P < 0.05)	Yes
Number of groups	6
Friedman statistic	47.27

Dunn's Multiple Comparison Test	Difference in rank sum	Significant? P < 0.05?	Summary
OVT vs XVT – h	11.50	No	ns
OVT vs XVT – m	19.50	No	ns
OVT vs OVT [□]	-16.50	No	ns
OVT vs XVT [□] - h	-16.50	No	ns
OVT vs XVT [□] - m	23.00	No	ns
XVT - h vs XVT – m	8.000	No	ns
XVT - h vs OVT [□]	-28.00	Yes	*
XVT - h vs XVT [□] - h	-28.00	Yes	*
XVT - h vs XVT [□] - m	11.50	No	ns
XVT - m vs OVT [□]	-36.00	Yes	****
XVT - m vs XVT [□] - h	-36.00	Yes	****
XVT - m vs XVT [□] - m	3.500	No	ns
OVT [□] vs XVT [□] - h	0.0	No	ns
OVT [□] vs XVT [□] - m	39.50	Yes	****
XVT [□] - h vs XVT [□] - m	39.50	Yes	****

Table VII - i: Statistical Comparisons of Langerhans Cells Staining Intensity

Parameter	Langerhans Cells		
Table Analyzed	Langerhans Cells		
Friedman test			
P value	< 0.0001		
Exact or approximate P value?	Gaussian Approximation		
P value summary	****		
Are means signif. different? (P < 0.05)	Yes		
Number of groups	6		
Friedman statistic	40.55		
Dunn's Multiple Comparison Test	Difference in rank sum	Significant? P < 0.05?	Summary
OVT vs XVT – h	9.500	No	Ns
OVT vs XVT – m	25.00	Yes	*
OVT vs OVT [□]	-11.50	No	Ns
OVT vs XVT [□] - h	21.00	No	Ns
OVT vs XVT [□] - m	28.00	Yes	*
XVT - h vs XVT – m	15.50	No	Ns
XVT - h vs OVT [□]	-21.00	No	Ns
XVT - h vs XVT [□] - h	11.50	No	Ns
XVT - h vs XVT [□] - m	18.50	No	Ns
XVT - m vs OVT [□]	-36.50	Yes	****
XVT - m vs XVT [□] - h	-4.000	No	Ns
XVT - m vs XVT [□] - m	3.000	No	Ns
OVT [□] vs XVT [□] - h	32.50	Yes	**
OVT [□] vs XVT [□] - m	39.50	Yes	****
XVT [□] - h vs XVT [□] - m	7.000	No	Ns

Table VII - j: Statistical Comparisons of VEGFR Staining Intensity

Parameter			
Table Analyzed	VEGFR		
Friedman test			
P value	0.0012		
Exact or approximate P value?	Gaussian Approximation		
P value summary	**		
Are means signif. different? (P < 0.05)	Yes		
Number of groups	6		
Friedman statistic	20.00		
Dunn's Multiple Comparison Test	Difference in rank sum	Significant? P < 0.05?	Summary
OVT vs XVT - h	12.00	No	ns
OVT vs XVT - m	15.00	No	ns
OVT vs OVT [□]	15.00	No	ns
OVT vs XVT [□] - h	15.00	No	ns
OVT vs XVT [□] - m	15.00	No	ns
XVT - h vs XVT - m	3.000	No	ns
XVT - h vs OVT [□]	3.000	No	ns
XVT - h vs XVT [□] - h	3.000	No	ns
XVT - h vs XVT [□] - m	0.0	No	ns
XVT - m vs OVT [□]	0.0	No	ns
XVT - m vs XVT [□] - h	0.0	No	ns
XVT - m vs XVT [□] - m	0.0	No	ns
OVT [□] vs XVT [□] - h	0.0	No	ns
OVT [□] vs XVT [□] - m	0.0	No	ns
XVT [□] - h vs XVT [□] - m	0.0	No	ns

